The Search for the Electric Dipole Moment of the Electron (eEDM) in Mercury Halides Using the Relativistic Coupled Cluster Theory

by

Srinivasa Prasannaa V

Indian Institute of Astrophysics, Bangalore

A thesis submitted in partial fulfillment for the
degree of Doctor of Philosophy to the

Department of Physics
University of Calicut
Calicut, Kerala

June 2017

CERTIFICATE

This is to certify that the thesis titled **The Search for the Electric Dipole Moment of the Electron (eEDM) in Mercury Halides Using the Relativistic Coupled Cluster Theory** is a bonafide record of the work done by Srinivasa Prasannaa V, under our joint supervision and that no part of it has been included previously for the award of any degree, either in this university or any other institution. The thesis has been checked for plagiarism, using the URKUND software, at the CHMK library, University of Calicut. Also, no changes were given by the thesis referees after evaluation, and therefore, there are no further corrections to be made in this thesis.

Supervisor:

Prof. Bhanu Pratap Das,
Indian Institute of Astrophysics,
Bangalore.

Co-supervisor:

Prof. Vishnu Mayya Bannur,
Department of Physics,
University of Calicut, Kerala.

DECLARATION

I hereby declare that the thesis titled **The Search for the Electric Dipole Moment of the Electron (eEDM) in Mercury Halides Using the Relativistic Coupled Cluster Theory** is an authentic record of research work carried out by me at the Indian Institute of Astrophysics under the supervision of Prof. Bhanu Pratap Das, and Prof. Vishnu Mayya Bannur. No part of this work has formed the basis for award of any other degree in any university or institution.

Srinivasa Prasannaa V
Indian Institute of Astrophysics
Bangalore 560 034
June 2017.

ACKNOWLEDGEMENTS

First and foremost, I would like to express my deepest gratitude to my thesis supervisor, Prof. Bhanu Pratap Das, for his invaluable guidance and encouragement provided during the work. It has been great pleasure working under him, and a wonderful learning experience too. I am grateful to him for teaching me each and every step of the relativistic quantum mechanics, lepton electric dipole moments, and the relativistic coupled cluster theory, the three major tools that are required to understand the processes involved in this work and move it further.

I am extremely grateful to Prof. Pravabati, for her help and guidance with matters related to the submission of my thesis, after my supervisor's retirement from IIA. In particular, she corresponded with the HoD and other faculty members at Calicut, and was present in my synopsis presentation. She also facilitated the official procedures that I had to comply with, at IIA. Finally, I wish to thank her for the useful discussions in physics, starting from my MSc days, when she taught me statistical mechanics and general relativity, till now. Her approach to physics helped me open my mind to different ways of thinking about a problem.

I wish to thank Dr. Minori Abe for her guidance with the codes. She explained to me several important details of the codes needed to do the computation, through several Skype calls, in spite of her very busy schedule. She did it very patiently, knowing the fact that I was completely unaware of these codes.

I thank the Director, Indian Institute of Astrophysics (IIA), Prof. Gangadhara from the Board of Graduate Studies, IIA , and all the administrative staff, who helped me in several stages with registration and administrative procedures. I also take this opportunity to thank the Vice Chancellor, University of Calicut. I thank Prof. Vishnu Mayya Bannur, my co-guide, for his useful suggestions in our work. I also take this opportunity to thank Dr. C. D. Ravikumar, for his help with my registration procedure.

I thank all my friends at IIA, for their several useful discussions in physics as well as other aspects of life, and standing by my side when I needed help.

I also thank Manpreet, and Anish for their kind help with Linux and the codes in my initial stages of PhD, and Dr. Baba Verghese for his help with Latex.

Last but not least, I thank my parents and my wife, Akshaya, for their support in each and every phase of my PhD.

CONTENTS

LIST OF FIGURES

NOTATIONS AND ABBREVIATIONS

EDM	Electric Dipole Moment
eEDM	Electron Electric Dipole Moment
SM	Standard Model
QCD	Quantum Chromodynamics
SUSY	Supersymmetry
P	Parity reversal
T	Time reversal
CP	Charge conjugation Parity reversal
CKM	Cabibo-Kobayashi-Masakawa matrix
BAU	Baryon Asymmetry in the Universe
CMBR	Cosmic Microwave Background Radiation
2HDM	Two-Higgs Doublet Model
GV/cm	Giga Volt per centimetre
PDM	Permanent Electric Dipole Moment
QED	Quantum Electrodynamics
HF	Hartree-Fock
DF	Dirac-Fock
GTO	Gaussian Type Orbital
STO	Slater Type Orbital
DZ	Double Zeta
TZ	Triple Zeta
QZ	Quadruple Zeta
cc-pV	correlation consistent, polarized valence
CI	Configuration Interaction
MCHF	Multiconfiguration Hartree-Fock
MBPT	Many-Body Perturbation Theory
CCM	Coupled Cluster Method
BCH	Baker Campbell Haussdorf

LOE	Level Of Excitation
CCSD	Coupled Cluster Singles and Doubles
NCCM	Normal Coupled Cluster Method
RCCM	Relativistic Coupled Cluster Method
AO	Atomic Orbital
MO	Molecular Orbital
SOMO	Singly Occupied Molecular Orbital
CASSCF	Complete Active Space Self Consistent Field
ECP	Effective Core Potential

LIST OF PUBLICATIONS

1. Permanent electric dipole moment of strontium monofluoride as a test of the accuracy of a relativistic coupled-cluster method, **V.S.Prasannaa**, M. Abe, and B. P. Das, PHYSICAL REVIEW A 90, 052507 (2014).

2. Mercury Monohalides: Suitability for Electron Electric Dipole Moment Searches, **V.S.Prasannaa**, A. C. Vutha, M. Abe and B. P. Das, PHYSICAL REVIEW LETTERS, 114, 183001 (2015).

3. Permanent electric dipole moments of alkaline-earth-metal monofluorides: Interplay of relativistic and correlation effects, **V.S.Prasannaa**, S. Sreerekha, M. Abe, V. M. Bannur, and B. P. Das, PHYSICAL REVIEW A 93, 042504 (2016).

4. Das, B. P., Nayak, M. K., Abe, M., and **V. S. Prasannaa**, Liu, W. (Ed.) Handbook of Relativistic Quantum Chemistry Relativistic Many-Body Aspects of the Electron Electric Dipole Moment Searches Using Molecules Springer Berlin Heidelberg, chapter 19, pages 581-610 (2016).

5. The Role of Molecular Electric Dipole Moments of Mercury Monohalides in the Search for the Electron Electric Dipole Moment, **V.S.Prasannaa**, M. Abe, and B. P. Das, ASIAN JOURNAL OF PHYSICS, in the issue, 'Advances in High Precision Spectroscopy and Tests of Fundamental Physics', Vol. 25, No 10 , page 1259 (2016).

6. Theoretical analysis of effective electric fields in mercury monohalides, **V. S. Prasannaa**, M. Abe, V. M. Bannur, and B. P. Das, PHYSICAL REVIEW A 95, 042513 (2017).

1

INTRODUCTION TO THE ELECTRIC DIPOLE MOMENT OF THE ELECTRON (EEDM)

1.1 Theoretical aspects

1.1.1 P and T violation

The electron's electric dipole moment (eEDM) is an excellent probe of beyond the Standard Model physics [1, 2]. The Standard Model (SM), which contains in it the electroweak theory and quantum chromodynamics (QCD), is by far the most successful theory of elementary particles and their interactions that has been verified by experiments till date. However, it stands incomplete, with phenomena like the oscillations of neutrinos and the nature of dark matter not being taken into account by it [3]. Several theories go beyond the SM, for example, supersymmetric (SUSY) models and their many variants.

The eEDM is a property that is intrinsic to an electron, just like its mass or charge. It arises when two discrete symmetries, namely parity reversal (P) and time reversal (T) symmetries, are simultaneously violated [4]. A proof of this is discussed below:

P basically switches $\vec{r} \rightarrow -\vec{r}$, where $\vec{r}$ refers to the usual spatial coordinates. The parity operator, $\boldsymbol{P}$, reverses the position operator's ($\boldsymbol{r}$) sign, that is, $\boldsymbol{PrP^{-1}} = -\boldsymbol{r}$. It is also unitary, that is, $\boldsymbol{P} = \boldsymbol{P^{-1}} = \boldsymbol{P^{\dagger}}$.

Consider a system, whose electric dipole moment (EDM) operator is $\boldsymbol{d}$. The EDM

operator has in it the displacement operator. Also, since $\boldsymbol{PrP^{-1}} = -\boldsymbol{r}$, $\boldsymbol{PdP^{-1}} = -\boldsymbol{d}$. When there is no external electric field, a stationary state, $|\varphi\rangle$, has a non-zero EDM, which is

$$\langle \boldsymbol{d} \rangle = \langle \varphi | \boldsymbol{d} | \varphi \rangle \tag{1.1}$$

If $\boldsymbol{P}$ acts on $|\varphi\rangle$, to give $|\varphi'\rangle$, then

$$\begin{aligned} \langle \boldsymbol{d} \rangle &= \langle \varphi | \boldsymbol{P^{\dagger} P d P^{-1} P} | \varphi \rangle \\ &= -\langle \varphi' | \boldsymbol{d} | \varphi' \rangle \end{aligned} \tag{1.2}$$

The following equation is satisfied by the stationary state:

$$\boldsymbol{H}|\varphi\rangle = E|\varphi\rangle \tag{1.3}$$

That is,

$$\begin{aligned} \boldsymbol{PHP^{-1}P}|\varphi\rangle &= E\boldsymbol{P}|\varphi\rangle \\ \boldsymbol{H}|\varphi'\rangle &= E|\varphi'\rangle \end{aligned} \tag{1.4}$$

Here, it is assumed that the Hamiltonian is invariant under space inversion, that is, $\boldsymbol{PHP^{-1}} = \boldsymbol{H}$.

Therefore, both $|\varphi\rangle$ and $|\varphi'\rangle$ describe stationary states whose energies are the same, given by E. If the energy level is non-degenerate, then $|\varphi'\rangle = c|\varphi\rangle$, where c is an eigenvalue of the parity operator, which means that it is either +1 or -1. Therefore,

$$\begin{aligned} \langle \varphi | \boldsymbol{d} | \varphi \rangle &= -\langle \varphi' | \boldsymbol{d} | \varphi' \rangle \\ &= -c^2 \langle \varphi | \boldsymbol{d} | \varphi \rangle \\ &= -\langle \varphi | \boldsymbol{d} | \varphi \rangle \end{aligned} \tag{1.5}$$

The above equation is true, only if $\langle \boldsymbol{d} \rangle = 0$. This means that if the Hamiltonian is invariant under parity, and if the stationary state is non-degenerate, then the EDM=0, for

that system.

$\boldsymbol{T}$ refers to $t \to -t$, where t denotes time. The physical interpretation of time reversal is that it is equivalent to motion reversal.

If the Hamiltonian were to be unchanged under rotations, then its eigenvectors, $\boldsymbol{J^2}$ and $\boldsymbol{J_z}$ form a complete set, given by $|E, j, m\rangle$. Here, we make an assumption that the degeneracy of these eigenvectors is associated with the $(2j + 1)$ values of m only. The Wigner-Eckart theorem gives the expression for the EDM in one of these states:

$$\langle E, j, m|\boldsymbol{d}|E, j, m\rangle = C_{E,j}\langle E, j, m|\boldsymbol{J}|E, j, m\rangle \tag{1.6}$$

Here, $\boldsymbol{J}$ is the angular momentum operator. Note that $C_{E,j}$ is not a function of m. We can show that if $|u'\rangle = \boldsymbol{T}|u\rangle$, and if $|v'\rangle = \boldsymbol{T}|v\rangle$, then $\langle u'|v'\rangle = \langle u|v\rangle^*$ [5]. If $|u\rangle$ is $|\varphi\rangle$, and $|v\rangle$ is $\boldsymbol{d_\alpha}|\varphi\rangle$, where $\boldsymbol{d_\alpha}$ is some component of the EDM operator, then

$$\begin{aligned} |u'\rangle = |\varphi'\rangle &= \boldsymbol{T}|\varphi\rangle \\ |v'\rangle = \boldsymbol{T}\boldsymbol{d_\alpha}|\varphi\rangle &= \boldsymbol{d_\alpha}|\varphi'\rangle \end{aligned}$$

The last equation uses the equality $\boldsymbol{T}\boldsymbol{d_\alpha} = \boldsymbol{d_\alpha}\boldsymbol{T}$. Therefore,

$$\langle\varphi'|\boldsymbol{d_\alpha}|\varphi'\rangle = \langle\varphi|\boldsymbol{d_\alpha}|\varphi\rangle^* \tag{1.7}$$

$\boldsymbol{d_\alpha}$ is a Hermitian operator, and therefore

$$\langle\varphi'|\boldsymbol{d_\alpha}|\varphi'\rangle = \langle\varphi|\boldsymbol{d_\alpha}|\varphi\rangle \tag{1.8}$$

In a similar way:

$$\langle\varphi'|\boldsymbol{J}|\varphi'\rangle = -\langle\varphi|\boldsymbol{J}|\varphi\rangle \tag{1.9}$$

This uses the equality $\boldsymbol{d_\alpha}\boldsymbol{J} = -\boldsymbol{J}\boldsymbol{d_\alpha}$. Moreover,

$$\boldsymbol{J_z}|E,j,m\rangle = \hbar m|E,j,m\rangle \tag{1.10}$$
$$\boldsymbol{T}\boldsymbol{J_z}\boldsymbol{T^{-1}}\boldsymbol{T}|E,j,m\rangle = \hbar m\boldsymbol{T}|E,j,m\rangle \tag{1.11}$$
$$\boldsymbol{J_z}(\boldsymbol{T}|E,j,m\rangle) = -\hbar m(\boldsymbol{T}|E,j,m\rangle) \tag{1.12}$$

Since $\boldsymbol{J_z}|E,j,-m\rangle = -\hbar m|E,j,-m\rangle$, $\boldsymbol{T}|E,j,m\rangle$ and $|E,j,-m\rangle$ are different only by a phase factor (note that the degeneracy is due to m only). Hence, if $|\varphi\rangle = |E,j,m\rangle$, and $|\varphi'\rangle = \boldsymbol{T}|E,j,m\rangle$, then

$$\langle\varphi|\boldsymbol{d_\alpha}|\varphi\rangle = \langle E,j,m|\boldsymbol{d_\alpha}|E,j,m\rangle \tag{1.13}$$
$$\langle\varphi'|\boldsymbol{d_\alpha}|\varphi'\rangle = \langle E,j,-m|\boldsymbol{d_\alpha}|E,j,-m\rangle \tag{1.14}$$

When the above two expressions are substituted into equation (1.8), we obtain:

$$\langle E,j,m|\boldsymbol{d_\alpha}|E,j,m\rangle = \langle E,j,-m|\boldsymbol{d_\alpha}|E,j,-m\rangle \tag{1.15}$$

Similarly,

$$\langle\varphi'|\boldsymbol{J}|\varphi'\rangle = \langle E,j,-m|\boldsymbol{J}|E,j,-m\rangle \tag{1.16}$$
$$\langle\varphi|\boldsymbol{J}|\varphi\rangle = \langle E,j,m|\boldsymbol{J}|E,j,m\rangle \tag{1.17}$$
$$\because \langle\varphi'|\boldsymbol{J}|\varphi'\rangle = -\langle\varphi|\boldsymbol{J}|\varphi\rangle,$$
$$\langle E,j,-m|\boldsymbol{J}|E,j,-m\rangle = -\langle E,j,m|\boldsymbol{J}|E,j,m\rangle \tag{1.18}$$

When the equations (1.15) and (1.18) are used in equation (1.6), one sees that the EDM vanishes. That is, under the assumptions of rotational invariance and time reversal invariance, as well as the assumption that the degeneracy is only due to m, the EDM=0. The proof that has been discussed follows Ballentine's approach [5]. Note that this proof is general, and is not limited only to the EDM of the electron (eEDM).

Hence, both P and T must be simultaneously violated for the electron, or for that matter, any other elementary particle, to possess an intrinsic EDM. Note that due to the well known CPT theorem, T violation would imply CP violation [6].

P,T violating electric and magnetic moments

Consider the Schroedinger's equation:

$$\boldsymbol{H}(\vec{r})\psi(\vec{r}) = E\psi(\vec{r}) \tag{1.19}$$

The wave functions, ψ, are assumed to be non-degenerate. Performing a parity operation ($\boldsymbol{P}$) on it, we obtain:

$$\boldsymbol{P}\boldsymbol{H}(\vec{\boldsymbol{r}})\boldsymbol{P}^{-1}\boldsymbol{P}\psi(\vec{r}) = \boldsymbol{P}E\psi(\vec{r}) \tag{1.20}$$

$$\boldsymbol{H}(\vec{r})\psi(-\vec{r}) = E\psi(-\vec{r}) \tag{1.21}$$

Note that the last line of the above equations assume that $\boldsymbol{H}$ is invariant under $\boldsymbol{P}$. In such a case, $[\boldsymbol{P}, \boldsymbol{H}] = 0$, and $\psi(\vec{r})$ are simultaneous eigenfunctions of $\boldsymbol{P}$ and $\boldsymbol{H}$. Eigenfunction of $\boldsymbol{P}$ would mean that:

$$\boldsymbol{P}\psi(\vec{r}) = \Pi\psi(\vec{r}) \tag{1.22}$$

Π is the eigenvalue, and it is either +1 (P-even) or -1 (P-odd). Independent of whether the eigenvalue is positive or negative unity, the state still has a definite parity. However, if the Hamiltonian were to have a P-odd term, then $[\boldsymbol{P}, \boldsymbol{H}]$ is not zero, that is, the state no longer is an eigenfunction of parity. The state is then said to not have a definite parity.

This idea indicates those moments that are P violating. Consider a system where the state is an eigenfunction of parity. Then,

$$\langle\psi_f|\boldsymbol{O}|\psi_i\rangle = \langle\psi_f|\boldsymbol{P}^{-1}\boldsymbol{P}\boldsymbol{O}\boldsymbol{P}^{-1}\boldsymbol{P}|\psi_i\rangle \tag{1.23}$$

$$= \Pi_f\Pi_i\langle\psi_f|\boldsymbol{P}\boldsymbol{O}\boldsymbol{P}^{-1}|\psi_i\rangle \tag{1.24}$$

Since we deal with expectation values, the bra and the ket are the same state, which means that $\Pi_f\Pi_i$ is one. Then, if the operator, $\boldsymbol{O}$, is P-even (note that for a state to have a definite parity, it is only the Hamiltonian that needs to be invariant under parity; here, we are referring to some operator, $\boldsymbol{O}$, which can be P-even or odd), then the matrix element may be non-zero, but if the operator, $\boldsymbol{O}$, is P-odd, then the matrix element is the negative of itself, thereby making it zero. Now, replace $\boldsymbol{O}$ by all the electric multipole moments' operators.

$\boldsymbol{E0}$ (electric monopole operator), $\boldsymbol{E2}$ (electric quadrupole operator), etc are P-even, so there is no restriction on the matrix elements. However, $\boldsymbol{E1}$ (electric dipole operator), $\boldsymbol{E3}$ (electric octupole operator), etc are P-odd, and hence their expectation values are zero.

Now, note that this is true only if $\boldsymbol{H}$ is even under parity. If $\boldsymbol{H}$ were to change sign when it is parity transformed, then the state is no longer an eigenfunction of parity, so the above analysis does not apply. That is, P-odd electric moments are not restricted to vanish, if $\boldsymbol{H}$ is odd under parity. In other words, $\boldsymbol{H}$ must be odd under parity, else, based on parity selection rules given above, the P-odd electric moments vanish.

Let us now discuss about the magnetic moments. $\boldsymbol{M0}$, $\boldsymbol{M2}$, etc are P-odd, while $\boldsymbol{M1}$, $\boldsymbol{M3}$, etc are P-even. Hence, if parity is violated, then those magnetic moments for which the rank is even can also exist.

To summarize, the expectation values of $\boldsymbol{E1}$, $\boldsymbol{E3}$, etc can be non-zero, if $\boldsymbol{H}$ is P-violating, while that of $\boldsymbol{M0}$, $\boldsymbol{M2}$, etc can be non-zero if the $\boldsymbol{H}$ is P-violating.

On a quick note, the reason why the odd electric moments are P-odd, while the even ones are P-even, can be understood by looking at their general expressions. The components of the electric multipole tensor operator can be shown to be [7]:

$$\boldsymbol{Q}_{\boldsymbol{E}\,l,\boldsymbol{m}} \propto r^l Y_{lm} \tag{1.25}$$

The operator's parity is $(-1)^l$. Therefore, the odd moments are P-odd, while the even ones are P-even.

Similarly, for the magnetic multipole:

$$\boldsymbol{Q}_{\boldsymbol{M}\,l,\boldsymbol{m}} \propto \boldsymbol{\nabla}(r^l Y_{lm}) \cdot \boldsymbol{S} \tag{1.26}$$

Note that S is P-even, Y_{lm}'s behaviour under parity is given by $(-1)^l$, and ∇ is P-odd. Therefore, the operator's parity is $(-1)^{l+1}$. This means that even moments are P-odd, and the odd ones are P-even.

Let us now discuss T-violating moments. An expectation value can be non-zero, where ψ is the eigenfunction of a Hamiltonian that is invariant under $\boldsymbol{T}$, when:
a. $\boldsymbol{O}$ is T-even, and the rank of the operator, l, is even, or b. $\boldsymbol{O}$ is T-odd, and l is odd.

The proof of the above statement is not discussed here, and can be found, for example, [7]. Now, the electric moment operators are T-even, and therefore l has to be even, if the expectation value must not vanish, that is, the expectation values of $\boldsymbol{E0}$, $\boldsymbol{E2}$, etc are

allowed. Now, the magnetic moment operators are T-odd, and hence the expectation values of $\boldsymbol{M1}$, $\boldsymbol{M3}$, etc are allowed.

However, if $\boldsymbol{H}$ is T-odd, then the above constraint does not hold, that is, the expectation value can be non-zero even if $\boldsymbol{O}$ is T-odd with l even, and $\boldsymbol{O}$ is T-even with l odd. Hence, in this case, even $\boldsymbol{E1}$, $\boldsymbol{E3}$, etc's expectation values are allowed. Similarly, those of $\boldsymbol{M0}$, $\boldsymbol{M2}$, etc are also not constrained to vanish, if $\boldsymbol{H}$ is T-odd.

To summarize:

$$\begin{aligned} P,T\ invariant &\longrightarrow \boldsymbol{E0}, \boldsymbol{E2}, \ldots \\ P,T\ violating &\longrightarrow \boldsymbol{E1}, \boldsymbol{E3}, \ldots are\ also\ allowed \\ P,T\ invariant &\longrightarrow \boldsymbol{M1}, \boldsymbol{M3}, \ldots \\ P,T\ violating &\longrightarrow \boldsymbol{M2}, \boldsymbol{M4}, \ldots are\ also\ allowed \end{aligned} \tag{1.27}$$

How many non-zero P,T violating electric and magnetic moments exist?

Consider the following expression from the Wigner-Eckart theorem: In a general matrix element, $\langle J'M'|\boldsymbol{O}^{\boldsymbol{k}}_{\boldsymbol{q}}|JM\rangle$, where $\boldsymbol{O}$ is a tensor operator of rank k, with one of its components being q, the matrix element is non-zero only if the condition $|J-K| \leq J' \leq J+K$ is satisfied (besides others).

For a free electron, the spin is 1/2, and it has no orbital angular momentum quantum number. Also, we evaluate an expectation value. Therefore, $J = J' = 1/2$. Hence, for the EDM, which involves an electric dipole operator, whose rank is 1, we can obtain J', which is 1/2, by subtracting J and K. This means that this matrix element can be non-zero. However, for the electric quadrupole moment, we can no longer satisfy the condition mentioned above. This holds also for all the subsequent higher moments. Also, the same argument can be extended to magnetic moments, where only the dipole moment is allowed by the Wigner-Eckart theorem. The only P,T violating moment that is allowed for a spin-1/2 elementary particle is the electric dipole moment. A final note: electric charge is allowed too (charge is a rank zero operator), but so is the magnetic monopole (a P,T violating moment)!

However, for a spin-1 system, for example, both dipole and quadrupole moments are allowed, for both the electric and the magnetic sectors. In this case, two P,T violating moments are allowed, the electric dipole moment, and the magnetic quadrupole moment.

Note that for both the cases of spin-1/2 and 1, there are up to 2S+1 P,T violating mo-

ments. This can also be found to be true for spins 3/2, 2, etc.

1.1.2 Connections with particle physics and matter-antimatter asymmetry

If the electron is treated to be a point particle, it would have no EDM, since then we have just a point charge. But, from a field theoretic viewpoint, the electron is viewed to be always surrounded by a cloud of virtual particles. When one says that the electron has an EDM, it basically refers to the asymmetry in this electron cloud.

In the SM, the first non-zero contribution to the eEDM arises only at the three-loop level. However, in SUSY, for example, the first non-zero contribution comes even at the one-loop level. This is because in SUSY, the complex phases involved in the emission and re-absorption of virtual particles need not be the same (SUSY generally allows for several CP violating phases, but the SM has just one (the phase in the CKM (Cabibo-Kobayashi- Masakawa) matrix)). In SM, for example, they are (because there is just one CP violating phase anyway), and hence they cancel out [1, 8, 9] (See figures 1, 2 and 3). Since the successively higher loops give rise to smaller and smaller contributions, the eEDM predicted by SM is much smaller than that in a SUSY. In fact, the SM predicts an eEDM less than 10^{-38} e cm, while SUSY and other beyond the SM theories predict much larger eEDMs, by a few orders in fact [1].

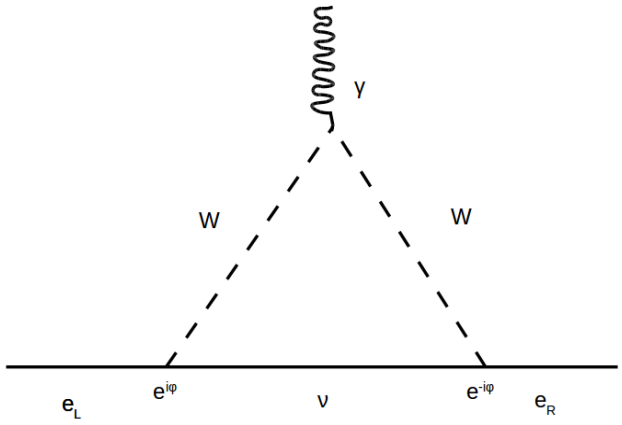

Figure 1.1: One of the Feynman diagrams showing the SM contribution to eEDM at the one-loop level: the phases (φ) at the two lower vertices cancel out. γ refers to the photon, W to the W- boson, and e is the electron. The subscripts L and R indicate left-handed and right-handed. In the SM case, $e_R = e_L$.

One sets an upper limit on the eEDM, by combining theory and experimental measurement. This is used to set stringent constrains on SM extension theories. The cur-

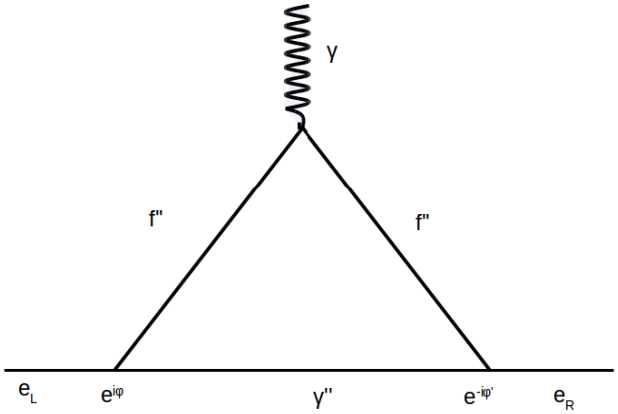

Figure 1.2: An illustration of how SUSY gives a contribution at the one-loop level: the phases do not cancel out. The superscript double prime means that the particle is a supersymmetric one.

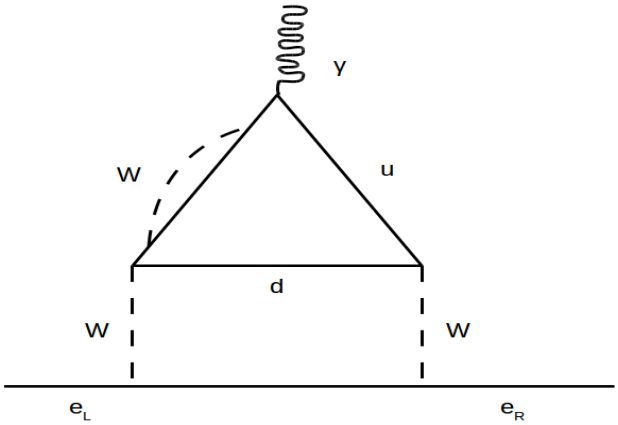

Figure 1.3: SM contribution to eEDM at the three-loop level. u and d refer to the up and down quarks respectively, and W refers to the W- boson. γ is a photon, and e refers to the electron.

rent best limit using atoms comes from Tl (20×10^{-28}e cm, with 90% confidence level), while from molecules, it is from ThO [10] (0.87×10^{-28}e cm), followed by YbF [11] (10.5×10^{-28}e cm), both at 90% confidence level (the latest in the race in HfF+, which has set an upper bound of 1.3×10^{-28}e cm, making it the second best [12]). Mercury monohalides are identified as promising candidates for eEDM searches, with their very large effective electric fields, and several attractive experimental features.

EDMs also shed light on the matter-antimatter asymmetry in the universe [13]. We believe that the early universe contained equal quantities of matter and antimatter. But, observations indicate strongly that the observable universe is currently dominated by matter. The baryon asymmetry in the universe (BAU) is given by η:

$$\eta = \frac{n_B}{n_\gamma} \approx 6.1^{+0.3}_{-0.2} \times 10^{-10} \tag{1.28}$$

Here, n_B refers to the number density of net baryons, which is the difference between the number density of baryons and that of anti-baryons. n_γ is the number density of the cosmic microwave background radiation (CMBR) photons.

Sakharov put forward three necessary conditions for baryogenesis [14]. Baryogenesis refers to the current BAU from an early universe, which was baryon symmetric. The three conditions, called the Sakharov conditions, are 1. baryon number violation, 2. C and CP violation, and 3. out-of-thermal equilibrium conditions. There are several models that describe baryogenesis, while satisfying the three conditions, for example, electroweak baryogenesis.

CP violation is a common condition for both the eEDM and the matter-antimatter asymmetry. In the SM, CP violation is predominantly from the CKM matrix. If we were to calculate the eEDM in the SM, as seen earlier, we get a value that is much smaller than what SM extensions predict. Since the SM is incomplete, the natural question in this regard is if there is any CP violation that is missing in this model. The SM value of η reinforces this, because it is of the order of 10^{-18}, whereas observations give $\approx 6.1^{+0.3}_{-0.2} \times 10^{-10}$. Hence, the search for a model to predict the right amount of CP violation so that one can reasonably describe both these seemingly unrelated phenomena becomes important.

Because only one real field remains after the Higgs mechanism in the SM, there is no CP violation from the Higgs sector. This is because one needs a complex phase for CP violation. This can be illustrated by using a simple example [8], the time dependent Schroedinger's equation:

$$i\hbar\frac{d\psi(\vec{x},t)}{dt} = -\frac{\hbar^2}{2m}\frac{d^2\psi(\vec{x},t)}{dx^2} + V(\vec{x})\psi(\vec{x},t) \tag{1.29}$$

For simplicity, V is made dependent on space and spin, but not time. Note that if V is real, that is, it has no complex terms in it, then the time reversed version of the Schroedinger's equation tells us that if $\psi(t)$ is a solution, so is $\psi^*(-t)$. This is because on the right hand side, not only does t go to -t, but also i to -i (since T is anti-unitary). However, if V were to be complex, that is, $V = |V|(cos(\phi) + isin(\phi))$, in other words, $V = Ve^(i\phi)$, where ϕ is called the complex phase, then T is violated, that is, upon operating the Schroedinger's equation with the time reversal operator, the equation no longer looks the same, due to an extra minus sign associated with the potential. We can say that

the complex phase, ϕ specifies the degree of T violation in the system, or the degree of CP violation (assuming CPT theorem). It is in a very similar way that complex phases in quantum field theory also imply T violation. The only complex phase associated with the weak sector in the SM is the CKM phase, which occurs in the CKM matrix.

Now, if one were to add another Higgs doublet (a two Higgs doublet model or 2HDM) to the SM, one has CP violation from the Higgs sector too. The next question to address is if this extra CP violation is sufficient to describe the observed BAU, and also connect it to eEDM. The scalar CP violating parameter was determined from cosmology, by Kazarian and Kuzmin, and from there, an estimate for the eEDM was obtained: $|d_e| > 10^{-27}$ e cm [13]. This idea was extended further by Nataraj and Das. The cut-off for d_e was from the then-best limit on eEDM, from the Tl atom. Their preliminary results indicated that η was still lower than the observed value, by a few orders [15]. They conclude that more sources of CP violation may be required.

1.2 Measuring eEDM

When an electric field ($\vec{E}$) is applied on a quantum mechanical system, for example, an electron, there is a shift in the energy of the system, by ΔE, which is given by

$$\Delta E = -\vec{d_e} \cdot \vec{E} \tag{1.30}$$

The proportionality constant is the eEDM, d_e. However, an electron just accelerates away when an electric field is applied on it, so one uses electrically neutral systems, such as atoms or molecules, with one unpaired electron (typically), to measure this shift in energy.

The idea behind an eEDM experiment is to look for spin precession of the electron (Larmour precession) (for example, refer [16]). In the presence of a magnetic field, an electron, with a magnetic dipole moment, say μ, precesses. This can be understood in a semi-classical way:
The electron experiences a torque, $\vec{\tau} = \vec{\mu} \times \vec{B}$, which tries to align $\vec{\mu} \propto \vec{L}$ ($\vec{L}$ is the spin itself, for a free electron) and $\vec{B}$ (since that's the lowest energy configuration). However, the torque also is the rate of change of angular momentum, and that change is perpendicular to $\vec{L}$. So, instead of aligning with the magnetic field, $\vec{L}$ (or $\vec{\mu}$) precesses around it. If ϕ is the angle between $\vec{L}$ and the line connecting the tail of $\vec{L}$ with the head of d$\vec{L}$, then:
$\omega = \frac{d\phi}{dt} = \frac{dL}{Ldt} = \frac{\tau dt}{Ldt} = \frac{dE}{L}$; L is $\hbar/2$, for a spin-1/2 particle like the electron.

So, if one can run the entire picture backward in time, the precession should be in the opposite direction. That is, if one can set up the experiment in such a way that it is somehow equivalent to running the experiment backward in time, and if the precession changes direction (and is different from the original precession frequency), it should be a test of T violation. However, this does not work, since the magnetic field too switches direction when $t \longrightarrow -t$. The resulting picture is not any different from the change in precession frequency when B is flipped, so there is nothing to distinguish a simple field flip and an actual time reversal. However, this idea can be extended to an electric field, since it does not flip sign under a time reversal!

As seen earlier, since an electron accelerates away in an electric field, one uses neutral systems like atoms or molecules. What one looks for is the spin precession in an electric field, of an unpaired electron with an EDM, in the molecule. A magnetic field is usually applied too, but for experimental purposes (more like a 'carrier signal', and nothing to do with T violation detection), having to do with the ease of detecting a small change in

a large signal (electric and magnetic fields), than a small change in a small signal (only electric field). However, its effect is taken out by performing two measurements, one with an electric field, and another with the electric field flipped. Then, the difference between them is measured.

$$\begin{aligned} \omega_1 &= -\vec{\mu}\cdot\vec{B} - \vec{d}\cdot\vec{E} && (1.31)\\ \omega_2 &= -\vec{\mu}\cdot\vec{B} + \vec{d}\cdot\vec{E} && (1.32)\\ \Delta\omega &= \omega_2 - \omega_1 \\ &= 2\vec{d}\cdot\vec{E} && (1.33) \end{aligned}$$

Note that the constants involved in the expression (like $\hbar$) are not explicitly mentioned. Finally, we add a quick note on how electric and magnetic fields behave under P and T reversal.

Electric and magnetic fields under P and T reversal

A convenient way to think of an electric field, is a field line from a positive to a negative charge. P $\Rightarrow$ the origin just flips, and so the direction of the arrow for the field changes too. Hence, $\vec{E}$ is P-odd. For a magnetic field, such an approach is not useful, since we then need to think of a field line from one monopole to another, and we would want to avoid monopoles. A convenient way is to think of a current loop, and P $\Rightarrow$ a tangent to the loop on the left side pointing downward becomes a tangent to the loop on the right side pointing upward. Since the direction of rotation is preserved, as seen from this, $\vec{B}$ is P-even.

$$\begin{aligned} \vec{\nabla}\cdot\vec{E} &= \rho && (1.34)\\ \vec{\nabla}\times\vec{B} &= \frac{\partial\vec{E}}{\partial t} + \vec{J} && (1.35) \end{aligned}$$

All the constants have been omitted for simplicity. Since the Maxwell's equations are invariant under T (so the right and left hand sides must be the same when a time reversal is performed), and since ρ is T-even (charge is a scalar, and hence so is charge density), while J is T-odd (since $\vec{j} = \rho\vec{v}$, and the velocity reverses sign under T), we can see that $\vec{E}$ is T-even, while $\vec{B}$ is T-odd.

1.3 eEDM from molecules

The interaction Hamiltonian of a diatomic, due to the eEDM is given by [17]

$$\boldsymbol{H_{eEDM}} - d_e \sum_{i=1}^{N_e} \boldsymbol{\beta \sigma_i \cdot E_i^{intl}} \tag{1.36}$$

The internal electric field, $\boldsymbol{E_i^{intl}}$, experienced by an electron, is due to the two nuclei and all the other electrons in the molecule. N_e is the number of electrons in the molecule. The experimental quantity is the energy shift due to the effective electric field, and it is given by

$$\begin{aligned} \Delta E &= \langle\psi|\boldsymbol{H_{eEDM}}|\psi\rangle \\ &= -d_e \sum_{i=1}^{N_e} \langle\psi|\beta \boldsymbol{\sigma_i \cdot E_i^{intl}}|\psi\rangle \\ &= -d_e E_{eff} \end{aligned} \tag{1.37}$$

$$\therefore E_{eff} = \sum_{i=1}^{N_e} \langle\psi|\beta \boldsymbol{\sigma_i . E_i^{intl}}|\psi\rangle \tag{1.38}$$

E_{eff} has to be evaluated using many-body theory. Hence, the energy shift is measured in an experiment, while the effective electric field is calculated from theory. The ratio of these two quantities is the eEDM. In the equation above, $|\psi\rangle$ is to the wave function of a molecule in some state. Relativistic calculations are necessary, since non-relativistic calculations give zero E_{eff}.

The evaluation of the two-body term in the expression for the internal electric field is complicated. Hence, the following expression can be used [18]:

$$\begin{aligned} -d_e \sum_{i=1}^{N_e} \beta \boldsymbol{\sigma_i . E^{intl}} &= [-\frac{d_e}{e}\beta \boldsymbol{\sigma} \cdot \boldsymbol{\nabla}, \boldsymbol{H_0}] \\ &+ 2icd_e \sum_{i=1}^{N_e} \beta\gamma_5 \boldsymbol{p}^2 \end{aligned} \tag{1.39}$$

The index, 'i', gives the summation over the electronic coordinates, and $\boldsymbol{H_0}$ is the Dirac-Coulomb Hamiltonian, which is given by

$$\begin{aligned} \boldsymbol{H_0} &= \sum_i [c\boldsymbol{\alpha}.\boldsymbol{p_i} + \beta mc^2 - \sum_A \frac{Z_A}{|\boldsymbol{r_i} - \boldsymbol{r_A}|}] \\ &+ \sum_{i \neq j} \frac{1}{|\boldsymbol{r_i} - \boldsymbol{r_j}|} \end{aligned} \tag{1.40}$$

Again, the summation over the electronic coordinates is given by i, and that over the nuclear coordinates by A. The position vector from the origin to the site of an electron is given by $\boldsymbol{r_i}$, and $\boldsymbol{r_A}$ is that from the origin to a nucleus. The atomic number of the A^{th} nucleus is given by Z_A.

Using the above relation, it can be shown that:

$$E_{eff} = \frac{2ic}{e} \sum_{i=1}^{N_e} \langle \psi | \beta \gamma_5 \boldsymbol{p_i^2} | \psi \rangle \tag{1.41}$$

$\beta\gamma_5 \boldsymbol{p_i^2}$ is a one-body operator. This expression is easier to evaluate, due to the absence of two-body operators. The derivation for this expression is given in Appendix B. The appendix also explains why the non relativistic E_{eff} is zero.

The eEDM a CP violating property, which is in the domain of particle physics. The property is observed using experiments performed on an atom/molecule. This would be under atomic, molecular and optical physics. The calculation of E_{eff} requires knowledge and application of relativistic quantum chemistry. Hence, eEDM searches involve the synergy of three different fields, as well as a combination of theory and experiment.

Recently, molecules have been preferred over atoms. This is because in molecules, there is hybridization of the atomic orbitals, and the implication may be that the matrix elements of the effective eEDM operator between some orbitals may be large. The effective electric field depends the internal electric field in the molecule (of the order of MV/cm), but in atoms,the effective electric fields are a function of an external electric field, of the order of kV/cm.

From an experimental viewpoint, the energy shift of a molecular state due to eEDM is given by

$$\Delta E = -d_e E_{eff} \eta(E_{external}); \tag{1.42}$$

$$\eta(E_{external}) \quad \propto \quad \langle \hat{z} \cdot \hat{n} \rangle \tag{1.43}$$

Here, η is called the polarization factor, and it is defined as being proportional to the dot product of the z axis' unit vector, defined by the applied electric field, and the internuclear axis' unit vector, $\hat{n}$. In an ideal case, when this quantity is unity, then the molecule is said to be fully polarized. What it means is that the external field and the internuclear axis are along the same axis.

η can be obtained from experiment. Since the shift in energy due to an eEDM is measured from experiment too, and E_{eff} is computed from many-body theory (relativistic), a combination of all these is required to set an upper limit on eEDM.

The figure of merit for an eEDM experiment is given by (for example, refer [19]):

$$\delta d_e \sim \frac{1}{2\pi E_{eff}\sqrt{NT\tau}\eta} \tag{1.44}$$

N refers to the number of uncorrelated molecules. T refers to the total time, and τ to the coherence time of the state in which the molecule is prepared. Note that only the effective field and polarization factor come outside of the square root. However, the latter has a multiplicative factor that is less than one always. Therefore, a large effective field plays a vital role in enhancing the sensitivity of the experiment.

Polarization factor

The sensitivity of an eEDM experiment also depends on what is known as the polarizing electric field, E_{pol}. This is an indicator of how much one can polarize a molecule, that is, align it in the direction of an external electric field. The lower the value of the external field applied, for a given E_{eff}, the better the sensitivity is. The is given by 2B/D, where B is the rotational constant for a molecule, and D is the permanent electric dipole moment of the molecule (PDM). A sample calculation is given below, for HgF:

$$\begin{aligned} E_{pol} &= 2B/D \\ B &= \frac{\hbar}{4\pi\mu r^2} \\ \therefore B &= \frac{1.054 \times 10^{-34} \times 10^{-9}}{4 \times \pi \times \mu(2.00686 \times 10^{-10})^2 \times 1.675 \times 10^{-27}} \end{aligned}$$

$$= \quad 7.16GHz$$

The numerator basically contains the reduced Plank's constant (SI units), and the 10^{-9} is because the original expression for B has c in the denominator, which is 3×10^8, and when we convert B to GHz, we multiply B in SI units with 0.3, and hence $\frac{0.3}{3\times10^8}$ gives us a factor of 10^{-9}. In the denominator, we have 1.675×10^{-27} to convert from AMU to SI units (kg), the reduced mass. We, hence, obtain 7.162 GHz.

Now, to convert the resulting E_{pol} in terms of kV/cm, convert this energy unit to J, which gives us 4.75×10^{-24}, and D into SI, which gives us 8.7027×10^{-30}, hence the electric field, which is the ratio of an energy term and a dipole term, is 5.457 kV/cm.

Let us quickly see how we arrive at the expression for polarization factor:

Consider a diatomic molecule in a state, $|\psi_\alpha^0\rangle$. An external field, E (a perturbation; this is an important approximation), is applied. Therefore, the new wave function is:
$|\psi_\alpha\rangle = |\psi_\alpha^0\rangle + |\psi_\alpha^1\rangle + \cdots$
Let us evaluate: $\langle\psi_\alpha|\boldsymbol{D}\cdot\boldsymbol{E}|\psi_\alpha\rangle$, where D is the PDM of the molecule. Note that E is along z, and D along n. Then:

$$\langle\psi_\alpha|\boldsymbol{D}\cdot\boldsymbol{E}|\psi_\alpha\rangle = D^2E^2\sum_{m\neq\alpha} 2\frac{|\langle\psi_\alpha^0|\boldsymbol{n}\cdot\boldsymbol{z}|\psi_m^0\rangle|^2}{\Delta E} \tag{1.45}$$

$$\therefore \langle\psi_\alpha|\boldsymbol{n}\cdot\boldsymbol{z}|\psi_\alpha\rangle \equiv \eta = DE\sum_{m\neq\alpha}\frac{|\langle J=0|\boldsymbol{n}\cdot\boldsymbol{z}|J=1\rangle|^2}{B} \tag{1.46}$$

Only the rotational states contribute significantly, since $\Delta E \sim 1GHz$, whereas for vibrational states, $\Delta E \sim 10THz$, and it is $\sim 100THz$ for electronic states. Also, note that in the last equation above, only mixing between $J = 0$ and $J = 1$ states has been considered. The matrix elements between rotational states of same parity vanish, and higher states' mixings contribute lesser and lesser.

Finally, we note that for good sensitivity in the experiment, we need a good polarization factor, which depends on the PDM of the molecule, the reduced mass of the system, the bond length, the external field, and how well the molecule aligns with the external field.

A toy example

To get a feel for the numbers involved, let us assume a typical $\delta E \approx 200\mu Hz$ [20]. Since $\delta E = \delta d_e E_{eff}$, and since E_{eff} is usually $\sim 10^9$ V/cm, we immediately see that $\delta d_e \sim 8 \times 10^{-28}$ e cm (after converting Hz to eV, so that δd_e is in e cm). Now, if the

effective field is two orders larger, the sensitivity is better by two orders!

1.4 Summary

To summarize, we have discussed about the eEDM, and why it requires P and T symmetries to be violated simultaneously, along with a few other interesting details. We have also discussed why the eEDM is important. It helps in extending physics beyond SM, using a non-accelerator approach, and also provides insights in BAU. We also saw how obtaining eEDM requires a combination of both theory and experiment, and how this area of research connects particle physics, molecular physics, and many-body electronic structure calculations. We also defined the effective electric field, E_{eff}, and saw that it can only be calculated, using relativistic many-body theory. At the end of the chapter, we also briefly mentioned the role of polarization factor, and got a feel for the numbers that are involved in the experiment. Since we need to employ many-electron theory in our computations, the next chapter shall serve as an introduction to it.

BIBLIOGRAPHY

[1] T. Fukuyama, Searching for new physics beyond the standard model in electric dipole moment, International Journal of Modern Physics A, 27(16):1230015 (2012).

[2] T. Ibrahim, A. Itani, and P. Nath, Electron electric dipole moment as a sensitive probe of PeV scale physics, Phys. Rev. D, 90:055006, (2014).

[3] Y. Nagashima, Beyond the Standard Model of Elementary Particle Physics, Wiley-VCH (2014).

[4] L. Landau, On the conservation laws for weak interactions, Nuclear Physics, 3(1):127-131 (1957).

[5] L. E. Ballentine, Quantum mechanics: A modern development, World scientific publishing, Singapore (1998).

[6] G. Lauders, Proof of the TCP theorem, Annals of Physics, 281(1-2):1004-1018 (2000).

[7] E. R. Boston, Theory of Parity Non-Conservation in Atoms, PhD thesis, University of Oxford (1990).

[8] N. Fortson, P. Sandars, S. Barr, The search for a permanent electric dipole moment, Physics Today (2003).

[9] W. Bernreuther, M. Suzuki, The electric dipole moment of the electron. Rev. Mod. Phys., 63:225-226 (1991).

[10] J. Baron et al, Order of magnitude smaller limit on the electric dipole moment of the electron, Science, 343(6168):269-272 (2014).

[11] J. J. Hudson, D. M. Kara, I. J. Smallman, B. E. Sauer, M. R. Tarbutt, and E. A. Hinds, Improved measurement of the shape of the electron, Nature, 473(7348):493-496 (2011).

[12] W. B. Cairncross et al, A precision measurement of the electron's electric dipole moment using trapped molecular ions, arXiV 1704.07928 (2017).

[13] A. Kazarian, S. Kuzmin and M.E. Shaposhnikov, Cosmological lower bound on the EDM of the electron, Phys. Lett. B 276, 131 (1992).

[14] A.D. Sakharov, Violation of CP Invariance, C Asymmetry, and Baryon Asymmetry of the Universe, Pisma Zh.Eksp.Teor.Fiz., 5:32–35 (1967).

[15] H. S. Nataraj, Electric dipole moment of the electron and its implications on matter-antimatter asymmetry in the universe, PhD thesis, Indian Institute of Astrophysics (2009).

[16] Hunter L R., Tests of time-reversal invariance in atoms, molecules, and the neutron, Science, 252 (5002), 73-79 (1991).

[17] E. E. Salpeter, Some atomic effects of an electronic electric dipole moment, Phys. Rev., 112:1642-1648 (1958).

[18] B. P. Das, Aspects of many-body effects in molecules and extended systems, page 411 (1989).

[19] Titov et al, P,T-Parity Violation Effects in Polar Heavy-Atom Molecules, pages 253-284, Proceedings of the 9th European Workshop on Quantum Systems in Chemistry and Physics (QSCP-IX) held at Les Houches, France (2004), Edited by Julien, J.-P., Maruani, J., Mayou, D., Delgado-Barrio, G.

[20] A. C. Vutha, A search for the electric dipole moment of the electron using thorium oxide, url: $https://www.prl.res.in/\ bijaya/pcpv-tho.pdf$.

2

MANY-ELECTRON THEORY

2.1 Introduction

Many-electron theory refers to the class of problems in quantum mechanics that involve two or more electrons. In the present report, we shall be considering atoms or molecules, which are many-electron systems. Such systems, when treated relativistically, are described by what are called relativistic many-electron theories. These theories are useful in understanding and predicting the behaviour and properties of atoms and molecules. One such example with atoms or molecules would be finding the electric dipole moment of the electron. These theories typically involve approximations to the wave function of the atom or molecule one works with. Only the hydrogen atom has an exact analytical solution. Typically, we deal with larger atoms or molecules, and therefore make certain approximations, and then proceed to solve for the atom or molecule's wave function and other properties. These theories are also very compute intensive. This report aims to give a brief overview of some of these many-electron theories.

2.1.1 Born-Oppenheimer approximation

For us to solve electronic structure problems in molecules, we need to solve the Schroedinger's (or Dirac's) equation:

$$\boldsymbol{H'}(\vec{r},\vec{R})\psi(\vec{r},\vec{R}) = E'\psi(\vec{r},\vec{R}) \tag{2.1}$$

H' contains in it the kinetic energy of N electrons, the kinetic energy of M nuclei, the

electron-nucleus interaction potential, the nucleus-nucleus interaction potential, and finally, the electron-electron interaction potential term. We do not consider any external fields for the time being. We make our very first approximation in the choice of the potentials. Instead of QED terms, we simply use classical Coulombic interactions as a first approximation. This turns out to be a very good approximation in most cases. Only in rare cases, such as highly charged ions, for example, the higher order terms, such as the Breit terms may become important. Now, solving the Schroedinger's (Dirac's) equation is a tedious task, since it is a second order (or first, if it is the Dirac equation) differential equation, in 3M+3N coordinates. We now make another approximation, the Born-Oppenheimer approximation, where the idea is that the time scales of motions of the electrons and the nuclei are different, and since it is the electronic structure that we are interested in, we can only solve the electronic Schroedinger's equation, if we treat the slower species on a different timescale. The slow moving nuclei are 'frozen'. This can be understood by observing that the mass of a nucleon is about a thousand times higher than that of an electron, and hence the kinetic energy term of the former can be ignored. Mathematically, then, we are left with H', but without the nuclear kinetic energy term. This equation is called the electronic Schroedinger's equation. The nucleus-nucleus term is a constant now, since the nuclei are fixed, and clamped nuclei means a constant bond length, R.

The approximations in quantum chemistry are at two levels, at the Hamiltonian level, and at the wave function level. The classical potentials and the Born-Oppenheimer approximation are at the level of the former. At the level of wave functions, we know that only the H_2^+ molecular ion has an exact solution, so we eventually need to resort to approximations. There are various ways to solve for the wave function, and the nature of the various approximations depend on the approach taken to solve for the wave function.

2.1.2 Atomic units

We shall adopt atomic units in the computations, since it makes the equations more convenient. It sets $\hbar = m_e = e = 4\pi\epsilon_o = 1$. The Schroedinger and Dirac Hamiltonians then become, respectively:

$$\boldsymbol{H_{NR}} = -\frac{1}{2}\boldsymbol{\nabla^2} - \frac{Z}{\boldsymbol{r}} + \frac{1}{\boldsymbol{r_{ij}}} \tag{2.2}$$

$$\boldsymbol{H_{rel}} = c\boldsymbol{\alpha}\cdot\boldsymbol{p} + \beta c^2 - \frac{Z}{\boldsymbol{r}} + \frac{1}{\boldsymbol{r_{ij}}} \tag{2.3}$$

2.2 Hartree-Fock equations

The Hartree-Fock (HF) method is used to obtain the approximate ground state wave function of a many electron system. Before describing this method, we present the Rayleigh-Ritz variational principle, on which it is based. The variational principle is used to get an upper bound on the ground state energy of a system, with Hamiltonian $\boldsymbol{H}$.

$$\boldsymbol{H}|\Phi_n\rangle = E_n|\Phi_n\rangle \tag{2.4}$$

Consider a general wavefunction, $|\psi\rangle = \sum_i C_i|\Phi_i\rangle$, with the normalization $|C_0|^2 + |C_1|^2 + \cdots = 1$. Let $\varepsilon = \langle\psi|\boldsymbol{H}|\psi\rangle = \langle\boldsymbol{H}\rangle$. Therefore,

$$\begin{aligned} \varepsilon &= \langle\psi|\boldsymbol{H}|\psi\rangle \\ &= \sum_{i,j} C_i^* C_j \langle\Phi_i|\boldsymbol{H}|\Phi_j\rangle \\ &= \sum_{i,j} C_i^* C_j E_j \delta_{ij} \end{aligned} \tag{2.5}$$

If $C_i, C_j \in \Re$, then

$$\begin{aligned} \varepsilon &= \sum_i |C_i|^2 E_i \\ &= |C_0|^2 E_0 + |C_1|^2 E_1 + \ldots \end{aligned} \tag{2.6}$$

Now,

$$\begin{aligned} \varepsilon &\geq |C_0|^2 E_0 + |C_1|^2 E_0 + \ldots \\ &= (|C_0|^2 + |C_1|^2 + \ldots) E_0 \end{aligned} \tag{2.7}$$

But, $|C_0|^2 + |C_1|^2 + \cdots = 1$, and hence

$$\varepsilon \geq E_0. \tag{2.8}$$

Here, ε will be the energy functional, and E_0 the ground state energy. $\langle \boldsymbol{H} \rangle$ is an overestimate of E_0, since if ψ happens to be one of the excited states, then obviously $\langle \boldsymbol{H} \rangle > E_0$.

For an N electron atom,

$$\begin{aligned} \boldsymbol{H} &= -\hbar^2/2m \sum_{i=1}^{n} \boldsymbol{\nabla_i^2} + \boldsymbol{V^{Nuclear}(r_i)} + \sum_{i>j} e^2/\boldsymbol{r_{ij}} \\ &= \sum_i \boldsymbol{t_i} + \sum_{i>j} \boldsymbol{v_{ij}} \end{aligned} \tag{2.9}$$

The approximate ground state wave function, $|\Phi_0\rangle$, can be written in terms of a Slater determinant:

$$|\Phi_0\rangle = \frac{1}{\sqrt{N!}} \begin{vmatrix} \phi_a(1) & \phi_a(2) & \cdots & \phi_a(n) \\ \phi_b(1) & \phi_b(2) & \cdots & \phi_b(n) \\ & & \cdot & \\ & & \cdot & \\ & & \cdot & \end{vmatrix} \tag{2.10}$$

Here, φ_a, φ_b, etc are the wave functions of single electrons, and they are referred to as orbitals. Note that terms as a function of both i and j coordinates are present in $\boldsymbol{H}$ but not in $|\Phi_0\rangle$. The variational principle is applied by constructing the energy functional given below, and minimizing it with respect to the individual orbitals. Let us first consider:

$$\begin{aligned} \varepsilon &= \langle \Phi_0 | \boldsymbol{H} | \Phi_0 \rangle \\ &= \sum_a \langle \varphi_a(1) | \boldsymbol{t(1)} | \varphi_a(1) \rangle + \sum_{a \neq b} \langle \varphi_a(1)\varphi_b(2) | \boldsymbol{v(1,2)} | \varphi_a(1)\varphi_b(2) \rangle \\ &- \sum_{a \neq b} \langle \varphi_a(1)\varphi_b(2) | \boldsymbol{v(1,2)} | \varphi_b(1)\varphi_a(2) \rangle \\ &= \sum_{a \neq c} \langle \varphi_a(1) | \boldsymbol{t(1)} | \varphi_a(1) \rangle + \langle \varphi_c(1) | \boldsymbol{t(1)} | \varphi_c(1) \rangle \\ &+ \sum_{a \neq b, a \neq c} \langle \varphi_a(1)\varphi_b(2) | \boldsymbol{v(1,2)} | \varphi_a(1)\varphi_b(2) \rangle \\ &- \sum_{a \neq b, a \neq c} \langle \varphi_a(1)\varphi_b(2) | \boldsymbol{v(1,2)} | \varphi_b(1)\varphi_a(2) \rangle \\ &+ \sum_b \langle \varphi_c(1)\varphi_b(2) | \boldsymbol{v(1,2)} | \varphi_c(1)\varphi_b(2) \rangle \end{aligned}$$

$$- \sum_b \langle \varphi_c(1)\varphi_b(2)|\boldsymbol{v(1,2)}|\varphi_b(1)\varphi_c(2)\rangle \tag{2.11}$$

The second line of the equation is obtained by using the Slater-Condon rules. It is used to evaluate the matrix elements for determinantal states, for one and two particle operators [1]. When $\varphi_c \longrightarrow \varphi_c + \delta\varphi_c$, $\varepsilon \longrightarrow \varepsilon + \delta\varepsilon$. Therefore,

$$\begin{aligned}
\varepsilon + \delta\varepsilon &= \sum_{a\neq c} \langle \varphi_a(1)|\boldsymbol{t(1)}|\varphi_a(1)\rangle + \langle \delta\varphi_c(1)|\boldsymbol{t(1)}|\varphi_c(1)\rangle \\
&+ \langle \varphi_c(1)|\boldsymbol{t(1)}|\delta\varphi_c(1)\rangle + \sum_{a\neq b, a\neq c} \langle \varphi_a(1)\varphi_b(2)|\boldsymbol{v(1,2)}|\varphi_a(1)\varphi_b(2)\rangle \\
&- \sum_{a\neq b, a\neq c} \langle \varphi_a(1)\varphi_b(2)|\boldsymbol{v(1,2)}|\varphi_b(1)\varphi_a(2)\rangle \\
&+ \sum_b \langle \delta\varphi_c(1)\varphi_b(2)|\boldsymbol{v(1,2)}|\varphi_c(1)\varphi_b(2)\rangle \\
&- \sum_b \langle \delta\varphi_c(1)\varphi_b(2)|\boldsymbol{v(1,2)}|\varphi_b(1)\varphi_c(2)\rangle \\
&+ \sum_b \langle \varphi_c(1)\varphi_b(2)|\boldsymbol{v(1,2)}|\delta\varphi_c(1)\varphi_b(2)\rangle \\
&- \sum_b \langle \varphi_c(1)\varphi_b(2)|\boldsymbol{v(1,2)}|\delta\varphi_b(1)\varphi_c(2)\rangle
\end{aligned} \tag{2.12}$$

Only the terms that are linear in $\delta\varphi_c$ are retained. Now,

$$\delta\varepsilon = (\varepsilon + \delta\varepsilon) - \varepsilon \tag{2.13}$$

$$\begin{aligned}
&= \langle \delta\varphi_c(1)|\boldsymbol{t(1)}|\varphi_c(1)\rangle + \langle \varphi_c(1)|\boldsymbol{t(1)}|\delta\varphi_c(1)\rangle \\
&+ \sum_b \langle \delta\varphi_c(1)\varphi_b(2)|\boldsymbol{v(1,2)}|\varphi_c(1)\varphi_b(2)\rangle \\
&- \sum_b \langle \delta\varphi_c(1)\varphi_b(2)|\boldsymbol{v(1,2)}|\varphi_b(1)\varphi_c(2)\rangle \\
&+ \sum_b \langle \varphi_c(1)\varphi_b(2)|\boldsymbol{v(1,2)}|\delta\varphi_c(1)\varphi_b(2)\rangle \\
&- \sum_b \langle \varphi_c(1)\varphi_b(2)|\boldsymbol{v(1,2)}|\delta\varphi_b(1)\varphi_c(2)\rangle
\end{aligned} \tag{2.14}$$

In order to apply the variational principle, a new energy functional is constructed, which is given by:

$$\varepsilon' = \varepsilon - \sum_a \epsilon_a \langle \varphi_a | \varphi_a \rangle \tag{2.15}$$

In the above equation, ϵ_as are Lagrange multipliers, which are introduced to enforce the normalization of the orbital, φ_a. Varying φ_c, we get:

$$\delta\varepsilon' = \delta\varepsilon - \epsilon_c(\langle \delta\varphi_c | \varphi_c \rangle + \langle \varphi_c | \delta\varphi_c \rangle) \tag{2.16}$$

That is,

$$\begin{aligned}
\delta\varepsilon' &= (\langle \delta\varphi_c(1) | \boldsymbol{t(1)} | \varphi_c(1) \rangle - \epsilon_c \langle \delta\varphi_c | \varphi_c \rangle \\
&+ \sum_b \langle \delta\varphi_c(1)\varphi_b(2) | \boldsymbol{v(1,2)} | \varphi_c(1)\varphi_b(2) \rangle \\
&- \sum_b \langle \delta\varphi_c(1)\varphi_b(2) | \boldsymbol{v(1,2)} | \varphi_b(1)\varphi_c(2) \rangle) \\
&+ (\langle \varphi_c(1) | \boldsymbol{t(1)} | \delta\varphi_c(1) \rangle - \epsilon_c \langle \varphi_c | \delta\varphi_c \rangle \\
&+ \sum_b \langle \varphi_c(1)\varphi_b(2) | \boldsymbol{v(1,2)} | \delta\varphi_c(1)\varphi_b(2) \rangle \\
&- \sum_b \langle \varphi_c(1)\varphi_b(2) | \boldsymbol{v(1,2)} | \varphi_b(1)\delta\varphi_c(2) \rangle)
\end{aligned} \tag{2.17}$$

According to the variational principle, since $\delta\varepsilon' = 0$, and also since $|\delta\varphi_c\rangle \neq 0$ and $\langle \delta\varphi_c | \neq 0$, we get:

$$\begin{aligned}
&\boldsymbol{t(1)} | \varphi_c(1) \rangle \\
&+ \sum_b \langle \varphi_b(2) | \boldsymbol{v(1,2)} | \varphi_b(2) \rangle | \varphi_c(1) \rangle \\
&- \sum_b \langle \varphi_b(2) | \boldsymbol{v(1,2)} | \varphi_c(2) \rangle | \varphi_b(1) \rangle &= \epsilon_c | \varphi_c \rangle
\end{aligned} \tag{2.18}$$

$$\begin{aligned}
&\langle \varphi_c(1) | \boldsymbol{t(1)} \\
&+ \sum_b \langle \varphi_c(1) | \langle \varphi_b(2) | \boldsymbol{v(1,2)} | \varphi_b(2) \rangle \\
&- \sum_b \langle \varphi_c(1) | \langle \varphi_b(2) | \boldsymbol{v(1,2)} | \varphi_b(1) \rangle &= \epsilon_c \langle \varphi_c |
\end{aligned} \tag{2.19}$$

The above set of coupled equations are called the Hartree-Fock equations. It is important to note that there is one equation for each orbital.

Note that the HF approach assumes that one Slater Determinant is sufficient to describe a wave function of a many-body system. This is not true always, for example, in systems with, say, two unpaired π electrons, the singlet π, the singlet π^*, and the triplet $\pi\pi^*$ corresponding to m=1 and -1 can be represented as a single determinant, whereas that corresponding to m=0 requires two such determinants. In this thesis, only those systems with one unpaired electron are considered. Therefore, the HF method is a good approximation.

2.2.1 Interpretation of the Hartree-Fock equations

The equations are interpreted using the information that the potential, $\phi(\vec{r})$, experienced by a particle at a point P, due to a charge distribution, whose charge density is $\rho(\vec{r})$, is given by:

$$\phi(\vec{r}) = \frac{\int \rho(\vec{r}')d\tau'}{|\vec{r} - \vec{r}'|} \tag{2.20}$$

where $d\tau$ is the three dimensional volume element at $\vec{r}'$, and $\vec{r}$ is the distance from the origin to the point P.

Also, one uses the fact that for a physical system with wavefunction $\psi(\vec{r})$ and with charge q, the charge density is given by:

$$\rho(\vec{r}) = q\psi^*(\vec{r})\psi(\vec{r}) \tag{2.21}$$

where $\psi^*(\vec{r})\psi(\vec{r})$ is the probability density of the system.

Now, with the above information, and substituting $\boldsymbol{v(1,2)} = \frac{e^2}{\boldsymbol{r_{12}}}$, one can interpret the Hartree Fock equations as follows:

$$\begin{aligned} & \boldsymbol{t(1)}\varphi_c(1) \\ + \sum_b \int_{r_2} & \varphi_b^*(2)\frac{e^2}{r_{12}}\varphi_b(2)d^3\vec{r}_2\varphi_c(1) \\ - \sum_b \int_{r_2} & \varphi_b^*(2)\frac{e^2}{r_{12}}\varphi_c(2)d^3\vec{r}_2\varphi_b(1) \quad = \quad \epsilon_c\varphi_c \end{aligned}$$

$$\begin{aligned}
&\boldsymbol{t(1)}\varphi_c(1) \\
&+\sum_{b\neq c}\int_{r_2}\varphi_b^*(2)\frac{e^2}{r_{12}}\varphi_b(2)d^3\vec{r}_2\varphi_c(1) \\
&-\sum_{b\neq c}\int_{r_2}\varphi_b^*(2)\frac{e^2}{r_{12}}\varphi_c(2)d^3\vec{r}_2\varphi_b(1) \\
&+\int_{r_2}\varphi_c^*(2)\frac{e^2}{r_{12}}\varphi_c(2)d^3\vec{r}_2\varphi_c(1) \\
&-\int_{r_2}\varphi_c^*(2)\frac{e^2}{r_{12}}\varphi_c(2)d^3\vec{r}_2\varphi_c(1) \quad = \quad \epsilon_c\varphi_c
\end{aligned}$$

$$\begin{aligned}
&\boldsymbol{t(1)}\varphi_c(1) \\
&+\sum_{b\neq c}\int_{r_2}\varphi_b^*(2)\frac{e^2}{r_{12}}\varphi_b(2)d^3\vec{r}_2\varphi_c(1) \\
&-\sum_{b\neq c}\int_{r_2}\varphi_b^*(2)\frac{e^2}{r_{12}}\varphi_c(2)d^3\vec{r}_2\varphi_b(1) \quad = \quad \epsilon_c\varphi_c
\end{aligned}$$

Now, $\frac{e\varphi_b^*(2)\varphi_b(2)}{r_{12}}$ is $\frac{\rho_b(2)}{r_{12}}$, and its integral over r_2 would be the potential, $\phi_b(r_1)$, and hence the Hartree-Fock equations become:

$$\begin{aligned}
&\boldsymbol{t(1)}\varphi_c(1)+\sum_{b\neq c}eU_b(1)\varphi_c(1) \\
&-\sum_{b\neq c}\int_{r_2}\varphi_b^*(2)\frac{e^2}{r_{12}}\varphi_c(2)d^3\vec{r}_2\varphi_b(1) \quad = \quad \epsilon_c\varphi_c; \\
&U_b(1) \quad = \quad \int_{r_2}\frac{\rho_b(2)}{r_{12}}d^3\vec{r}_2 \qquad (2.22)
\end{aligned}$$

In the second term, $\sum_{b\neq c}eU_b(\vec{r}_1)$ is the potential energy of the electron in coordinate 1 and state c, due to $(N-1)$ electrons' charge distribution, in coordinate 2. There are a total of N such equations for the N electrons. So, the Hartree Fock equations can be rewritten as:

$$\boldsymbol{t(1)}\varphi_c(1)+\boldsymbol{V_{direct}}\varphi_c(1)-\boldsymbol{V_{exchange}}\varphi_b(1) \quad = \quad \epsilon_c\varphi_c$$

It is to be noted that the direct term appears even if the trial wavefunction is a simple product, that is, the trial wavefunction is not antisymmetrized. It is also to be noted that the exchange term doesn't have a classical counterpart, it is a purely quantum effect.

To solve the Hartree Fock equations, one guesses $\varphi_c(2)$, solve for $\varphi_c(1)$, substitute it back into the integral, and continue doing this till the solution converges. However, note that one only solves for the approximate wavefunction here. This is because although the Hamiltonian takes into account the electron-electron interaction, the trial wavefunction, namely the Slater determinant, doesn't! However, it turns out that if one takes a linear combination of the Slater determinants, one obtains the exact wavefunction of the system.

2.2.2 Relativistic Hartree-Fock(Dirac-Fock) equations

When one uses the relativistic Hamiltonian; ie, the Dirac-Coulomb Hamiltonian, H takes the form:

$\boldsymbol{H} = \sum_i \{c\boldsymbol{\alpha_i}.\boldsymbol{p_i} + \beta c^2 + \boldsymbol{V_i^{Nuclear}}\} + \sum_{i>j} 1/\boldsymbol{r_{ij}}$,

and an orbital (single particle wave function) for the relativistic case can be expressed as:

$$\varphi = \begin{pmatrix} \varphi_1 \\ \varphi_2 \\ \varphi_3 \\ \varphi_4 \end{pmatrix} = \begin{pmatrix} v \\ w \end{pmatrix} = \begin{pmatrix} g(r)\chi_{\kappa m} \\ if(r)\chi_{-\kappa m} \end{pmatrix}; \tag{2.23}$$

where $g(r)$ and $f(r)$ are the large and small components of the wave function, and $\chi_{\kappa m}$ represents a spin angular function of J^2, J_Z, L^2, and S^2, and is given by:

$$\chi_{\kappa m} = \sqrt{\frac{l+m+\frac{1}{2}}{2l+1}} Y_{lm-\frac{1}{2}} \begin{pmatrix} 1 \\ 0 \end{pmatrix} + \sqrt{\frac{l-m+\frac{1}{2}}{2l+1}} Y_{lm+\frac{1}{2}} \begin{pmatrix} 0 \\ 1 \end{pmatrix}; l = j - \frac{1}{2} \tag{2.24}$$

$$\chi_{-\kappa m} = -\sqrt{\frac{l-m+\frac{1}{2}}{2l+1}} Y_{lm-\frac{1}{2}} \begin{pmatrix} 1 \\ 0 \end{pmatrix} + \sqrt{\frac{l+m+\frac{1}{2}}{2l+1}} Y_{lm+\frac{1}{2}} \begin{pmatrix} 0 \\ 1 \end{pmatrix}; l = j + \frac{1}{2} \tag{2.25}$$

instead of the usual non-relativistic one, the same calculations as shown above repeats with the changed Hamiltonian, and the resulting set of equations are called Dirac-Fock (DF) equations. These equations are used for relativistic calculations. In the above set of

equations,

$$\begin{aligned} \kappa &= -(l+1), forj = l + \frac{1}{2} \\ &= l, forj = l - \frac{1}{2} \end{aligned} \tag{2.26}$$

Mathematically, the orbitals are now four-component spinors.

2.2.3 Matrix formulation of Hartree-Fock/Dirac-Fock equations

The mean field equations, i.e HF/DF can be expressed as:

$$\boldsymbol{t}|\varphi_c\rangle + \boldsymbol{V_{DF}}|\varphi_c\rangle = E_c|\varphi_c\rangle; \tag{2.27}$$

$$\begin{aligned} \boldsymbol{V_{DF}}|\varphi_c\rangle &= \sum_{b=1}^{N_c}\langle\varphi_b|\boldsymbol{v}|\varphi_b\rangle|\varphi_c\rangle \\ &- \sum_{b=1}^{N_c}\langle\varphi_b|\boldsymbol{v}|\varphi_c\rangle|\varphi_b\rangle \end{aligned} \tag{2.28}$$

Here, $\boldsymbol{V_{DF}}$ is the HF/DF potential and N_c refers to the number of core orbitals. Note that the summation is over N_c, and not $N_c - 1$. Both the former and the latter would be the same, since when $b = c$, the second and third terms on the right hand side of $\boldsymbol{V_{DF}}$ cancel out. Also, the coordinates are left out just for simplicity of writing down the equations, they are very much present. The above set of equations are for the core. Let $|\varphi_p\rangle$ be a virtual orbital. Then:

$$\boldsymbol{t}|\varphi_p\rangle + \boldsymbol{V_{DF}}|\varphi_p\rangle = E_p|\varphi_p\rangle; \tag{2.29}$$

$$\begin{aligned} \boldsymbol{V_{DF}}|\varphi_p\rangle &= \sum_{b=1}^{N_c}\langle\varphi_b|\boldsymbol{v}|\varphi_b\rangle|\varphi_p\rangle \\ &- \sum_{b=1}^{N_c}\langle\varphi_b|\boldsymbol{v}|\varphi_p\rangle|\varphi_b\rangle \end{aligned} \tag{2.30}$$

$\boldsymbol{V_{DF}}$, in this case, is a V^{N-1} potential, that is, an electron sees a mean potential due to the other $N - 1$ electrons, as discussed earlier.

It is possible to combine the two equations into a single equation:

$$\boldsymbol{t}|\varphi_i\rangle + \boldsymbol{V_{DF}}|\varphi_i\rangle = E_i|\varphi_i\rangle; \tag{2.31}$$

$$\begin{aligned} \boldsymbol{V_{DF}}|\varphi_i\rangle &= \sum_{b=1}^{N_c}\langle\varphi_b|\boldsymbol{v}|\varphi_b\rangle|\varphi_i\rangle \\ &- \sum_{b=1}^{N_c}\langle\varphi_b|\boldsymbol{v}|\varphi_i\rangle|\varphi_b\rangle \end{aligned} \tag{2.32}$$

Here, $|\varphi_i\rangle$ is a general orbital. Now, we want to solve the above equation. Let $\boldsymbol{F} \equiv \boldsymbol{t} + \boldsymbol{V_{DF}}$. Then:

$$\begin{aligned} \boldsymbol{F}|\varphi_i\rangle &= E_i|\varphi_i\rangle && (2.33)\\ Let\ |\varphi_i\rangle &= \sum_n C_{in}|\chi_n\rangle && (2.34)\\ \therefore \sum_n \langle\chi_m|\boldsymbol{F}|\chi_n\rangle C_{in} &= E_i \sum_n C_{in}\langle\chi_m|\chi_n\rangle && (2.35)\\ \sum_n F_{mn}C_{in} &= E_i \sum_n S_{mn}C_{in}; S_{mn} = \langle\chi_m|\chi_n\rangle && (2.36)\\ \boldsymbol{F}C &= ESC && (2.37)\\ \boldsymbol{F}S^{-1/2}S^{1/2}C &= ES^{1/2}S^{1/2}C \\ \boldsymbol{F}S^{-1/2}C' &= ES^{1/2}C' \\ S^{-1/2}\boldsymbol{F}S^{-1/2}C' &= EC' \\ \boldsymbol{F'}C' &= EC'; \boldsymbol{F'} = S^{-1/2}\boldsymbol{F}S^{-1/2} && (2.38) \end{aligned}$$

The above equation is an eigenvalue equation. The unknown is C'. One solves the above equation to get C' and hence C. Now, one needs to construct $\boldsymbol{F}$.

$$\begin{aligned} \boldsymbol{F} &= \boldsymbol{t} + \boldsymbol{V_{DF}} \\ F_{mn} &= t_{mn} + (V_{DF})_{mn} && (2.39)\\ t_{mn} &= \langle\chi_m|\boldsymbol{t}|\chi_n\rangle && (2.40)\\ (V_{DF})_{mn} &= \langle\chi_m|\boldsymbol{V_{DF}}|\chi_n\rangle && (2.41) \end{aligned}$$

Now,

$$\begin{aligned}
\boldsymbol{V_{DF}}|\varphi_i\rangle &= \sum_{b=1}^{N_c}\langle\varphi_b|\boldsymbol{v}|\varphi_b\rangle|\varphi_i\rangle - \sum_{b=1}^{N_c}\langle\varphi_b|\boldsymbol{v}|\varphi_i\rangle|\varphi_b\rangle \\
|\varphi_i\rangle &= \sum_n C_{in}|\chi_n\rangle \qquad (2.42)\\
|\varphi_b\rangle &= \sum_k C_{bk}|\chi_k\rangle \qquad (2.43)
\end{aligned}$$

This gives:

$$\begin{aligned}
\boldsymbol{V_{DF}}\sum_n C_{in}|\chi_n\rangle &= \sum_{b=1}^{N_c}(\sum_{kln} C^*_{bk}C_{bl}\langle\chi_k|\boldsymbol{v}|\chi_l\rangle C_{in}|\chi_n\rangle \\
&- \sum_{kln} C^*_{bk}C_{bl}\langle\chi_k|\boldsymbol{v}|\chi_n\rangle C_{in}|\chi_l\rangle) \qquad (2.44)
\end{aligned}$$

For a given value of i,

$$\begin{aligned}
\sum_n\langle\chi_m|\boldsymbol{V_{DF}}|\chi_n\rangle C_n &= \sum_{b=1}^{N_c}(\sum_{kln} C_nC^*_{bk}C_{bl}\langle\chi_m\chi_k|\boldsymbol{v}|\chi_l\chi_n\rangle \\
&- \sum_{b=1}^{N_c}(\sum_{kln} C_nC^*_{bk}C_{bl}\langle\chi_m\chi_k|\boldsymbol{v}|\chi_n\chi_l\rangle) \qquad (2.45)
\end{aligned}$$

For a given n,

$$\begin{aligned}
\langle\chi_m|\boldsymbol{V_{DF}}|\chi_n\rangle &= \sum_{b=1}^{N_c}(\sum_{kl} C^*_{bk}C_{bl}[\langle mk|\boldsymbol{v}|ln\rangle - \langle mk|\boldsymbol{v}|nl\rangle]) \qquad (2.46)\\
&= \sum_{kl} P_{kl}[\langle mk|\boldsymbol{v}|ln\rangle - \langle mk|\boldsymbol{v}|nl\rangle]; \qquad (2.47)
\end{aligned}$$

where

$$m = \chi_m, k = \chi_k,\ etc,\ and\ P_{kl} = \sum_b C^*_{bk}C_{bl}$$

P_{kl} is called the density matrix.

For the relativistic case,

$$\varphi_i = \begin{pmatrix} \varphi_{large} \\ \varphi_{small} \end{pmatrix} \tag{2.48}$$

For each of these components, one solves for the coefficients. That means that if there are N coefficients for the non-relativistic case, then there would be 2N coefficients for the relativistic case.

So, if one knows the χs, the matrix elements of t, $\boldsymbol{V_{DF}}$, $\boldsymbol{F}$, S and $\boldsymbol{F'}$ can be constructed. We now consider the form of χ:

$$\chi_k(r) \propto r^{n_k} e^{-\zeta_k r^2} \tag{2.49}$$

For example,

$$\varphi_i(r) = \sum_{k=1}^{N} C_{ik}\chi_k(r) \tag{2.50}$$

$$\therefore \varphi_i(r) = \sum_{k=1}^{N} C_{ik}\chi_k(r) \propto \sum_{k=1}^{N} C_{ik} r^{n_k} e^{-\zeta_k r^2} \tag{2.51}$$

The χs are called basis sets, and must be chosen by us, to give as an input to the code/ program, from a suitable database. ζ decides the 'width' of the orbital. For example, a small ζ gives a diffuse function, while a large one a tight function. The former is useful to account for far nuclear region properties, while the latter for near-nuclear regions. The basis sets must be kinetically balanced, i.e., the large and small components should satisfy a proper relationship. [2] The relation is as follows:

$$\varphi_p^L = \sum_i C_i^L \chi_i^L \tag{2.52}$$

$$\varphi_p^S = \sum_i C_i^S \chi_i^S \tag{2.53}$$

$$\chi^L = (constant)(\frac{d}{dr} + \frac{\kappa}{r})\chi^S \tag{2.54}$$

The superscripts, 'L' and 'S', refer to the large and small components, respectively. We

shall shortly discuss why kinetic balance is necessary:

When one uses finite basis sets for calculations (of properties like energy, for example), a common problem that is encountered is that of variational collapse. What this means is that because the Dirac equation admits negative continuum in its spectrum, during numerical computations of a bound state, single particle state can have very large negative energy. When one employs the kinetic balance condition, it ensures that there is no variational collapse, but with errors of the order of c^{-4} for the total DF energy [3]. Also, kinetic balance first ensures that the kinetic energy is properly represented in the non-relativistic limit [2].

Lastly, we shall discuss the form of χ. The form written above is called a Gaussian Type Orbital (GTO). Another alternative is to use Slater Type Orbitals (STOs). They fall as $e^{-}\zeta_k r$, and this is closer to the actual hydrogenic wave function. However, computing molecular matrix elements is far harder than in the case of GTOs, since the latter satisfy the Gaussian Product Theorem, which tells us that the product of two Gaussians (while evaluating matrix elements, we either encounter two or four of the GTOs, depending on whether we want to evaluate one or two electron integrals) gives another Gaussian (with some other centre) [4]. This means that for a two electron integral, which has four centres (and hence is also called a four-centre integral), we can apply the product theorem and reduce it to a two-centre integral. This greatly simplifies the matrix elements, thereby saving a lot of computational time and effort. Also, one can use a linear combination of GTOs to mimic an STO! Due to these two major reasons, GTOs are preferred nowadays.

The GTOs can be either centred around nuclei (atom-centred), or somewhere along the bond length. We use the former. If an atomic orbital is described by one basis function, it is called a minimal basis. If we use two functions to describe an orbital, it is called a double zeta (DZ) basis, three is called triple zeta (TZ), and so on. For example, the carbon atom has 5 orbitals, so a minimal basis has 5 functions, DZ has 10, and so on. QZ sets are generally more accurate than TZ, and TZ more than DZ sets. However, the accuracy comes at heavy computational cost. If the finite basis sets are expanded sufficiently, and if they approach towards an infinite set of complete functions, it is referred to as approaching the basis set limit. Computational complexity severely limits going beyond QZ basis sets for fairly large molecules. An orbital in a molecule can get polarized (get shifted) in the presence of another orbital, for example, an s orbital can get polarized by p, etc. Those functions that polarize orbitals in an atom are called polarizing functions. Dunning et al realized that basis sets prepared by optimizing them at the HF level may be insufficient for correlation calculations. Those sets that are optimized using a correlated scheme, like CI, are called correlation consistent sets. Also, since valence electrons play the major role in chemistry,

only valence valence correlations are considered, while obtaining basis sets. If all these factors are put into basis sets, they are called cc-pVNZ (correlation consistent, polarized, valence N zeta, where N can stand for double, triple, etc). If diffuse functions are added, a prefix, 'aug' is added. Diffuse functions have very small values of ζ, which means that the Gaussian decays slower, that is, it accounts for regions far away from the nucleus (the 'tail' regions of an atomic orbital). This is particularly useful when we evaluate properties that are sensitive to the far-nuclear region. Most of the above discussions on basis sets can be found in several resources online, especially Ref.s [5, 6]

2.2.4 Dirac-Fock energy calculations for some atoms

The DF energies of some atoms were calculated using the GRASP2 (General Purpose Relativistic Atomic Structure Program 2) code. [7] The DF energy is given by :

$$\begin{aligned} E_{DF} &= \langle \Phi_0 | \boldsymbol{H} | \Phi_0 \rangle \\ &= \sum_a \langle \varphi_a(1) | \boldsymbol{t(1)} | \varphi_a(1) \rangle + \sum_{a \neq b} \langle \varphi_a(1)\varphi_b(2) | \boldsymbol{v(1,2)} | \varphi_a(1)\varphi_b(2) \rangle \\ &- \sum_{a \neq b} \langle \varphi_a(1)\varphi_b(2) | \boldsymbol{v(1,2)} | \varphi_b(1)\varphi_a(2) \rangle \end{aligned} \tag{2.55}$$

Here, H is the Dirac-Coulomb Hamiltonian, and the Φ_0 is built out of four-component single particle wave functions, φ_i. φ_a and φ_b refer to the occupied orbitals.

We calculated the energies of the following atoms:

The first column gives the atomic number of the atom. The second column gives the names of the atoms chosen. The third column gives the DF energies calculated using GRASP (in au). The fourth column gives the HF energies (in au) [8, 9]. The last column gives the difference between the HF and the DF energies. Note that as the atomic number increases, the difference in the energy $E_{DF} - E_{HF}$ increases substantially. This is because as the atomic number increases, the nuclear charge increases. Hence, the electrons have to move faster. The higher the velocity of an object, the more the relativistic effects. The trend in the previous table illustrates the same. Figure 1 shows atomic number (Z) versus the difference in the energy $E_{DF} - E_{HF}$

The above table gives the atomic number and the name of the elements, and the expectation values of the 1s and the 2s orbitals (in au). Note that for a given element, the former is lesser than the latter. This can be explained by the fact that the inner orbital electrons

Table 2.1

Z	$Element$	E_{DF}	E_{HF}	$E_{DF} - E_{HF}$	$\frac{E_{DF}-E_{HF}}{E_{DF}} \times 100$
4	Be	-14.57589	-14.57302	-2.87×10^{-3}	0.02
5	B	-24.53661	-24.52906	-7.55×10^{-3}	0.03
10	Ne	-128.69193	-128.54710	-0.14483	0.11
12	Mg	-199.93480	-199.61463	-0.32017	0.16
13	Al	-242.33112	-241.87671	-0.45441	0.19
18	Ar	-528.63762	526.81751	-1.82011	0.34
20	Ca	-679.71015	-676.75818	-2.95197	0.43
31	Ga	-1942.56614	-1923.26100	-19.30514	0.99
36	Kr	-2788.86060	-2752.05500	-36.80560	1.32
38	Sr	-3178.07998	-3131.54570	-46.53478	1.46
49	In	-5880.43779	-5740.16910	-140.26869	2.38
54	Xe	-7446.89516	-7232.1384	-214.75676	2.88
56	Ba	-8135.64446	-7883.54380	-252.10066	3.09
70	Yb	-14067.67141	-13391.45600	-676.21541	4.81
80	Hg	-19468.87432	-18408.99100	-1239.88332	5.44
81	Tl	-20269.38272	-18961.82500	-1307.55772	6.45

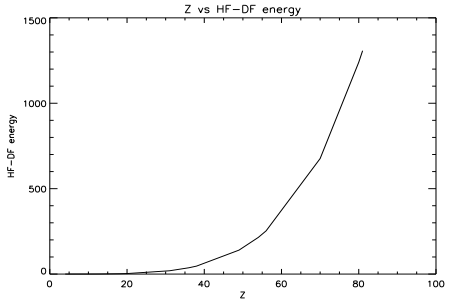

Figure 2.1: Z vs difference between DF and HF energies

experience more nuclear charge, and hence more attraction, due to which the electrons move faster. Hence, the inner electrons have more pronounced relativistic effects than the outer ones. This means that they would experience more length contraction than the outer electrons.

This can also be understood in the following way: when the velocity of an inner electron in the vicinity of a nucleus increases, so does its rest mass. The average distance of an electron from the nucleus is the inverse of the rest mass (the Bohr radius is inversely proportional to the mass of the electron), and hence the orbital contracts. The outer orbitals then "fall down" towards the contracted inner ones, and hence they too are contracted. In fact, mercury being a liquid can be explained using this effect. Since the 6s orbital contracts, it mimics a closed shell, and hence less reactivity, and therefore, the weak Vander-Waal

Table 2.2

Z	$Element$	$\langle r \rangle_{1s}$	$\langle r \rangle_{2s}$
4	Be	4.1×10^{-1}	2.64
5	B	3.25×10^{-1}	1.97
10	Ne	1.5×10^{-1}	1.64
12	Mg	1.3×10^{-1}	6.8×10^{-1}
13	Al	1.2×10^{-1}	6.2×10^{-1}
18	Ar	8.6×10^{-2}	4.1×10^{-1}
20	Ca	7.6×10^{-2}	3.6×10^{-1}
31	Ga	4.8×10^{-2}	2.2×10^{-1}
36	Kr	4.1×10^{-2}	1.8×10^{-1}
38	Sr	3.9×10^{-2}	1.7×10^{-1}
49	In	2.9×10^{-2}	1.3×10^{-1}
54	Xe	2.7×10^{-2}	1.14×10^{-1}
56	Ba	2.5×10^{-2}	1.09×10^{-1}
70	Yb	1.9×10^{-2}	8.3×10^{-2}
80	Hg	1.65×10^{-2}	6.9×10^{-2}
81	Tl	1.63×10^{-2}	6.8×10^{-2}
88	Ra	1.4×10^{-2}	6.0×10^{-2}

bonds between Hg-Hg lead to not a solid, but a liquid.

A more mathematical way to understand this is as follows:

$$
\begin{aligned}
l' &= l\sqrt{1 - \frac{v^2}{c^2}} \\
\therefore a'_o &= a_o\sqrt{1 - \frac{v^2}{c^2}} \\
r &= 2n^2h^2\epsilon_o/m_eZe^2 \\
\because n^2(h/2\pi)^2 &= mvr, \\
v &= Ze^2/2nh\epsilon_o
\end{aligned}
$$

In atomic units,

$$v = Z/n \therefore a'_o = a_o\sqrt{1 - \frac{Z^2}{(nc)^2}}$$

This gives us a relation between the atomic number of the atom, the principal quantum number of the electron that we are considering, and the length contracted atomic orbital.

This result is not too different in molecules.

Also, note that as the atomic number increases, for a given orbital, the expectation value decreases. This also can be explained by the fact that for a given orbital, more the atomic number, more the nuclear charge experienced, and greater the speed of the electrons. And since the faster electrons experience more relativistic effects than slower ones, the orbitals of a heavier element is expected to experience more length contraction.

2.3 Electron correlation

Electron correlation refers to the physical effects beyond those embodied in the mean field approximation. In other words, we must take into account not just the interaction of an electron with a mean potential due to other electrons, but its instantaneous interaction with each of the remaining electrons. In the real space, electrons scatter, and this, in the orbital picture, is viewed as excitations from an occupied orbital to an unoccupied (virtual) one [10].

If E is the actual energy of a many-electron system, that is, E is the energy that is obtained by solving the Schroedinger's equation exactly, and if E_{DF} is the energy obtained for the same system at the DF level, then the correlation energy is given by:

$$E_{corr} = E - E_{DF} \tag{2.56}$$

Examples of many-electron theories that take electron correlation into account are: Configuration interaction (CI), Multi-Configuration Hartree-Fock (MCHF), Many-Body Perturbation Theory (MBPT), Coupled Cluster Methods (CCM), and their relativistic extensions.

2.4 Configuration Interaction

Consider a wavefunction, $|\psi\rangle$, such that:

$$|\psi\rangle = c_1|\Phi_1\rangle + c_2|\Phi_2\rangle \tag{2.57}$$

$$So, \langle\psi| = \langle\Phi_1|c_1 + \langle\Phi_2|c_2 \tag{2.58}$$

c_1 and c_2 are assumed to be real in the above case. c_1 and c_2 are the unknowns, and $|\varphi_1\rangle$ and $|\varphi_2\rangle$ are known. Let the energy functional to be minimized be ε.

$$\varepsilon = \langle\psi|\boldsymbol{H}|\psi\rangle - E\langle\psi|\psi\rangle \tag{2.59}$$

The Lagrange multiplier imposes the constraint that the wave function will be normalized.

$$\begin{aligned} x &= \langle\psi|\boldsymbol{H}|\psi\rangle && (2.60)\\ &= (\langle\Phi_1|c_1 + \langle\Phi_2|c_2)\boldsymbol{H}(c_1|\Phi_1\rangle + c_2|\Phi_2\rangle) \\ &= \langle\psi_1|c_1\boldsymbol{H}c_1|\Phi_1\rangle + \langle\psi_1|c_1\boldsymbol{H}c_2|\Phi_2\rangle \\ &+ \langle\psi_2|c_2\boldsymbol{H}c_1|\Phi_1\rangle + \langle\psi_2|c_2\boldsymbol{H}c_2|\Phi_2\rangle \\ &= c_1^2\langle\Phi_1|\boldsymbol{H}|\Phi_1\rangle + c_1c_2\langle\Phi_1|\boldsymbol{H}|\Phi_2\rangle \\ &+ c_2c_1\langle\Phi_2|\boldsymbol{H}|\Phi_1\rangle + c_2^2\langle\Phi_2|\boldsymbol{H}|\Phi_2\rangle && (2.61) \end{aligned}$$

If we call $\langle\Phi_1|\boldsymbol{H}|\Phi_1\rangle$ as H_{11}, and so on, for short-hand. Also, H_{ij} is a number. So are c_1 and c_2. So, they commute. Also, H is Hermitian, and hence $H_{12} = H_{21}$. Therefore:

$$\langle\psi|\boldsymbol{H}|\psi\rangle = c_1^2H_{11} + 2c_1c_2H_{12} + c_2^2H_{22} \tag{2.62}$$

$$\frac{\delta\varepsilon}{\delta c_1} = 0 \Longrightarrow 2c_1H_{11} + 2c_2H_{12} = 2Ec_1 \tag{2.63}$$

$$\frac{\delta\varepsilon}{\delta c_2} = 0 \Longrightarrow 2c_2H_{22} + 2c_2H_{21} = 2Ec_2 \tag{2.64}$$

That is,

$$\begin{pmatrix} H_{11} & H_{12} \\ H_{21} & H_{22} \end{pmatrix} \begin{pmatrix} c_1 \\ c_2 \end{pmatrix} = E \begin{pmatrix} c_1 \\ c_2 \end{pmatrix} \tag{2.65}$$

This is basically an eigenvalue problem.

The above set of equations can be generalized to any number of configurations:

$$\begin{aligned} |\psi\rangle &= c_0|\Phi_0\rangle + \sum_{ia} c_i^a|\Phi_i^a\rangle + \sum_{a.b,i.j} c_{ij}^{ab}|\Phi_{ij}^{ab}\rangle + \dots && (2.66)\\ &= (c_0 + \sum_{ia} c_i^a a^\dagger i + \sum_{a.b,i.j} c_{ij}^{ab} a^\dagger b^\dagger j i + \dots)|\Phi_0\rangle && (2.67)\\ &= (c_0 + \boldsymbol{C_1} + \boldsymbol{C_2} + \dots)|\Phi_0\rangle && (2.68) \end{aligned}$$

Note that in the notation that we have adopted, we are not explicitly indicating the creation and annihilation operators in bold font. The entire analysis can be extended to its relativistic version, where one uses the Dirac-Coulomb Hamiltonian, and the non-relativistic wave function is replaced by the four-component one, just as we had discussed in the section that describes the HF method.

2.5 Multiconfiguration Hartree-Fock(MCHF)

In CI, the single particle orbitals, φs, are known, and the coefficients are the unknowns, and one varies the energy functional with respect to the coefficients. In SCF (example: HF/DF), the φs are unknown, the coefficient is known, and one varies the energy functional with respect to the φs. In multiconfiguration Hartree-Fock/Dirac-Fock(MCHF/DF), the energy functional is varied with respect to both the φs and the coefficients.

$$\begin{aligned} \varepsilon &= \langle\psi|\boldsymbol{H}|\psi\rangle - \sum_a \varepsilon_a \langle\varphi_a|\varphi_a\rangle; && (2.69)\\ |\psi\rangle &= \sum_n C_n |\Phi_n\rangle && (2.70)\\ \therefore \varepsilon &= \sum_{mn} C_m C_n \langle\Phi_m|\boldsymbol{H}|\Phi_n\rangle - \sum_a \varepsilon_a \langle\varphi_a|\varphi_a\rangle && (2.71) \end{aligned}$$

Here, $|\Phi_n\rangle$ is the n^{th} Slater determinant. The single particle orbitals in the Slater determinants can be either occupied or virtual. Note that in the HF/DF case, the single particle orbitals are all occupied.

The variational parameters in MCHF/DF are both the single particle orbitals and the coefficients. The equations obtained by varying the orbitals and the coefficients are respectively:

$$\begin{aligned} \boldsymbol{h_{MCHF/DF}}|\varphi_i\rangle &= \varepsilon_i|\varphi_i\rangle && (2.72)\\ \boldsymbol{H}C &= EC && (2.73) \end{aligned}$$

The single-particle Hamiltonian, $h_{MCHF/DF}$, contains the generalized direct and exchange potentials, which depend on the orbitals and the coefficients. Here, both the orbitals and the coefficients are guessed, then substituted into the above two equations. The first equation gives new orbitals, and the second new coefficients, which are in turn put into the equations as the second set of guesses. This is done iteratively till the solutions converge.

Again, this too can be extended into the relativistic domain.

2.6 Many Body Perturbation Theory

If H_0 is the unperturbed Hamiltonian, and E_0 the mean field(Hartree-Fock/Dirac-Fock) energy, then the unperturbed Schroedinger equation would be:

$$\begin{aligned} \boldsymbol{H_0}|\psi_0\rangle &= E_0|\psi_0\rangle; \\ \boldsymbol{H_0} &= \sum_i \boldsymbol{t_i} + \sum_i \boldsymbol{V_i^{DF}} \end{aligned} \tag{2.74}$$

The Schroedinger equation corresponding to the actual wavefunction of the system would be:

$$\begin{aligned} \boldsymbol{H}|\psi\rangle &= E|\psi\rangle; \\ \boldsymbol{H} &= \sum_i \boldsymbol{t_i} + \sum_{ij} \frac{1}{\boldsymbol{r_{ij}}} \\ \therefore \boldsymbol{H'} &= \boldsymbol{H} - \boldsymbol{H_0} \\ &= \sum_{ij} \frac{1}{\boldsymbol{r_{ij}}} - \sum_i \boldsymbol{V_i^{DF}} \end{aligned} \tag{2.75}$$

$$And, |\psi\rangle = |\Phi_0\rangle + |\Phi_0^{(1)}\rangle + |\Phi_0^{(2)}\rangle + \dots \tag{2.76}$$

$$And, |\psi\rangle = |\Phi_0\rangle + |\Phi_0^{(1)}\rangle + |\Phi_0^{(2)}\rangle + \dots \tag{2.77}$$

where $|\varphi_0^{(1)}\rangle$ contains one order of $\boldsymbol{H'}$, $|\varphi_0^{(2)}\rangle$ contains two orders of $\boldsymbol{H'}$, etc.

This holds for both the relativistic (denoted by the subscript rel) and non-relativistic cases (denoted by the subscript NR).

$$\boldsymbol{t_{i,NR}} = -\hbar^2/2 \sum_{i=1}^{n} \boldsymbol{\nabla_i^2} + \boldsymbol{V^{Nuclear}(r_i)} \tag{2.78}$$

$$\boldsymbol{t_{i,rel}} = \sum_i c\boldsymbol{\alpha_i}.\boldsymbol{p_i} + \beta c^2 + \boldsymbol{V_i^{Nuclear}} \tag{2.79}$$

One can also use a relativistic version of MBPT, as described in earlier sections.

2.7 Coupled Cluster Method

The coupled cluster method's wave function is given by:

$$|\psi\rangle = e^{\boldsymbol{T}}|\Phi_0\rangle \tag{2.80}$$

Here, $\boldsymbol{T}$ is called the cluster operator. This method is considered to be the gold standard of electronic structure theory. Since this is the method that will be employed in the work related to this thesis, this approach shall be discussed elaborately in the next chapter.

2.8 Summary

This chapter was an introduction to many-electron theory. The chapter begins with the Born-Oppenheimer approximation, and atomic units. We discussed the Hartree-Fock method in detail, since it is this wavefunction that is chosen as the model state for coupled cluster calculations, in the subsequent chapters. The subsections included the interpretation of the HF/DF equations, matrix formalism, and also DF calculations in some atoms, that illustrated the importance of relativistic effects. We then discussed electron correlation, and some theories that take into account this phenomenon. We conclude the chapter with a very brief section on the coupled cluster method. The next chapter will elaborate on it in great detail. It will also discuss our implementation of the method for problems of our interest.

BIBLIOGRAPHY

[1] Slater, J. C., The Theory of Complex Spectra, Phys. Rev. 34 (10): 1293–1322 (1929); Condon, E. U., The Theory of Complex Spectra, Phys. Rev. 36 (7): 1121–1133 (1930).

[2] K. G. Dyall, and K. Faegri, Introduction to Relativistic Quantum Chemistry, Chapter 11, Oxford University Press (2007).

[3] R. E. Stanton and S. Havriliak, Kinetic balance: A partial solution to the problem of variational safety in Dirac calculations, J Chem Phys, 81, 1910 (1984); doi: http://dx.doi.org/10.1063/1.447865.

[4] T. Helgaker, P. Jorgensen, J. Olsen, Molecular Electronic Structure Theory, John Wiley and Sons (2012).

[5] $http://vergil.chemistry.gatech.edu/courses/chem6485/pdf/basis-sets.pdf$.

[6] $http://www.helsinki.fi/kemia/fysikaalinen/opetus/jlk/luennot/Lecture5.pdf$.

[7] F. A. Parpia, C. F. Fischer and I. P. Grant, GRASP92: A package for large-scale relativistic atomic structure calculations, Computer physics communications, Volume 94, Issues 2–3, Pages 249-271 (1996).

[8] C.F. Fischer, The Hartree-Fock Approach for Atoms, Wiley, 1977.

[9] C. F. Bunge et al, Hartree-Fock and Roothaan-Hartree-Fock energies for the ground states of He through Xe, Physical Review A, 46, 3691 (1992).

[10] T. Helgaker, Convergence properties of the coupled-cluster method, the accurate calculation of molecular properties for light systems, CMA–CTCC workshop on computational quantum mechanics, Department of Chemistry, University of Oslo, Norway, June 18–19, 2010.

3

THE COUPLED CLUSTER METHOD

3.1 The Coupled Cluster wave function

The coupled cluster method (CCM) is the current gold standard of all electronic structure calculations. It is a non-perturbative approach. The coupled cluster ansatz is:

$$|\psi\rangle = e^{\boldsymbol{T}}|\Phi_0\rangle \tag{3.1}$$

where Φ_0 refers to the Hartree-Fock or Dirac-Fock wavefunction. Consider the atom Beryllium (Be) as an example to describe the coupled cluster method. The 1s and 2s orbitals have two electrons each, and these together are called occupied orbitals. The orbitals 2p, 3s, and so on, are called unoccupied or virtual orbitals. Now, electron correlations involve interactions between electrons leading to virtual excitations. In this case, the electrons from the 1s and 2s orbitals interact and lead to virtual excitations of one or more of these electrons into the virtual orbitals. All the occupied orbitals are called holes, and all the virtual orbitals are called particles, pretty much in the sense of an excited particle leaving behind a hole. This is the standard notation. In the above expression, Φ_0, which is in fact the Fermi vacuum, is taken as the model state, that is, a state on which some operator(s) act to lead to the virtual excitations. In this case, the states 1s and 2s constitute the model state, and some operator(s) act on them to excite them to different virtual states.

Let us consider a single excitation, that is, one of the electrons get excited to some virtual orbital. This is also called a one hole-one particle excitation, because the electron that gets excited leaves behind a hole, creating a particle in that virtual orbital to which it is excited. Mathematically, this can be described as an annihilation operator acting on the

model state to destroy an electron from it, and a creation operator acting on this state to create a particle in some virtual orbital:

$$|\Phi_i^a\rangle = a_a^\dagger a_i |\Phi_0\rangle \tag{3.2}$$

$$= a^\dagger i |\Phi_0\rangle \tag{3.3}$$

The above equation basically says that a hole i from the Fermi vacuum goes to a particle a, leading to the state $|\Phi_i^a\rangle$. The notation of a_a being replaced by just a, and a_i by just i is used in the last line of the above equation. Also, we adopt the notation where the creation and annihilation operators are not represented in bold, like the other operators. Note that since a single excitation, say, from 2s to 3s is easier than one from 1s to 3s, the former has more weightage when one writes down the probability amplitude for these excitations. Let us call that weight t_i^a. Also, since any one of the four electrons in the Fermi vacuum can get excited to any of the virtual orbitals, we consider all possible single excitations. Hence, we obtain the following amplitude for all possible single excitations:

$$\sum_{ia} t_i^a |\Phi_i^a\rangle \tag{3.4}$$

We sum over all possible single excitations in the sense that either a single excitation occurs from 1s to 3s, or a single excitation can occur from 1s to 3p, and so on. In other words, it means that each of these excitations are independent events where either of them occur, but not more than one simultaneously.

In a similar way, one also takes into account double excitations, or two hole- two particle excitations. They give rise to the amplitude, based on arguments similar to that presented for single excitations:

$$\sum_{i>j,a>b} t_{ij}^{ab} |\Phi_{ij}^{ab}\rangle \tag{3.5}$$

Likewise, one can write down amplitudes for triple excitations and quadruple excitations. For Beryllium, the highest excitation possible is a quadruple excitation. But for atoms with more electrons, it goes higher accordingly. So, in general, one obtains for the probability amplitude:

$$|\psi\rangle = |\Phi_0\rangle + \sum_{ia} t_i^a |\Phi_i^a\rangle + \sum_{i>j,a>b} t_{ij}^{ab} |\Phi_{ij}^{ab}\rangle + \ldots \tag{3.6}$$

$$= |\Phi_0\rangle + \boldsymbol{T_1}|\Phi_0\rangle + \boldsymbol{T_2}|\Phi_0\rangle + \ldots \tag{3.7}$$

where $\boldsymbol{T_1} = \sum_{ia} t_i^a a^\dagger i$, etc. Here, $\boldsymbol{T_1}$, $\boldsymbol{T_2}$, etc are called clusters.

One notices that there can be more possible excitations. For example, there can be two one hole-one particle excitations happening simultaneously. The amplitude for such an excitation would be given by:

$$\sum_{i>j,a>b} t_i^a t_j^b |\Phi_{ij}^{ab}\rangle = \frac{1}{2!}\boldsymbol{T_1^2}|\Phi_0\rangle \tag{3.8}$$

The factor of $\frac{1}{2!}$ is to avoid overcounting. Likewise, one gets $\frac{1}{3!}\boldsymbol{T_1^3}$, $\frac{1}{4!}\boldsymbol{T_1^4}$, etc. Also, there would be terms like $\frac{1}{3!}\boldsymbol{T_2^3}$, $\frac{1}{4!}\boldsymbol{T_2^4}$, etc.

There can also be terms that involve simultaneous single and double excitations, single and triple excitations, and so on. Each of those terms that contain $\boldsymbol{T_1 T_2}$, $\boldsymbol{T_2^2}$, etc are said to be coupled clusters. For example, the coupled cluster $\boldsymbol{T_1 T_2}$ contains the clusters $\boldsymbol{T_1}$ and $\boldsymbol{T_2}$.

When one takes all of these excitations into account, the probability amplitude automatically takes an exponential form:

$$|\psi\rangle = e^{\boldsymbol{T}}|\Phi_0\rangle \tag{3.9}$$

which is the coupled cluster wave function!

The coupled cluster method is valid both in the non-relativistic and the relativistic regimes. For the relativistic case, the reference state, $|\Phi_0\rangle$, is a determinantal state, which is built out of 4-component orbitals (single particle wave functions). Also, the Hamiltonian typically contains the one-electron Dirac terms and the two-electron Coulomb interactions.

3.2 Baker Campbell Hausdorff expansion

The expansion is given by:

$$e^{-\boldsymbol{T}}\boldsymbol{A}e^{\boldsymbol{T}} = \sum_{n=0}^{\infty}\frac{1}{n!}[\boldsymbol{A},\boldsymbol{T}]^{(n)} \tag{3.10}$$

A and T are operators. Also, $[\boldsymbol{A},\boldsymbol{T}]^{(n)} = [[\boldsymbol{A},\boldsymbol{T}]^{(n-1)},\boldsymbol{T}]$.
Proof of Baker Campbell Hausdorff (BCH) expansion:
Let $\boldsymbol{A'}(\lambda) \equiv e^{-\lambda\boldsymbol{T}}\boldsymbol{A}e^{\lambda\boldsymbol{T}}$.

$$\begin{aligned}
\frac{d}{d\lambda}\boldsymbol{A'}(\lambda) &= -e^{-\lambda\boldsymbol{T}}\boldsymbol{T}\boldsymbol{A}e^{\lambda\boldsymbol{T}} + e^{-\lambda\boldsymbol{T}}\boldsymbol{A}\boldsymbol{T}e^{\lambda\boldsymbol{T}} \\
&= e^{-\lambda\boldsymbol{T}}(\boldsymbol{A}\boldsymbol{T} - \boldsymbol{T}\boldsymbol{A})e^{\lambda\boldsymbol{T}} \\
&= e^{-\lambda\boldsymbol{T}}[\boldsymbol{A},\boldsymbol{T}]e^{\lambda\boldsymbol{T}} \\
\frac{d^2}{d\lambda^2}\boldsymbol{A'}(\lambda) &= -e^{-\lambda\boldsymbol{T}}\boldsymbol{T}[\boldsymbol{A},\boldsymbol{T}]e^{\lambda\boldsymbol{T}} + e^{-\lambda\boldsymbol{T}}[\boldsymbol{A},\boldsymbol{T}]\boldsymbol{T}e^{\lambda\boldsymbol{T}} \\
&= e^{-\lambda\boldsymbol{T}}[[\boldsymbol{A},\boldsymbol{T}],\boldsymbol{T}]e^{\lambda\boldsymbol{T}}, etc. \\
\therefore \boldsymbol{A'}(\lambda) &= \boldsymbol{A'}(0) + \lambda\frac{d}{d\lambda}\boldsymbol{A'}(0) + \frac{1}{2!}\lambda^2\frac{d^2}{d\lambda^2}\boldsymbol{A'}(0) + \ldots \\
&= \boldsymbol{A} + \lambda[\boldsymbol{A},\boldsymbol{T}] + \frac{1}{2!}\lambda^2[[\boldsymbol{A},\boldsymbol{T}],\boldsymbol{T}] + \ldots \\
\boldsymbol{A'}(1) &= \boldsymbol{A} + [\boldsymbol{A},\boldsymbol{T}] + \frac{1}{2!}[[\boldsymbol{A},\boldsymbol{T}],\boldsymbol{T}] + \ldots \\
or,\ e^{-\boldsymbol{T}}\boldsymbol{A}e^{\boldsymbol{T}} &= \boldsymbol{A} + [\boldsymbol{A},\boldsymbol{T}] + \frac{1}{2!}[[\boldsymbol{A},\boldsymbol{T}],\boldsymbol{T}] + \ldots \\
&= \sum_{n=0}^{\infty}\frac{1}{n!}[\boldsymbol{A},\boldsymbol{T}]^{(n)}
\end{aligned} \tag{3.11}$$

3.3 The linked cluster theorem

We first begin with a few basic ideas that will be used in the proof of the linked cluster theorem. Let $\boldsymbol{ABC}\ldots$ represent a string of creation and annihilation operators. Then, the normal product of this string is defined by: $\{\boldsymbol{ABC}\ldots\} : i^\dagger$ and a to the right of other operators, that is, all hole creation and particle annihilation operators are to the right of the other operators in the string. It follows that:

$$\langle\Phi_o|\{\boldsymbol{ABC}\ldots\}|\Phi_0\rangle = 0 \tag{3.12}$$

This is because further holes cannot be created in the Fermi vacuum, and particles cannot be destroyed from it since there is none.

Contraction of two general operators $p^\dagger$ and q is defined by:

$$\overbrace{p^\dagger q} = p^\dagger q - \{p^\dagger q\} \tag{3.13}$$

Consider the cases where p and q are particles, and the cases where they are holes, with either p or q serving as a creation operator, and the other as an annihilation operator:

Case 1:

$$ba^\dagger = \{ba^\dagger\} + \overbrace{ba^\dagger} \tag{3.14}$$

Now, $[a^\dagger, b]_+ = \delta_{ab}$, that is, $ba^\dagger = -a^\dagger b + \delta_{ab}$. So, $\{ba^\dagger\} = -a^\dagger b$. Hence, $ba^\dagger = -a^\dagger b + \overbrace{ba^\dagger}$. Therefore,

$$\overbrace{ba^\dagger} = \delta_{ab} \tag{3.15}$$

Case 2:

$$a^\dagger b = \{a^\dagger b\} + \overbrace{a^\dagger b} \tag{3.16}$$
$$Note\ that\ \{a^\dagger b\} = a^\dagger b \tag{3.17}$$
$$\therefore \overbrace{a^\dagger b} = 0 \tag{3.18}$$

Case 3:

$$i^\dagger j = \{i^\dagger j\} + \overbrace{i^\dagger j} \tag{3.19}$$
$$Note\ that\ \{i^\dagger j\} = -ji^\dagger \tag{3.20}$$
$$\therefore \overbrace{i^\dagger j} = \delta_{ij} \tag{3.21}$$

Case 4:

$$ij^\dagger = \{ij^\dagger\} + \overbrace{ij^\dagger} \tag{3.22}$$
$$Note\ that\ \{ij^\dagger\} = ij^\dagger \tag{3.23}$$
$$\therefore \overbrace{ij^\dagger} = 0 \tag{3.24}$$

Wick's theorem tells that if $\boldsymbol{ABC}\ldots$ are a string of creation and annihilation operators, then:

$$\begin{aligned} \boldsymbol{ABC}\ldots &= \{\boldsymbol{ABC}\ldots\} + \sum_{single\ contractions} \overbrace{\boldsymbol{AB}}\boldsymbol{CDE}\ldots \\ &+ \sum_{double\ contractions} \overbrace{\boldsymbol{AB}}\overbrace{\boldsymbol{CD}}\boldsymbol{E}\ldots + \ldots \end{aligned} \tag{3.25}$$

$$\langle\Phi_0|\boldsymbol{ABC}\ldots|\Phi_0\rangle = \sum_{fully\ contracted\ products} \overbrace{\langle\Phi_0|\boldsymbol{A}\,\boldsymbol{B}\overbrace{\boldsymbol{C}\ldots}|\Phi_0\rangle} \tag{3.26}$$

Normal product form of an operator, $\boldsymbol{A}$, is defined also by:

$$\boldsymbol{A_N} = \boldsymbol{A} - \langle\Phi_0|\boldsymbol{A}|\Phi_0\rangle \tag{3.27}$$

For the Hamiltonian,

$$\boldsymbol{H_N} = \boldsymbol{H} - \langle\Phi_0|\boldsymbol{H}|\Phi_0\rangle \tag{3.28}$$

The normal ordered Hamiltonian is, in second quantized form:

$$\boldsymbol{H_N} = \sum_{pq} h_{pq}\{p^\dagger q\} + \frac{1}{4}\sum_{pqrs}\langle pq||rs\rangle p^\dagger q^\dagger sr; \tag{3.29}$$

$$\langle pq||rs\rangle = \langle pq|\boldsymbol{v}|rs\rangle - \langle pq|\boldsymbol{v}|sr\rangle \tag{3.30}$$

An object is defined as an arbitrary operator containing the same number of creation and annihilation operators standing inside a normal product. Let $\boldsymbol{A}$ and $\boldsymbol{B}$ be two different objects. From the generalized Wick's theorem:

$$\boldsymbol{AB} = \{\boldsymbol{AB}\} + \widehat{\boldsymbol{AB}} \tag{3.31}$$

$$\boldsymbol{BA} = \{\boldsymbol{BA}\} + \widehat{\boldsymbol{BA}} \tag{3.32}$$

Since $\boldsymbol{A}$ and $\boldsymbol{B}$ are made up of even number of creation and annihilation operators, one obtains:

$\{\boldsymbol{AB}\} = \{\boldsymbol{BA}\}$

Then,

$$\boldsymbol{AB} - \boldsymbol{BA} = [\boldsymbol{A}, \boldsymbol{B}] \tag{3.33}$$

$$= \{\boldsymbol{AB}\} + \widehat{\boldsymbol{AB}} - \{\boldsymbol{BA}\} - \widehat{\boldsymbol{BA}} \tag{3.34}$$

$$= \widehat{\boldsymbol{AB}} - \widehat{\boldsymbol{BA}} \tag{3.35}$$

Now, consider the Schroedinger equation:

$$\boldsymbol{H}|\psi\rangle = E|\psi\rangle \tag{3.36}$$

$$\boldsymbol{H}e^{\boldsymbol{T}}|\Phi_0\rangle = Ee^{\boldsymbol{T}}|\Phi_0\rangle \tag{3.37}$$

$$e^{-\boldsymbol{T}}\boldsymbol{H}e^{\boldsymbol{T}}|\Phi_0\rangle = E|\Phi_0\rangle \tag{3.38}$$

Let us consider the part $e^{-\boldsymbol{T}}\boldsymbol{H}e^{\boldsymbol{T}}$ from the right hand side. Let us use an object, $\boldsymbol{A}$, for a more general treatment. Then, from the Baker Campbell Hausdorff expansion seen in the previous section, one obtains:

$$e^{-\boldsymbol{T}}\boldsymbol{A}e^{\boldsymbol{T}} = \sum_{n=0}^{\infty}\frac{1}{n!}[\boldsymbol{A},\boldsymbol{T}]^{(n)} \tag{3.39}$$

The first term, which would be just $\boldsymbol{A}$, is connected, since it is just a single piece. The second term would be:

$[\boldsymbol{A},\boldsymbol{T}] = \widehat{\boldsymbol{AT}} - \widehat{\boldsymbol{TA}}$

Now, a normal ordered operator is defined in two ways:

$$\boldsymbol{A_N} = \boldsymbol{A} - \langle\Phi_0|\boldsymbol{A}|\Phi_0\rangle \tag{3.40}$$

$$\boldsymbol{A_N} = \boldsymbol{A} - \widehat{\boldsymbol{A}} \tag{3.41}$$

$$\therefore \widehat{\boldsymbol{A}} = \langle\Phi_0|\boldsymbol{A}|\Phi_0\rangle \tag{3.42}$$

This would mean that the second term in $[\boldsymbol{A},\boldsymbol{T}]$ would be zero, since $\widehat{\boldsymbol{TA}} = \langle\Phi_0|\boldsymbol{TA}|\Phi_0\rangle$, and the action of a cluster operator T on the bra model state gives a zero.

The second term is zero, since a particle creation operator acting on the bra model state gives a zero. Therefore,

$[\boldsymbol{A},\boldsymbol{T}] = \widehat{\boldsymbol{AT}}$

The third term gives:

$$\begin{aligned}[\boldsymbol{A},\boldsymbol{T}]^{(2)} &= [[\boldsymbol{A},\boldsymbol{T}],\boldsymbol{T}] \\ &= [\widehat{\boldsymbol{AT}},\boldsymbol{T}] \\ &= \widehat{\widehat{\boldsymbol{AT}}\,\boldsymbol{T}} - \widehat{\widehat{\boldsymbol{TA}}\,\boldsymbol{T}}\end{aligned}$$

$$= \overbrace{\overbrace{\boldsymbol{AT}}\boldsymbol{T}} \tag{3.43}$$

The above result uses the fact that the contraction between two $\boldsymbol{T}$s is zero. In general,

$$[\boldsymbol{A}, \boldsymbol{T}]^{(n)} = \overbrace{\overbrace{\boldsymbol{AT} \ldots T}} \tag{3.44}$$

Therefore, one can write:

$$e^{-\boldsymbol{T}} \boldsymbol{A} e^{\boldsymbol{T}} = \{\boldsymbol{A} e^{\boldsymbol{T}}\}_c \tag{3.45}$$

where the subscript c indicates that only the connected terms are taken into account. This is the linked cluster theorem.

There are two approaches to obtaining the energy and amplitude equations. One is the algebraic approach, where one uses the idea of the BCH expansion and the fact that the commutators terminate after certain number of terms, depending on the operator in question. The second is the diagrammatic approach, where one uses the linked cluster theorem to rewrite $e^{-\boldsymbol{T}} \boldsymbol{A} e^{\boldsymbol{T}}$ as $\{\boldsymbol{A} e^{\boldsymbol{T}}\}_c$, and then use the idea of level of excitation to obtain the energy and amplitude equations through Feynman-like diagrams, called the Goldstone diagrams.

3.4 Energy and amplitude equations

$$\boldsymbol{H}|\psi\rangle = E|\psi\rangle \tag{3.46}$$

$$(\boldsymbol{H} - E_{DF})|\psi\rangle = (E - E_{DF})|\psi\rangle; E_{DF} = \langle\Phi_0|\boldsymbol{H}|\Phi_0\rangle \tag{3.47}$$

$$\boldsymbol{H_N}|\psi\rangle = \Delta E|\psi\rangle \tag{3.48}$$

$$\boldsymbol{H_N}e^{\boldsymbol{T}}|\Phi_0\rangle = \Delta E e^{\boldsymbol{T}}|\Phi_0\rangle \tag{3.49}$$

$$e^{-\boldsymbol{T}}\boldsymbol{H_N}e^{\boldsymbol{T}}|\Phi_0\rangle = \Delta E|\Phi_0\rangle \tag{3.50}$$

$$\therefore \Delta E = \langle\Phi_0|e^{-\boldsymbol{T}}\boldsymbol{H_N}e^{\boldsymbol{T}}|\Phi_0\rangle \tag{3.51}$$

$$And, \langle\Phi_{ij\ldots}^{ab\cdots}|e^{-\boldsymbol{T}}\boldsymbol{H_N}e^{\boldsymbol{T}}|\Phi_0\rangle = 0 \tag{3.52}$$

The last two equations are called the energy and amplitude equations.

3.5 Coupled Cluster Singles and Doubles approximation: energy and amplitude equations

In the CCM, if one takes $\boldsymbol{T} = \boldsymbol{T_1} + \boldsymbol{T_2}$, then it is called the Coupled Cluster Singles and Doubles (CCSD) approximation, that is, only the single and double excitations are taken into account. The energy equation remains the same, but there would only be two amplitude equations:

$$\langle \Phi_0 | e^{-\boldsymbol{T}} \boldsymbol{H_N} e^{\boldsymbol{T}} | \Phi_0 \rangle = \Delta E \tag{3.53}$$

$$\langle \Phi_i^a | e^{-\boldsymbol{T}} \boldsymbol{H_N} e^{\boldsymbol{T}} | \Phi_0 \rangle = 0 \tag{3.54}$$

$$\langle \Phi_{ij}^{ab} | e^{-\boldsymbol{T}} \boldsymbol{H_N} e^{\boldsymbol{T}} | \Phi_0 \rangle = 0 \tag{3.55}$$

Consider the energy equation:

$$\Delta E = \langle \Phi_0 | e^{-\boldsymbol{T}} \boldsymbol{H_N} e^{\boldsymbol{T}} | \Phi_0 \rangle \tag{3.56}$$

$$= \langle \Phi_0 | (\boldsymbol{H_N} e^{\boldsymbol{T}})_c | \Phi_0 \rangle \tag{3.57}$$

Now, in the above equation, if we expand the series $e^{\boldsymbol{T}}$, we see that the first term $\langle \Phi_0 | \boldsymbol{H_N} | \Phi_0 \rangle = 0$. This is because the normal ordered Hamiltonian has hole creation and particle annihilation operators to its right, which act on the ket Fermi vacuum to give zero. Also, terms from $\boldsymbol{T_3}$ and beyond, as well as their higher powers do not contribute. Also, $\boldsymbol{T_2^2}$ and higher powers do not contribute. And $\boldsymbol{T_1^3}$ and higher powers do not contribute. This can be seen using the idea that the maximum number of operators the normal ordered Hamiltonian can have is four, and that those terms of $\boldsymbol{T}$ that have beyond four operators cannot contract fully with $\boldsymbol{H_N}$. Therefore, one gets:

$$\Delta E = \langle \Phi_0 | \boldsymbol{H_N T_1} + \boldsymbol{H_N T_2} + \boldsymbol{H_N} \frac{\boldsymbol{T_1^2}}{2!} | \Phi_0 \rangle \tag{3.58}$$

To obtain a more specific form, one uses the fact that the normal ordered Hamiltonian is made up of a one-electron part and a two-electron part. Then, one sees that the energy equation for CCSD takes the form:

$$\begin{aligned}\Delta E &= \sum_{ia} f_{ia} t_i^a + \frac{1}{4} \sum_{a>b,i>j} \langle ij||ab\rangle t_{ij}^{ab} \\ &+ \frac{1}{2} \sum_{a>b,i>j} \langle ij||ab\rangle t_i^a t_j^b \end{aligned} \tag{3.59}$$

In a similar way, we obtain the amplitude equations for CCSD:

Singles amplitude equation:

$$\begin{aligned}&\sum_c f_{ac} t_i^c - \sum_k f_{ki} t_k^a + \sum_{kc} \langle ka||ci\rangle t_k^c + \frac{1}{2} \sum_{kcd} \langle ka||cd\rangle t_{ki}^{cd} - \frac{1}{2} \sum_{kcl} \langle kl||ci\rangle t_{kl}^{ca} \\ &+ \sum_{kcd} \langle ka||cd\rangle t_k^c t_i^d - \sum_{kcl} \langle kl||ci\rangle t_k^c t_l^a - \sum_{klcd} \langle kl||cd\rangle t_k^c t_i^d t_l^a + \sum_{klcd} \langle kl||cd\rangle t_k^c t_{li}^{da} \\ &- \frac{1}{2} \sum_{klcd} \langle kl||cd\rangle t_{ki}^{cd} t_l^a - \frac{1}{2} \sum_{klcd} \langle kl||cd\rangle t_{kl}^{ca} t_i^d t_i^d = 0 \end{aligned} \tag{3.60}$$

Doubles amplitude equation:

$$\begin{aligned}&\sum_c \langle ab||cj\rangle t_i^c - \sum_c \langle ab||ci\rangle t_j^c - \sum_k \langle kb||ij\rangle t_k^a + \sum_k \langle ka||ij\rangle t_k^b \\ &+ \sum_c f_{bc} t_{ij}^{ac} - \sum_c f_{ac} t_{ij}^{bc} - \sum_k f_{kj} t_{ik}^{ab} + \sum_k f_{ki} t_{jk}^{ab} + \frac{1}{2} \sum_{kl} \langle kl||ij\rangle t_{kl}^{ab} + \frac{1}{2} \sum_{cd} \langle ab||cd\rangle t_{ij}^{cd} \\ &+ \sum_{kc} \langle kb||cj\rangle t_{ik}^{ac} - \sum_{kc} \langle kb||ci\rangle t_{jk}^{ac} - \sum_{kc} \langle ka||cj\rangle t_{ik}^{bc} + \sum_{kc} \langle ka||ci\rangle t_{jk}^{bc} \\ &+ \sum_{kc} \langle ak||ci\rangle t_{jk}^{cb} - \sum_{kc} \langle bk||ci\rangle t_{jk}^{ca} + \frac{1}{2} \sum_{kl} \langle kl||ij\rangle t_k^a t_l^b - \frac{1}{2} \sum_{kl} \langle kl||ij\rangle t_k^b t_l^a \\ &+ \frac{1}{2} \sum_{cd} \langle ab||cd\rangle t_i^c t_j^d - \frac{1}{2} \sum_{cd} \langle ab||cd\rangle t_j^c t_i^d - \sum_{kc} \langle kb||ic\rangle t_k^a t_j^c + \sum_{kc} \langle kb||jc\rangle t_k^a t_i^c \\ &+ \sum_{kc} \langle ka||ic\rangle t_k^b t_j^c - \sum_{kc} \langle ka||jc\rangle t_k^b t_i^c + \frac{1}{2} \sum_{klcd} \langle kl||cd\rangle t_{ik}^{ac} t_{lj}^{db} - \frac{1}{2} \sum_{klcd} \langle kl||cd\rangle t_{jk}^{ac} t_{li}^{db} \\ &- \frac{1}{2} \sum_{klcd} \langle kl||cd\rangle t_{ik}^{bc} t_{lj}^{da} + \frac{1}{2} \sum_{klcd} \langle kl||cd\rangle t_{jk}^{bc} t_{li}^{da} + \frac{1}{4} \sum_{klcd} \langle kl||cd\rangle t_{ij}^{cd} t_{kl}^{ab} - \frac{1}{2} \sum_{klcd} \langle kl||cd\rangle t_{ij}^{ac} t_{kl}^{bd} \\ &+ \frac{1}{2} \sum_{klcd} \langle kl||cd\rangle t_{ij}^{bc} t_{kl}^{ad} - \frac{1}{2} \sum_{klcd} \langle kl||cd\rangle t_{ik}^{ab} t_{jl}^{cd} + \frac{1}{2} \sum_{klcd} \langle kl||cd\rangle t_{jk}^{ab} t_{il}^{cd} - \frac{1}{2} \sum_{klcd} \langle kl||cd\rangle t_{il}^{ac} t_{kj}^{db} \\ &+ \frac{1}{2} \sum_{klcd} \langle kl||cd\rangle t_{il}^{bc} t_{kj}^{da} - \frac{1}{2} \sum_{klcd} \langle kl||cd\rangle t_{ik}^{ac} t_{lj}^{bd} + \frac{1}{2} \sum_{klcd} \langle kl||cd\rangle t_{ik}^{bc} t_{lj}^{ad} + \frac{1}{2} \sum_{klcd} \langle kl||cd\rangle t_{ki}^{ac} t_{lj}^{bd} \end{aligned}$$

$$
\begin{aligned}
&-\frac{1}{2}\sum_{klcd}\langle kl||cd\rangle t_{kj}^{ac}t_{li}^{bd}+\frac{1}{2}\sum_{klcd}\langle kl||cd\rangle t_{il}^{ca}t_{kj}^{db}-\frac{1}{2}\sum_{klcd}\langle kl||cd\rangle t_{il}^{cb}t_{kj}^{da}-\frac{1}{2}\sum_{klcd}\langle kl||cd\rangle t_{kl}^{ac}t_{ij}^{db}\\
&+\frac{1}{2}\sum_{klcd}\langle kl||cd\rangle t_{kl}^{ac}t_{ji}^{db}+\frac{1}{2}\sum_{kcd}\langle kb||cd\rangle t_{j}^{c}t_{i}^{d}t_{k}^{a}+\frac{1}{2}\sum_{kcd}\langle ka||cd\rangle t_{i}^{c}t_{j}^{d}t_{k}^{b}-\frac{1}{2}\sum_{kcd}\langle kb||cd\rangle t_{i}^{c}t_{j}^{d}t_{k}^{a}\\
&-\frac{1}{2}\sum_{kcd}\langle ka||cd\rangle t_{j}^{c}t_{i}^{d}t_{k}^{b}+\frac{1}{2}\sum_{kcl}\langle kl||cj\rangle t_{i}^{c}t_{l}^{b}t_{k}^{a}-\frac{1}{2}\sum_{kcl}\langle kl||cj\rangle t_{i}^{c}t_{k}^{b}t_{l}^{a}-\frac{1}{2}\sum_{kcl}\langle kl||ci\rangle t_{j}^{c}t_{l}^{b}t_{k}^{a}\\
&+\frac{1}{2}\sum_{kcl}\langle kl||ci\rangle t_{j}^{c}t_{k}^{b}t_{l}^{a}-\sum_{kcl}\langle kl||ci\rangle t_{k}^{c}t_{lj}^{ab}+\sum_{kcl}\langle kl||cj\rangle t_{k}^{c}t_{li}^{ab}+\sum_{kcd}\langle ka||cd\rangle t_{k}^{c}t_{ij}^{db}\\
&-\sum_{kcd}\langle kb||cd\rangle t_{k}^{c}t_{ij}^{da}+\sum_{kcd}\langle ak||dc\rangle t_{i}^{d}t_{jk}^{bc}-\sum_{kcd}\langle ak||dc\rangle t_{j}^{d}t_{ik}^{bc}-\sum_{kcd}\langle bk||dc\rangle t_{i}^{d}t_{jk}^{ac}\\
&+\sum_{kcd}\langle bk||dc\rangle t_{j}^{d}t_{ik}^{ac}+\sum_{kcl}\langle kl||ic\rangle t_{l}^{a}t_{jk}^{bc}-\sum_{kcl}\langle kl||jc\rangle t_{l}^{a}t_{ik}^{bc}-\sum_{kcl}\langle kl||ic\rangle t_{l}^{b}t_{jk}^{ac}\\
&+\sum_{kcl}\langle kl||jc\rangle t_{l}^{b}t_{ik}^{ac}+\frac{1}{2}\sum_{kcl}\langle kl||cj\rangle t_{i}^{c}t_{kl}^{ab}-\frac{1}{2}\sum_{kcl}\langle kl||ci\rangle t_{j}^{c}t_{kl}^{ab}-\frac{1}{2}\sum_{kcd}\langle kb||cd\rangle t_{k}^{a}t_{ij}^{cd}\\
&+\frac{1}{2}\sum_{kcd}\langle ka||cd\rangle t_{k}^{b}t_{ij}^{cd}+\sum_{kcd}\langle ak||dc\rangle t_{i}^{c}t_{jk}^{db}-\sum_{kcd}\langle ak||dc\rangle t_{j}^{c}t_{ik}^{db}+\sum_{kcl}\langle kl||ic\rangle t_{k}^{a}t_{lj}^{cb}\\
&-\sum_{kcl}\langle kl||ic\rangle t_{k}^{b}t_{lj}^{ca}-\sum_{kcb}\langle ak||bc\rangle t_{j}^{c}t_{ik}^{bd}+\sum_{kcb}\langle ak||bc\rangle t_{i}^{c}t_{jk}^{bd}-\sum_{kcl}\langle kl||cj\rangle t_{l}^{c}t_{ki}^{ab}\\
&+\sum_{kcl}\langle kl||cj\rangle t_{l}^{c}t_{ki}^{ba}-\sum_{kcd}\langle ka||cd\rangle t_{k}^{d}t_{ij}^{cb}+\sum_{kcd}\langle ka||cd\rangle t_{k}^{d}t_{ji}^{cb}-\sum_{kcl}\langle kl||ic\rangle t_{k}^{a}t_{jl}^{cb}\\
&+\sum_{kcl}\langle kl||ic\rangle t_{k}^{b}t_{jl}^{ca}+\sum_{kcld}\langle kl||cd\rangle t_{i}^{c}t_{k}^{a}t_{j}^{d}t_{l}^{b}-\sum_{kcld}\langle kl||cd\rangle t_{k}^{c}t_{i}^{d}t_{lj}^{ab}+\sum_{kcld}\langle kl||cd\rangle t_{k}^{c}t_{j}^{d}t_{li}^{ab}\\
&-\sum_{kcld}\langle kl||cd\rangle t_{k}^{c}t_{l}^{a}t_{ij}^{db}+\sum_{kcld}\langle kl||cd\rangle t_{k}^{c}t_{l}^{b}t_{ij}^{da}+\frac{1}{2}\sum_{kcld}\langle kl||cd\rangle t_{i}^{c}t_{j}^{d}t_{kl}^{ab}-\frac{1}{2}\sum_{kcld}\langle kl||cd\rangle t_{j}^{c}t_{i}^{d}t_{kl}^{ab}\\
&+\frac{1}{2}\sum_{kcld}\langle kl||cd\rangle t_{k}^{a}t_{l}^{b}t_{ij}^{cd}-\frac{1}{2}\sum_{kcld}\langle kl||cd\rangle t_{k}^{b}t_{l}^{a}t_{ij}^{cd}-\sum_{kcld}\langle kl||cd\rangle t_{i}^{c}t_{k}^{a}t_{lj}^{db}+\sum_{kcld}\langle kl||cd\rangle t_{j}^{c}t_{k}^{a}t_{li}^{db}\\
&+\sum_{kcld}\langle kl||cd\rangle t_{i}^{c}t_{k}^{d}t_{lj}^{ab}-\sum_{kcld}\langle kl||cd\rangle t_{i}^{c}t_{k}^{d}t_{lj}^{ba}+\sum_{kcld}\langle kl||cd\rangle t_{k}^{a}t_{i}^{d}t_{lj}^{cb}-\sum_{kcld}\langle kl||cd\rangle t_{j}^{d}t_{k}^{a}t_{li}^{cb}\\
&+\sum_{kcld}\langle kl||cd\rangle t_{i}^{c}t_{k}^{a}t_{jl}^{db}-\sum_{kcld}\langle kl||cd\rangle t_{i}^{c}t_{k}^{b}t_{lj}^{da}=0
\end{aligned}
\tag{3.61}
$$

One of the common criticisms of the truncated CCM is that it is not variational, and hence, we cannot say how reliable the energies that we obtain by solving them are. This is because unlike a variational theory, the calculated energy is not an upper bound to the exact energy. However, we can address this in the following way: full CI is variational, and full CI and full CC give the same energy. And if CCSD, for example, is a good approximation to full CC (as we shall see subsequently, by comparing CC with MBPT), then we expect the energy obtained from CCSD to be close to that from full CC. And therefore, the CCSD

energy is indeed reliable.

3.6 CCM vs MBPT

We begin by examining the MBPT wave function, and then connecting it with the CCM terms:

$$|\psi\rangle_{MBPT} = |\Phi_{0,\alpha}\rangle + |\Phi_\alpha^{(1)}\rangle + |\Phi_\alpha^{(2)}\rangle + \cdots \tag{3.62}$$

$$|\Phi_\alpha^{(1)}\rangle = \sum_S (\boldsymbol{C_S^{(1)}} + \boldsymbol{C_D^{(1)}} + \dots)|\Phi_{0,\alpha}\rangle \tag{3.63}$$

$$|\Phi_\alpha^{(2)}\rangle = \sum_S (\boldsymbol{C_S^{(2)}} + \boldsymbol{C_D^{(2)}} + \dots)|\Phi_{0,\alpha}\rangle \tag{3.64}$$

We are basically rewriting the perturbative corrections to the wave function at a particular order as a summation over single, double, $\cdots$ excitations, at that order. This is justified, since if we take the corrections to the wave functions in this form, to all orders, and add them up, we get back the coupled cluster wave function. This already tells us that CCSD, for example, contains in it single and double excitations, to all orders of perturbation in the residual Coulomb interaction.

Now, let us consider the first order correction to the wave function, in MBPT:

$$|\Phi_\alpha^{(1)}\rangle = \sum_{n\neq\alpha} \frac{|\Phi_n\rangle\langle\Phi_n|\boldsymbol{H'}|\Phi_{0,\alpha}\rangle}{E_\alpha - E_n} \tag{3.65}$$

$$\boldsymbol{H'} = \boldsymbol{v} - \boldsymbol{v^{HF}} \tag{3.66}$$

If $|\Phi_n\rangle = |\Phi_i^a\rangle$, then note that the bra is a one-hole one-particle excitation, while the ket is the reference state. Therefore, this matrix element represents $\boldsymbol{T_1}$. Specifically, it is that part of $\boldsymbol{T_1}$ that is contained in $\boldsymbol{C_s^{(1)}}$.

If $|\Phi_n\rangle = |\Phi_{ij}^{ab}\rangle$, then:

$$\langle\Phi_n|\boldsymbol{H'}|\Phi_{0,\alpha}\rangle = \langle ab|\boldsymbol{v}|ij\rangle - Exch \tag{3.67}$$

This is like $\boldsymbol{T_2}$, more specifically the part of $\boldsymbol{T_2}$ that is contained in $\boldsymbol{C_D^{(1)}}$.

The second order correction to the wave function, in MBPT, is:

$$|\Phi_\alpha^{(2)}\rangle = \sum_{m,n\neq\alpha} \frac{|\Phi_n\rangle\langle\Phi_n|\boldsymbol{H'}|\Phi_m\rangle\langle\psi_m|\boldsymbol{H'}|\Phi_{0,\alpha}\rangle}{(E_\alpha - E_n)(E_\alpha - E_m)} \tag{3.68}$$

We can already see that if Φ_n is a Slater determinant with two holes excited to two particles, and if Φ_m is one with one-hole one-particle excitation, then both the matrix elements look like $\boldsymbol{T_1}$ each, and therefore the entire term is like the part of $\boldsymbol{T_1^2}$, which is contained in $\boldsymbol{C_D^{(2)}}$. Note that if Φ_n is a single excitation determinant, while Φ_m is double, then we obtain a term that contains in it $\boldsymbol{T_1 T_2}$. This mapping can be repeated for all the other excitations. Note that this way of looking at CC helps us to intuitively identify which excitations may be important (for energy calculations). Consider an example, both $\boldsymbol{T_1}$ and $\boldsymbol{T_2}$ occur in first order in perturbation, while $\boldsymbol{T_!^2}$ occurs in second. Since in perturbation theory, the second order correction is supposed to be smaller than the first, this analysis points that $\boldsymbol{T_1}$ and $\boldsymbol{T_2}$ may be more important than $\boldsymbol{T_1 T_2}$.

3.7 CCM vs CI

In CI, consider the Configuration Interaction Singles Doubles (CISD) approximation:

$$\begin{aligned} \boldsymbol{C_1} &= \boldsymbol{T_1} \\ \boldsymbol{C_2} &= \boldsymbol{T_1^2} + \boldsymbol{T_2} \end{aligned} \tag{3.69}$$

On the other hand, with the same level of hole-particle excitations, $|\psi_{CCSD}\rangle = e^{(T_1+T_2)}|\Phi_0\rangle$. We see that the CCSD approximation contains all the powers of T_1 and T_2. This is due to the exponential nature of the CCSD wave function. Of course, in an actual calculation, we cannot take into account all the terms.

CCM is size extensive independent of the level of truncation. Only full CI is size extensive, any truncation to it makes it lose the property of size extensivity. Consider an N particle system with the ground state wave function $|\psi\rangle$. If the system is made up of two sub-systems, A and B, such that there are N_a particles in A and N_B particles in B, then at $r \to \infty$, $\boldsymbol{H_{AB}} \longrightarrow \boldsymbol{H_A} + \boldsymbol{H_B}$; $[\boldsymbol{H_A}, \boldsymbol{H_B}] = 0$. That would imply that:

$$E_{AB} = E_A + E_B \tag{3.70}$$

$$|\psi\rangle = |\psi_A\rangle \otimes |\psi_B\rangle \tag{3.71}$$

A system is said to be size extensive if it satisfies the above two equations.

Now, consider the SUBn scheme, that is, the m-body partitions of the operator S (for CCM) or F (for CI) are truncated, such that one retains only the components with $m \leq n$. All the higher partitions $m > n$ is set to zero. Consider the SUB2 scheme. In CCM, it is the CCSD approximation:

$$\begin{aligned} |\psi\rangle &= e^{\boldsymbol{T}}|\Phi_0\rangle \\ &= e^{\boldsymbol{T_A}+\boldsymbol{T_B}}|\Phi_0\rangle \\ &= e^{\boldsymbol{T_1^A}+\boldsymbol{T_2^A}+\boldsymbol{T_1^B}+\boldsymbol{T_2^B}}|\Phi_0\rangle \end{aligned} \tag{3.72}$$

Now,

$$\begin{aligned} |\psi^A\rangle \otimes |\psi^B\rangle &= e^{\boldsymbol{T_A}}|\Phi_0^A\rangle \otimes e^{\boldsymbol{T_B}}|\Phi_0^B\rangle \\ &= e^{\boldsymbol{T_A}+\boldsymbol{T_B}}|\Phi_0^A\rangle \otimes |\Phi_0^B\rangle \\ &= e^{\boldsymbol{T_A}+\boldsymbol{T_B}}|\Phi_0\rangle \\ &= e^{\boldsymbol{T_1^A}+\boldsymbol{T_2^A}+\boldsymbol{T_1^B}+\boldsymbol{T_2^B}}|\Phi_0\rangle \end{aligned} \tag{3.73}$$

Both the expressions for $|\psi\rangle$ are the same.

For CISD (Configuration Interaction Singles and Doubles) scheme:

$$\begin{aligned} |\psi\rangle &= (1+\boldsymbol{C_1}+\boldsymbol{C_2})|\Phi_0\rangle \\ &= (1+\boldsymbol{C_1^A}+\boldsymbol{C_1^B}+\boldsymbol{C_2^A}+\boldsymbol{C_2^B})|\Phi_0\rangle \end{aligned} \tag{3.74}$$

Now,

$$\begin{aligned} |\psi^A\rangle &= (1+\boldsymbol{C_1^A}+\boldsymbol{C_2^A}+\dots)|\Phi_0\rangle \\ |\psi^B\rangle &= (1+\boldsymbol{C_1^B}+\boldsymbol{C_2^B}+\dots)|\Phi_0\rangle \\ |\psi^A\rangle \otimes |\psi^B\rangle &= (1+\boldsymbol{C_1^B}+\boldsymbol{C_2^B}+\boldsymbol{C_1^A}+\boldsymbol{C_1^A C_1^B}+\boldsymbol{C_1^A C_2^B} \\ &+ \boldsymbol{C_2^A}+\boldsymbol{C_2^A C_1^B}+\boldsymbol{C_2^A C_2^B})|\Phi_0\rangle \end{aligned} \tag{3.75}$$

Clearly, the above two expressions for $|\psi\rangle$ are not the same. Hence, CISD is not size extensive. In a similar way, it can be shown that any order of truncation leads to loss of size extensivity. Diagrammatically, the extra terms would correspond to the unlinked diagrams.

3.8 The expectation value

We know that:

$$|\psi\rangle = e^{\boldsymbol{T}}|\Phi_0\rangle \tag{3.76}$$
$$\langle\psi| = \langle\Phi_0|(e^{\boldsymbol{T}})^\dagger \tag{3.77}$$

Then, the expectation value of a general operator,$\boldsymbol{A}$, in CCM is given by:

$$\langle A\rangle = \frac{\langle\psi|A|\psi\rangle}{\langle\psi|\psi\rangle} \tag{3.78}$$
$$= \frac{\langle\Phi_0|(e^{\boldsymbol{T}})^\dagger A e^{\boldsymbol{T}}|\Phi_0\rangle}{\langle\Phi_0|(e^{\boldsymbol{T}})^\dagger e^{\boldsymbol{T}}|\Phi_0\rangle} \tag{3.79}$$
$$= \langle\Phi_0|e^{\boldsymbol{T}\dagger}A_N e^{\boldsymbol{T}}|\Phi_0\rangle_C + \langle\Phi_0|A|\Phi_0\rangle \tag{3.80}$$

The last expression is due to Cizek [1]. N means that the operator is normal ordered, and C refers to the condition that each term must be connected. This form of expectation value vastly simplifies the expression, where we need to truncate both the numerator and the denominator. Note that the expression still requires us to truncate the two infinite series' in the numerator. A 'proof' of the expression will be discussed in the section where the diagrammatic reformulation of CCM is presented.

3.9 The relativistic CCM

The relativistic version of the CCM uses the Dirac Hamiltonian, instead of the Schroedinger one, and also uses a four-component wave function, similar to that discussed in the relativistic Hartree-Fock equations' section.

Usually, one chooses the Dirac-Coulomb Hamiltonian (as seen in the Dirac-Fock section), where the electron-nucleus and the electron-electron interactions are classical, Coulombic ones:

$\boldsymbol{H} = \sum_i \{c\boldsymbol{\alpha_i}.\boldsymbol{p_i} + \beta c^2 + \boldsymbol{V_i^{Nuclear}}\} + \sum_{i>j} 1/\boldsymbol{r_{ij}}$,

Again, as discussed in the Dirac-Fock section, a general orbital is represented as:

$$\varphi = \begin{pmatrix} \varphi_1 \\ \varphi_2 \\ \varphi_3 \\ \varphi_4 \end{pmatrix} = \begin{pmatrix} v \\ w \end{pmatrix} = \begin{pmatrix} g(r)\chi_{\kappa m} \\ if(r)\chi_{-\kappa m} \end{pmatrix}; \tag{3.81}$$

3.10 The Normal Coupled Cluster Method (NCCM)

In this variant of the coupled cluster method, the bra and the ket are defined differently:

$$\boldsymbol{H}|\psi\rangle = E|\psi\rangle \tag{3.82}$$
$$\langle\widetilde{\psi}|\boldsymbol{H} = \langle\widetilde{\psi}|E \tag{3.83}$$

where

$$|\psi\rangle = e^{\boldsymbol{T}}|\Phi_0\rangle; \boldsymbol{T} = \sum_{I\neq 0} T_I C_I^+ \tag{3.84}$$
$$\langle\widetilde{\psi}| = \widetilde{\boldsymbol{T}}e^{-\boldsymbol{T}}\langle\Phi_0|; \widetilde{\boldsymbol{T}} = \sum_{I\neq 0} 1 + \widetilde{T}_I C_I^- \tag{3.85}$$

In the above equations, T_Is refer to the t amplitudes, and C_I^+ to the usual operators associated with hole-particle excitations. C_I^- refers to the set of creation and annihilation operators that are associated with de-excitation.

3.10.1 Amplitude equations by variational principle

Consider the energy functional:

$$x = \langle\widetilde{\psi}|\boldsymbol{H}|\psi\rangle \tag{3.86}$$
$$= \langle\Phi_0|(\sum_{I\neq 0}\widetilde{T}_I C_I^- + 1)e^{-\sum_{I\neq 0} T_I C_I^+}\boldsymbol{H}e^{\sum_{I\neq 0} T_I C_I^+}|\Phi_0\rangle \tag{3.87}$$

According to the variational principle:

$$\frac{\delta x}{\delta\widetilde{T}_I} = 0 \Longrightarrow \langle\Phi_0|C_I^+ e^{-\boldsymbol{T}}\boldsymbol{H}e^{\boldsymbol{T}}|\Phi_0\rangle = 0 \tag{3.88}$$
$$\frac{\delta x}{\delta T_I} = 0 \tag{3.89}$$
$$\Longrightarrow \frac{\delta}{\delta T_I}\langle\Phi_0|(\sum_{I\neq 0}\widetilde{T}_I C_I^- + 1)e^{-\sum_{I\neq 0} T_I C_I^+}\boldsymbol{H}e^{\sum_{I\neq 0} T_I C_I^+}|\Phi_0\rangle = 0 \tag{3.90}$$

Using $\sum_{I\neq 0} \widetilde{T}_I C_I^- = \widetilde{T} - 1$, we get:

$$\frac{\delta}{\delta T_I}\langle\Phi_0|\widetilde{T}e^{-\sum_{I\neq 0} T_I C_I^+}\boldsymbol{H}e^{\sum_{I\neq 0} T_I C_I^+}|\Phi_0\rangle = 0$$
$$\langle\Phi_0|\widetilde{T}e^{-\boldsymbol{T}}\boldsymbol{H}C_I^+e^{\boldsymbol{T}}|\Phi_0\rangle - \langle\Phi_0|\widetilde{T}C_I^+e^{-\boldsymbol{T}}\boldsymbol{H}e^{\boldsymbol{T}}|\Phi_0\rangle = 0 \tag{3.91}$$

In the second term in the left hand side, the order of C_I^+ and $e^{-\boldsymbol{T}}$ can be changed, since they commute. Therefore, we get:

$$\langle\Phi_0|\widetilde{T}e^{-\boldsymbol{T}}[\boldsymbol{H}, C_I^+]e^{\boldsymbol{T}}|\Phi_0\rangle = 0 \tag{3.92}$$

3.10.2 Amplitude equations by projection

A general bra state, $\langle\Phi_{gen}|$, looks like:

$\langle\Phi_{gen}| = \langle\Phi_0|C_I^-$

Here, $\langle\Phi_{gen}|$ can be $\langle\Phi_i^a|$, $\langle\Phi_{ij}^{ab}|$, etc. So, a compact notation for the ket amplitude equations would be:

$$\langle\Phi_0|C_I^+e^{-\boldsymbol{T}}\boldsymbol{H}e^{\boldsymbol{T}}|\Phi_0\rangle = 0 \tag{3.93}$$

Now,

$$\begin{aligned}
\langle\widetilde{\psi}|\boldsymbol{H} &= \langle\widetilde{\psi}|E \\
\langle\Phi_0|\widetilde{\boldsymbol{T}}e^{-\boldsymbol{T}}\boldsymbol{H} &= \langle\Phi_0|\widetilde{\boldsymbol{T}}e^{-\boldsymbol{T}}E \\
\langle\Phi_0|\widetilde{T}e^{-\boldsymbol{T}}\boldsymbol{H}e^{\boldsymbol{T}} &= \langle\Phi_0|\widetilde{\boldsymbol{T}}E \\
\langle\Phi_0|\widetilde{T}e^{-\boldsymbol{T}}\boldsymbol{H}e^{\boldsymbol{T}}C_I^+|\Phi_0\rangle &= \langle\Phi_0|\widetilde{\boldsymbol{T}}EC_I^+|\Phi_0\rangle
\end{aligned} \tag{3.94}$$

Consider the right hand side:

$$\begin{aligned}
\langle\Phi_0|\widetilde{\boldsymbol{T}}EC_I^+|\Phi_0\rangle &= \langle\varphi_0|\widetilde{\boldsymbol{T}}C_I^+E|\Phi_0\rangle \\
&= \langle\Phi_0|\widetilde{\boldsymbol{T}}C_I^+e^{-\boldsymbol{T}}Ee^{\boldsymbol{T}}|\Phi_0\rangle \\
&= \langle\Phi_0|\widetilde{\boldsymbol{T}}C_I^+e^{-\boldsymbol{T}}E|\psi\rangle
\end{aligned}$$

$$\begin{aligned} &= \langle\Phi_0|\widetilde{\boldsymbol{T}}C_I^+ e^{-\boldsymbol{T}}\boldsymbol{H}e^{\boldsymbol{T}}|\Phi_0\rangle \\ &= \langle\Phi_0|\widetilde{\boldsymbol{T}}e^{-T}C_I^+\boldsymbol{H}e^{\boldsymbol{T}}|\Phi_0\rangle \end{aligned} \tag{3.95}$$

Therefore, we get:

$$\langle\Phi_0|\widetilde{\boldsymbol{T}}e^{-\boldsymbol{T}}\boldsymbol{H}e^{\boldsymbol{T}}C_I^+|\Phi_0\rangle - \langle\Phi_0|\widetilde{e}^{-\boldsymbol{T}}C_I^+\boldsymbol{H}e^{\boldsymbol{T}}|\Phi_0\rangle = 0 \tag{3.96}$$

$$\langle\Phi_0|\widetilde{\boldsymbol{T}}e^{-\boldsymbol{T}}[\boldsymbol{H}, C_I^+]e^{\boldsymbol{T}}|\Phi_0\rangle = 0 \tag{3.97}$$

3.10.3 The expectation value

It was seen in an earlier section on the expectation value computed using CCM that the numerator as well as the denominator were infinite series', and that they are terminated on physical grounds. It was also seen in earlier sections that the BCH expansion terminates automatically owing to the nature of the Hamiltonian. If the bra and the ket states are treated differently so as to allow the BCH expansion to automatically terminate the infinite series, the need to approximately terminate terms on physical grounds is avoided. That is exactly what NCCM achieves.

$$\langle\boldsymbol{A}\rangle = \frac{\langle\widetilde{\psi}|\boldsymbol{A}|\psi\rangle}{\langle\psi|\psi\rangle} \tag{3.98}$$

$$= \frac{\langle\Phi_0|\widetilde{\boldsymbol{T}}e^{-\boldsymbol{T}}\boldsymbol{A}e^{\boldsymbol{T}}|\Phi_0\rangle}{\langle\Phi_0|\widetilde{\boldsymbol{T}}|\Phi_0\rangle} \tag{3.99}$$

The denominator gives(for NCCSD, say):

$$\begin{aligned} \langle\Phi_0|\widetilde{\boldsymbol{T}}|\Phi_0\rangle &= \langle\Phi_0|(1 + \widetilde{\boldsymbol{T_1}} + \widetilde{\boldsymbol{T_2}})|\Phi_0\rangle \\ &= 1 \end{aligned}$$

This is because:

$$\begin{aligned} \langle\Phi_0|1|\Phi_0\rangle &= 1 \\ \langle\Phi_0|\widetilde{\boldsymbol{T_1}}|\Phi_0\rangle &= \langle\Phi_0|t_a^i i^\dagger a|\Phi_0\rangle \\ &= 0 \end{aligned}$$

$$Likewise, \langle \Phi_0 | \widetilde{\boldsymbol{T_2}} | \Phi_0 \rangle \quad = \quad 0$$

Therefore,

$$\langle \boldsymbol{A} \rangle = \langle \Phi_0 | \widetilde{\boldsymbol{T}} e^{-\boldsymbol{T}} \boldsymbol{A} e^{\boldsymbol{T}} | \Phi_0 \rangle \tag{3.100}$$

Since the denominator is unity (and hence no infinite series) and since $e^{-\boldsymbol{T}} \boldsymbol{A} e^{\boldsymbol{T}}$ terminates depending on the rank of $\boldsymbol{A}$, for example, $e^{-\boldsymbol{T}} \boldsymbol{H} e^{\boldsymbol{T}}$ terminates at the fourth commutator, NCCM expectation value avoids the issue of truncating a series.

3.11 Diagrammatic representation of the CCM

In this section, we shall introduce the diagrammatic approach to CCM. This becomes particularly useful, when we need to evaluate expectation values, for example, where we can directly arrive at the form of an expectation value, without going through any of the tedious algebra.

Let us revisit the linked cluster theorem:

$$e^{-\boldsymbol{T}}\boldsymbol{A}e^{\boldsymbol{T}} = \{\boldsymbol{A}e^{\boldsymbol{T}}\}_c \tag{3.101}$$

Let us write down the normal ordered Hamiltonian, which we saw earlier:

$$\begin{aligned} \boldsymbol{H_N} &= \sum_{pq} h_{pq}\{p^\dagger q\} + \frac{1}{4}\sum_{pqrs}\langle pq||rs\rangle p^\dagger q^\dagger sr; & (3.102)\\ \langle pq||rs\rangle &= \langle pq|\boldsymbol{v}|rs\rangle - \langle pq|\boldsymbol{v}|sr\rangle & (3.103) \end{aligned}$$

We shall expand the one-body part of the Hamiltonian in the following way:

$$\begin{aligned} \sum_{pq} h_{pq}\{p^\dagger q\} &= \sum_{ab} h_{ab}\{a^\dagger b\} + \sum_{ij} h_{ij}\{i^\dagger j\} \\ &+ \sum_{ai} h_{ai}\{a^\dagger i\} + \sum_{ai} h_{ia}\{i^\dagger a\} & (3.104)\\ &= I + II + III + IV & (3.105) \end{aligned}$$

The four terms above correspond to the four diagrams in Figure 1, respectively. These type of diagrams are Feynman-like, and are called the Goldstone diagrams. The figure does not explicitly contain the symbols in the text, but upward arrows indicate particle lines, and downward hole lines. We shall, at this point, introduce the idea of level of excitation (LOE). We assign an LOE of 0 for diagrams a and b, 1 for c, and -1 for d. This can be understood in the following way: In figure a, s particle 'excites' into a particle, and hence no LOE is assigned to it. The same holds for b. However, in c, a hole excites into a particle, and we assign an low of 1. When a particle de-excites into a hole, then we say that the low is -1.

We can rewrite the two-body part of $\boldsymbol{H_N}$ in a similar way, and associate with each term a diagram, with a certain LOE.

$$\begin{aligned}
\sum_{pqrs}\langle pq||rs\rangle p^\dagger q^\dagger sr &= \sum_{abcd}\langle ab||cd\rangle a^\dagger b^\dagger dc \\
&+ \sum_{ajbi}\langle aj||bi\rangle a^\dagger j^\dagger ib + \sum_{abci}\langle ab||ci\rangle a^\dagger b^\dagger ic \\
&+ \sum_{aibc}\langle ai||bc\rangle a^\dagger i^\dagger bc + \sum_{ijkl}\langle ij||kl\rangle i^\dagger j^\dagger lk \\
&+ \sum_{kaij}\langle ka||ij\rangle k^\dagger a^\dagger ji + \sum_{jkia}\langle jk||ia\rangle j^\dagger k^\dagger ai \\
&+ \sum_{abij}\langle ab||ij\rangle a^\dagger b^\dagger ji + \sum_{ajbi}\langle aj||bi\rangle a^\dagger j^\dagger ib \\
&+ \sum_{ijab}\langle ij||ab\rangle i^\dagger j^\dagger ba \qquad (3.106) \\
&= I + II + III + IV + V + VI + VII + VIII + IX \qquad (3.107)
\end{aligned}$$

Note that the second and the ninth diagrams are actually one and the same (Refer Figure 3.2).

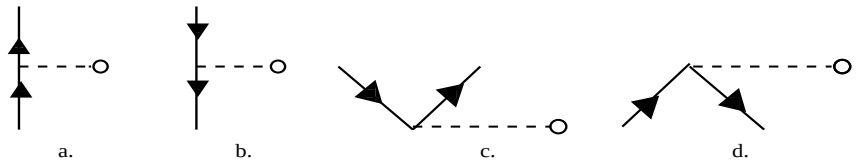

Figure 3.1: One-body normal ordered operators

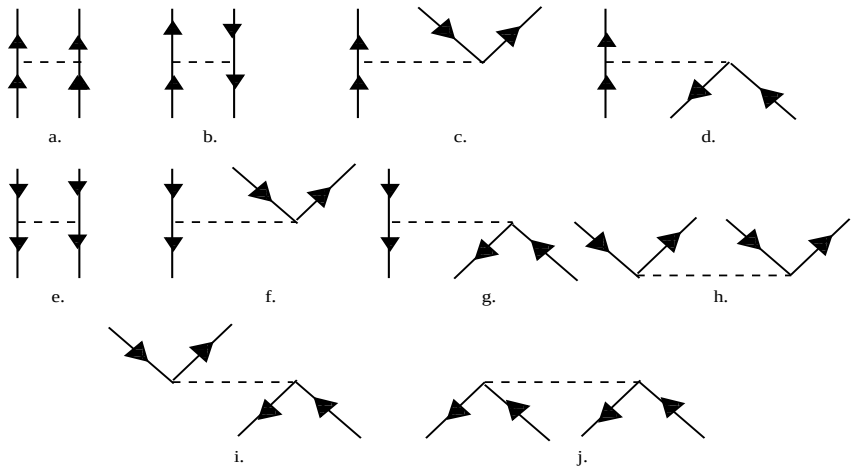

Figure 3.2: Two-body normal ordered operators

These diagrams are one set of the building blocks of Goldstone diagrams that we would use to either solve the CCSD equations or expectation value expressions. Let us consider

the latter situation. Consider an expectation value problem, in the CCSD framework. We still need the diagrammatic counterpart for the T operators. Since they basically excite a hole to a particle, their diagrams ($\boldsymbol{T_1}$ and $\boldsymbol{T_2}$) are as shown in Fig. 3.3.

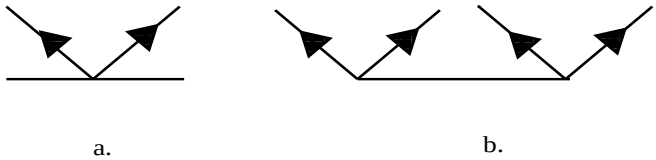

Figure 3.3: Coupled cluster operators, $\boldsymbol{T_1}$ and $\boldsymbol{T_2}$

Finally, since the expression by Cizek requires that each of the terms must be connected, we illustrate what a connected diagram is, in Fig. 3.4.

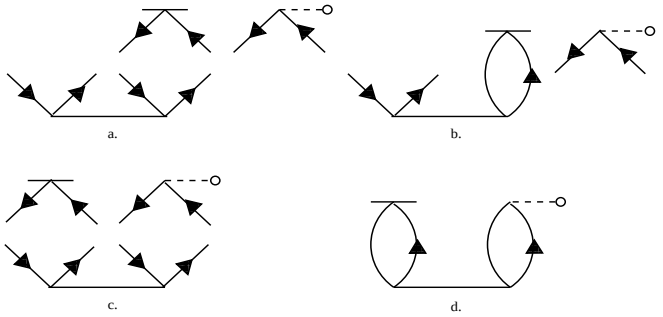

Figure 3.4: Connected and unconnected diagrams: an example

One has to assemble the different blocks for each term in the expectation value expression, with accordance to the rules of LOE.

For example, the CCSD energy equation's diagrams are constructed as follows: We already saw that only $\boldsymbol{T_1}$, $\boldsymbol{T_2}$, and $\boldsymbol{T_1^2}$ terms contribute. We can also understand this diagrammatically. The energy equation is:

$$\Delta E = \langle \Phi_0 | e^{-\boldsymbol{T}} \boldsymbol{H_N} e^{\boldsymbol{T}} | \Phi_0 \rangle \tag{3.108}$$

$$= \langle \Phi_0 | (\boldsymbol{H_N} e^{\boldsymbol{T}})_c | \Phi_0 \rangle \tag{3.109}$$

From the left hand side of the equation, it is clear that the LOE=0 (since the correlation energy is just a number). Hence, the right hand side must have the same LOE too. Hence, if we were to construct a diagram with $\boldsymbol{T_1}$, whose LOE=1, the other block(s) must have an LOE=-1. We also require that the final diagram be connected. There is also an additional requirement that there must be no open lines. With these considerations, we get a. from Fig. 5. Similarly, we see that with $\boldsymbol{T_2}$, we obtain b. from Figure 3.5. We also obtain another diagram satisfying these conditions, for $\boldsymbol{T_1^2}$.

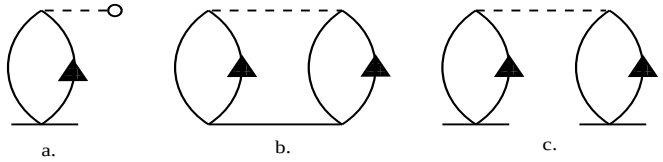

Figure 3.5: CCSD energy diagrams

Before proceeding to show how the diagrammatic approach to solving a CCSD expectation value problem simplifies things, a quick outline of Cizek's expression shall be presented. This largely follows the approach in Bartlett's book; mostly qualitative, but still retaining the essential concepts in an otherwise complicated derivation.

The expectation value of an operator, $\boldsymbol{A}$, as seen earlier, is:

$$\langle \boldsymbol{A} \rangle = \frac{\langle \psi | \boldsymbol{A} | \psi \rangle}{\langle \psi | \psi \rangle} \tag{3.110}$$

Now, the identity $\boldsymbol{A_N} = \boldsymbol{A} - \langle \Phi_0 | \boldsymbol{A} | \Phi_0 \rangle$ seen earlier implies that $\langle \psi | \boldsymbol{A_N} | \psi \rangle = \langle \psi | \boldsymbol{A} | \psi \rangle - \langle \Phi_0 | \boldsymbol{A} | \Phi_0 \rangle \langle \psi | \psi \rangle$. Therefore,

$$\langle \boldsymbol{A} \rangle = \frac{\langle \psi | \boldsymbol{A_N} | \psi \rangle}{\langle \psi | \psi \rangle} + \langle \Phi_0 | \boldsymbol{A} | \Phi_0 \rangle \tag{3.111}$$

$$= \frac{\langle \Phi_0 | (e^{\boldsymbol{T}})^\dagger \boldsymbol{A} e^{\boldsymbol{T}} | \Phi_0 \rangle}{\langle \Phi_0 | (e^{\boldsymbol{T}})^\dagger e^{\boldsymbol{T}} | \Phi_0 \rangle} + \langle \Phi_0 | \boldsymbol{A} | \Phi_0 \rangle \tag{3.112}$$

The basic approach is to factorize the numerator, preferably into terms of which one has the same form as the denominator. Note that all the diagrams in the denominator are, by definition, connected, since the open lines of a $\boldsymbol{T}^\dagger$ term 'connects' with those of a $\boldsymbol{T}$ term. The numerator will have several terms, with the diagrams of each term having connected and disconnected parts. For example, consider $\langle \Phi_0 | \boldsymbol{T_2^\dagger T_1^\dagger O_N T_2} | \Phi_0 \rangle$. The diagrams corresponding to this term are shown in Fig. 3.6. Now, when one achieves such a factorization, the common term in the numerator and the denominator cancel, leaving behind the expression for the expectation value as:

$$\langle \boldsymbol{A} \rangle = \langle \Phi_0 | (e^{\boldsymbol{T}})^\dagger \boldsymbol{A_N} e_C^{\boldsymbol{T}} + \langle \Phi_0 | \boldsymbol{A} | \Phi_0 \rangle \tag{3.113}$$

A sample example of how expressions can be directly obtained through diagrams, with-

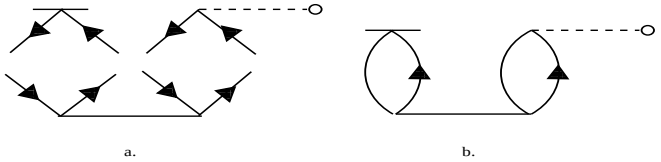

Figure 3.6: Expectation value diagrams: a sample

out having to go through the tedious procedure of applying Wick's theorem, is as follows: Consider the contraction of the one-body operator denoted as d in Figure 3.1, and IV in the expression for the one-body part of the Hamiltonian, with T_1. The one-body part is $\sum_{ia} i^\dagger a$, and the T_1 part is $\sum_{jb} t_j^b a^\dagger j$. Diagrammatically, we just join the hole arm of one diagram to the hole arm of the other, and the particle arm of one to the particle arm of the other. This corresponds to a full contraction, and therefore the net summation has only i and a now. We are then left with $\sum_{ia} t_i^a h_{ia}$. This approach helps a lot when we apply it to terms like $\langle\Phi_0|\boldsymbol{T_2^\dagger T_1^\dagger O_N T_2}|\Phi_0\rangle$, for example. Let us look at this using Figure 3.6. There are two ways of joining the hole arm to a hole arm and a particle arm to a particle arm. The figure shows one of those two ways (called the direct term, the other gives the exchange term). We now simply say that there are four contractions in the two loops, and only four indices are left behind: two hole indices and two particle indices. We therefore obtain: $\sum_{i>j\ a>b} t_a^i t_{ij}^{ab} h_{jb}$. We also need to take into account the sign changes that occur due to the anti-commutation relations, when we follow the algebraic way. This is taken care of by using the rule: $(-1)^{h+l}$, for the sign, where h is the number of hole lines and l is the number of loops. Also, to avoid over counting, we add a factor of 1/2, for equivalent vertices. Using these rules, one can quickly obtain the final expressions for any term in an expectation value expression.

3.12 Calculating the effective electric field using CCM

The effective electric field, like most other properties, is an expectation value problem. In order to calculate it, we need the wave function of the molecule. We obtain that by solving the relativistic CCSD equations. We already saw that we need to have already solved the DF equations, in order to solve the CCSD equations. Therefore, we first solve the DF equations. This is done in a program called UTChem [2]. We also perform atomic orbital (AO) to molecular orbital (MO) integral transformations here. We use the C_8 molecular symmetry to reduce the computational cost [3]. Note that to solve the DF equations, we need to give as input the bond length of the molecule that we are interested in, and also the basis sets, which are, as seen earlier, the trial functions that are used for solving the DF equations. We then need to obtain the t amplitudes, by solving the CCSD equations. This is done by the Dirac08 program [4].

The RCCM equations are solved in Dirac08 using the Jacobi method. The idea is to rewrite the CC equations in the form $AX = B$.
$A_{11}X_1 + A_{12}X_2 + \cdots + A_{1n}X_n = B_1 \Rightarrow X_1 = (B_1 - (A_{12}X_2 + \cdots + A_{1n}X_n))/A_{11}$
$A_{21}X_1 + A_{22}X_2 + \cdots + A_{2n}X_n = B_2 \Rightarrow X_2 = (B_2 - (A_{22}X_2 + \cdots + A_{2n}X_n))/A_{22}$
$\cdots$
$\therefore\ X_i^n = B_i - \sum_{j \neq i} \frac{A_{ij}X_j^{(n-1)}}{A_{ii}}$
Subsequently, the idea is to guess the amplitudes, obtain a new set of amplitudes, and repeat, till convergence is obtained.

We also use what is called the T_1 diagnostic, to see how reliable our CCSD calculations are. It is defined by:

$$T_1 = \sqrt{\frac{t_1 \cdot t_1}{N}} \tag{3.114}$$

The numerator is the dot product of the single excitation amplitude with itself, and the denominator, N, is the number of independent correlated electrons. Empirically, if this quantity is greater than or equal to 0.02, the employed coupled cluster method is probably not too reliable, and the results may not be very accurate [5, 6].

We then need to write an expectation value code to obtain the final value of E_{eff}. Note that this is the algorithm for solving any expectation value problem, using a single reference RCCM. Therefore, we can also compute the PDM of a molecule, using this procedure.

Finally, we add a quick note on the no-pair approximation, where all the excited configurations are built up of positive energy orbitals. If this were not so, the result would

be spurious, since negative energy states can't be treated properly within the conventional formulation of these methods [7]. All our calculations are performed in the no-pair approximation.

3.13 Interplay between relativistic and correlation effects

3.13.1 Introduction

Before applying the RCCM to the HgX molecules, we evaluated the PDM of the SrF molecule [8], and compared it with experiment. This was a good test of the accuracy of our RCCM. SrF was chosen, because Sr is a moderately heavy atom, due to which the relativistic effects are pronounced, as compared to a fluoride of a lighter alkaline earth atom like Mg or Ca. An alkaline earth monofluoride was chosen since it contains only a single valence electron, making it a suitable candidate to test a single reference coupled cluster method, the type that one would use for molecules such as HgX. Also, a high precision measurement of the molecule's PDM is available for comparison with experiment [9].

Moreover, it is among the few molecules that have been laser-cooled thus far [10]. A knowledge of the PDM is also useful in determining the long-range dipole-dipole interaction [11], among ultracold molecules in optical lattices. These interactions will give rise to novel quantum phases, for example, the elusive supersolid state (the simultaneous existence of the superfluid and the density wave phases) [12]. At ultracold temperatures, these molecules can also be used for high precision spectroscopy [13, 14]. An experiment for the search for parity violation using this molecule is currently underway [15].

Later, this work was extended to all the alkaline earth monofluorides, up to BaF, and with a larger basis. This was motivated by the fact that the entire class of molecules and their PDMs are of importance in many applications. For example, after SrF, experiments to laser cool CaF and BaF are in progress. In turn, this opens new avenues for various high precision experiments on the molecules, for example, for CaF, see: Ref. [16]. BaF becomes importance in the context of the NAM [17, 18].

Also, this provides us with a test bed to try understand the interplay between relativistic and correlation effects. For example, the effective electric field (E_{eff}) and the coupling constant of the nuclear anapole moment (NAM), κ_A, depend on the degree of hybridization of the orbitals. Hence, there are similarities in the correlation trends for these properties [19]. Furthermore, E_{eff} arises entirely from relativistic interactions [20, 19, 21, 22], while κ_A is enhanced by relativistic effects. Our work on the interplay between relativistic and correlation effects should be useful in the context of theoretical studies for E_{eff}, and also κ_A.

Moreover, the PDMs of these molecules have been extensively computed, using several approaches [23, 24, 25, 26, 27, 28, 29, 30, 8, 31], and just as in SrF, high precision experimental data are available for some of these molecules [32, 33].

PDMs are also important in determining the polarizing electric field, E_{pol} [34], which plays a role in the sensitivity of eEDM search experiments. Experimental measurements of the PDM are not always available for a proposed eEDM candidate, and in such cases, accurate many-body calculations of the PDM become necessary. This point shall be discussed later in Chapter 6, where we compute the PDMs of the HgX molecules.

3.13.2 Theory

The PDM of a molecule, D, is given by:

$$\begin{aligned} D &= \frac{\langle\psi|\boldsymbol{D}|\psi\rangle}{\langle\psi|\psi\rangle} \\ &= \langle\Phi_0|e^{\boldsymbol{T}\dagger}\boldsymbol{D_N}e^{\boldsymbol{T}}|\Phi_0\rangle_C + \langle\Phi_0|\boldsymbol{D}|\Phi_0\rangle \\ &= \langle\Phi_0|e^{\boldsymbol{T}\dagger}\boldsymbol{D_N}e^{\boldsymbol{T}}|\Phi_0\rangle_C + \langle\Phi_0|(-\sum_i e\boldsymbol{r_i} + \sum_A Z_A e\boldsymbol{r_A})|\Phi_0\rangle \\ &= \langle\Phi_0|e^{T\dagger}D_N e^{T}|\Phi_0\rangle_C + \langle\Phi_0|(-\sum_i e\boldsymbol{r_i})|\Phi_0\rangle \\ &+ \sum_A Z_A e\boldsymbol{r_A}\langle\Phi_0|\Phi_0\rangle \\ &= \langle\Phi_0|e^{\boldsymbol{T}\dagger}\boldsymbol{D_N}e^{\boldsymbol{T}}|\Phi_0\rangle_C + \langle\Phi_0|(-\sum_i e\boldsymbol{r_i})|\Phi_0\rangle \\ &+ \sum_A Z_A e\boldsymbol{r_A} \end{aligned} \tag{3.115}$$

where $\boldsymbol{D}$ is the electric dipole moment operator and e is the charge of the electron. The summation over the electronic coordinates is indicated by i, and that over the nuclear coordinates is indicated by A. $\boldsymbol{r_i}$ is the position vector from the origin to the site of an electron, and $\boldsymbol{r_A}$ is the position vector from the origin to the coordinate of a nucleus. Z_A is the atomic number of the A^{th} nucleus. We have invoked the Born-Oppenheimer approximation in the fourth line of the equations given above. The fluorine atom chosen to be at the origin. Hence, the PDM can be expressed as

$$\begin{aligned} D &= \langle\Phi_0|(1+\boldsymbol{T_1}+\boldsymbol{T_2})^\dagger\boldsymbol{D_N}(1+\boldsymbol{T_1}+\boldsymbol{T_2})|\Phi_0\rangle_C \\ &+ \langle\Phi_0|(-\sum_i e\boldsymbol{r_i})|\Phi_0\rangle + Z_A e r_e \end{aligned} \tag{3.116}$$

where r_e is the equilibrium bond length for the molecule AF, with A=Be, Mg, Ca, Sr or Ba. Note that the $e^{\boldsymbol{T}}$ term has only been expanded linearly in $\boldsymbol{T}$. Later, we shall check

the validity of this approximation too, and conclude that this is indeed a very reasonable approximation. The first term captures the electron correlation effects, while the second is the electronic contribution from the DF calculations. The third gives the nuclear contribution. We shall define the first two terms as the electronic terms, and the third as the nuclear term. The PDM depends on the mixing of opposite parity orbitals. Since their orbitals are hybridized, this is achieved already in polar molecules.

We shall add a quick note on the origin dependence of the PDM. It can be shown that for a system whose net charge is zero, for example, neutral molecules such as those that we considered, the PDM is independent of origin. If the original PDM, D (with some origin that we chose and then calculated), were to be computed after shifting the origin by a, then the new PDM, D_a would be:

$$\begin{aligned} D_a &= \int r'_a \rho(r') d\tau' \\ &= \int (r' - a)\rho(r') d\tau' \\ &= \int r'\rho(r') D\tau' + a \int \rho(r') d\tau' \\ &= D + aQ \end{aligned}$$

In the above equations, ρ refers to the charge density, and Q is the total charge of the system. For a neutral molecule, Q is zero, and hence the PDM does not change, when we displace the origin. We tested this for BeF and MgF, and found that the maximum change in the PDM was for MgF at the QZ level, at about three percent.

3.13.3 Calculation and results

The bond lengths used for BeF, MgF, CaF, SrF and BaF are 1.361, 1.75, 1.967, 2.075 [25, 35] and 2.16 [26, 36] Angstrom respectively.

The details of the basis sets used are shown below in Table I.

The exponential parameters for Sr and Ba were taken from Dyall's basis sets [37]. Then, diffuse and polarization functions from the Sapporo-DKH3 [38] basis sets were added to it. The exponential parameters of the cc-pV (correlation consistent-polarized valence) basis sets from the EMSL Basis Set Exchange Library [39, 40] were used, for Be, Mg, Ca and F. The calculations were done at the DZ, TZ, and QZ levels.

Basis sets optimized using Hartree-Fock theory may not be suitable for studying correlations, and hence correlation consistent basis sets were employed. Polarization functions

are added, to take into account the fact that one orbital may be polarized by another, for example, the s orbital due to p, etc [41]. Also, diffuse functions are added to Sr and Ba to capture effects associated with far nuclear region. This is especially relevant, for properties like the PDM and E_{eff}. The basis sets for Ca does not contain aug-cc-pV diffuse functions, since they are not available for it. For Be, the difference in the PDMs at the QZ level between cc-pV and the aug-cc-pV basis sets is negligible at the CCSD level (1.1 and 1.12 for cc-pV and aug-cc-pV respectively). For MgF, the CCSD PDM increases by around 2 percent (3.07 and 3.13D respectively for cc-pV and aug-cc-pV). Hence, for the lighter elements, diffuse functions do not seem to modify the PDM significantly. For CaF, adding diffuse functions to Ca, by combining Dyall and Saporro basis sets, changes the PDM by 2.2 percent. The PDM of SrF, however, changes by over 6 percent when diffuse functions are added to it [42]! Hence, diffuse functions may become important for heavier systems. Note that diffuse functions have not been added to F, since adding diffuse functions to F does not significantly modify the PDM [42].

Table 3.1: Details of the basis sets used

Atom	Basis
Be	cc-pVDZ: 9s, 4p, 1d cc-pVTZ: 11s, 5p, 2d, 1f cc-pVQZ: 12s, 6p, 3d, 2f, 1g
Mg	cc-pVDZ: 12s, 8p, 1d cc-pVTZ: 15s, 10p, 2d, 1f cc-pVQZ: 16s, 12p, 3d, 2f, 1g
Ca	cc-pVDZ: 14s, 11p, 5d cc-pVTZ: 20s, 14p, 6d, 1f cc-pVQZ: 22s, 16p, 7d, 2f, 1g
Sr	Dyall+Sapporo: 20s, 14p, 9d Dyall+Sapporo: 28s, 20p, 13d, 2f Dyall+Sapporo: 33s, 25p, 15d, 4f, 2g
Ba	Dyall+Sapporo: 25s, 19p, 13d Dyall+Sapporo: 31s, 25p, 15d, 2f Dyall+Sapporo: 37s, 30p, 18d, 3f, 2g
F	cc-pVDZ: 9s, 4p, 1d cc-pVTZ: 10s, 5p, 2d, 1f cc-pVQZ: 12s, 6p, 3d, 2f, 1g

Table II presents the results of the calculations of energies and the PDMs of the molecules, both at the DF and the CCSD levels. The values have been rounded off to the second decimal place.

As the molecules get heavier (more relativistic), the absolute value of the correlation

Table 3.2: Summary of the calculated results of the present work

$Molecule$	$Method$	$Basis$	$E(au)$	$PDM(D)$
BeF	DF	DZ	-114.07	1.32
	DF	TZ	-114.23	1.31
	DF	QZ	-114.26	1.30
	CCSD	DZ	-114.38	0.93
	CCSD	TZ	-114.59	1.06
	CCSD	QZ	-114.67	1.10
	Expt	-	-	-
MgF	DF	DZ	-299.51	3.21
	DF	TZ	-299.52	3.21
	DF	QZ	-299.57	3.16
	CCSD	DZ	-299.96	2.84
	CCSD	TZ	-300.02	3.02
	CCSD	QZ	-300.11	3.07
	Expt	-	-	-
CaF	DF	DZ	-779.31	2.89
	DF	TZ	-779.33	2.82
	DF	QZ	-779.37	2.77
	CCSD	DZ	-780.09	3.01
	CCSD	TZ	-780.21	3.13
	CCSD	QZ	-780.31	3.16
	Expt	-	-	$3.07(7)$
SrF	DF	DZ	-3277.67	2.83
	DF	TZ	-3277.70	2.95
	DF	QZ	-3277.74	3.01
	CCSD	DZ	-3278.85	2.95
	CCSD	TZ	-3279.01	3.42
	CCSD	QZ	-3279.13	3.60
	Expt	-	-	$3.4676(1)$
BaF	DF	DZ	-8235.25	2.42
	DF	TZ	-8235.27	2.28
	DF	QZ	-8235.31	2.65
	CCSD	DZ	-8236.55	2.69
	CCSD	TZ	-8236.71	3
	CCSD	QZ	-8236.82	3.40
	Expt	-	-	$3.170(3)$

energy increases. For a given molecule, the CCSD value of the PDM increases with the size of the basis set.

We can partially understand this, by rewriting the terms in equation 3.116. This shall be done only for the DF and the $\langle\Phi_0|\boldsymbol{D_N T_1}|\Phi_0\rangle_C$ (called the DT_1 term hereafter) terms,

since these are the terms that contribute in a significant way to the PDM. The former can be rewritten as:

$$\begin{aligned} D^{DF} &= \langle\Phi_0|\boldsymbol{D}|\Phi_0\rangle \\ &= \sum_m \langle\varphi_m|\boldsymbol{d}|\varphi_m\rangle \qquad (3.117) \\ &= \sum_m \sum_{k,l} C^{*L}_{m,k} C^{*L}_{m,l} \langle\chi^L_{mk}|\boldsymbol{d}|\chi^L_{ml}\rangle \\ &+ \sum_m \sum_{k,l} C^{*S}_{m,k} C^{*S}_{m,l} \langle\chi^S_{mk}|\boldsymbol{d}|\chi^S_{ml}\rangle \qquad (3.118) \end{aligned}$$

The summation, m, is over the MOs, while k and l are over the AOs. φ_m is the m^{th} MO. χ refers to an AO. The superscripts, L and S, refer to the large and small components, respectively.

In a similar way, the DT_1 term can be rewritten in the following way (the subscript, 'C', is dropped hereafter):

$$\begin{aligned} \langle\Phi_0|\boldsymbol{D_N T_1}|\Phi_0\rangle &= \sum_{i,a} t^a_i \langle\varphi_i|\boldsymbol{d_N}|\varphi_a\rangle \\ &= \sum_{i,a} \sum_{k,l} t^a_i C^{*L}_{i,k} C^{*L}_{a,l} \langle\chi^L_{ik}|\boldsymbol{d}|\chi^L_{al}\rangle \\ &+ \sum_{i,a} \sum_{k,l} t^a_i C^{*S}_{i,k} C^{*S}_{a,l} \langle\chi^S_{ik}|\boldsymbol{d}|\chi^S_{al}\rangle \qquad (3.119) \end{aligned}$$

The final value of PDM depends on the cancellation between these terms, with some of them being positive, while others negative. As the basis set is increased from DZ to TZ, and then to QZ, the number of χs per MO increase. In this class of molecules, the net CCSD PDM increases with increase in basis, after all the cancellations. Physically, one can expect the PDM to change with basis, since the QZ set is closer to the actual wave function than the TZ set, and TZ closer than DZ. Hence, a change in basis would translate into some change in the PDM, depending on how the results converge. Here, convergence refers to the difference in QZ and TZ PDMs being less than that between TZ and DZ. The CCSD PDMs do show convergence, except for BaF. It may be attributed to either of the following two cases, or both: 1. there may be more correlation effects to account for, or 2. insufficient optimization of the basis sets. The PDM increases from BeF to SrF, that is, the quantity increases with the system becoming more relativistic. However, the PDM drops

from SrF to BaF. Also, the absolute value of the correlation effects monotonically increase with the system becoming more relativistic (from 0.2 D for BeF to 0.75 D for BaF), with MgF as an exception. The T_1 diagnostic was around 0.02 or lesser, for all of the molecules, and for all the basis sets.

At the QZ level, the PDMs that we calculated differ from experiment by about 3, 4 and 7 percent, for CaF, SrF and BaF respectively.

The CCSD values of the electronic (QZ) and nuclear contribution to the PDM for the molecules are shown in Table III.

Table 3.3: Electronic (at the CCSD level, with QZ basis sets) and nuclear contributions to the PDM for all the alkaline earth monofluorides

Molecule	Electronic terms	Nuclear term
BeF	-25.05	26.15
MgF	-97.80	100.87
CaF	-185.81	188.97
SrF	-375.16	378.76
BaF	-577.64	581.04

The nuclear term depends on two parameters: the atomic number of the alkaline earth atom (Z), and the equilibrium bond length. Hence, this term increases from BeF to BaF. The electronic terms, on the other hand, depend on the many-body theory used to evaluate the wave function, that is, how much correlation a method (under a given truncation scheme) captures, and on the choice of basis sets. The ratio of the absolute values of the electronic and the nuclear terms can provide us with a sense of which term 'grows' faster among them. From BeF to BaF, they are 0.96, 0.97, 0.98, 0.99 and 0.99 respectively. The ratio is slightly higher (in the third decimal place) for BaF, than SrF. This implies that the electronic term 'grows' faster, with increase in Z. Since the nuclear term is proportional to Z, the electronic terms may be a slightly more sensitive function of Z.

The contributions from each of the 10 terms in Eq. 3.116 is considered, in order to inspect the correlation trends. The last term is the DF contribution. Since D is a one-body operator, when the Slater-Condon rules are applied to the $\langle\Phi_0|\boldsymbol{D_N T_2}|\Phi_0\rangle_C$ (which will be denoted by DT_2 hereafter, and so on for the other terms) and the $T_2^\dagger D$ terms, they vanish. Also, the $\langle\Phi_0|\boldsymbol{D_N}|\Phi_0\rangle_C$ is zero, since the expectation value of a normal ordered operator between Slater determinants vanishes.

The DF term contributes the most to the PDM, followed by the DT_1 term. The latter includes in it important pair correlation effects, like the Breukner pair effect [43]. The DT_1 term is not very significant in BeF and MgF though. In fact, for MgF, the dominant correlation term is $T_2^\dagger D T_2$. The DT_1 term can be understood as the off-diagonal matrix el-

Table 3.4: Contributions from the individual terms to the PDM for all the alkaline earth monofluorides

Term	BeF	MgF	CaF	SrF	BaF
DF	-24.85	-97.72	-186.20	-375.75	-578.39
DT_1	-0.08	-0.02	0.21	0.31	0.4
DT_2	0	0	0	0	0
$T_1^\dagger D$	-0.08	-0.02	0.21	0.31	0.4
$T_1^\dagger D T_1$	-0.02	-0.02	-0.02	-0.03	-0.05
$T_1^\dagger D T_2$	0.02	0.01	0.02	0.02	0.02
$T_2^\dagger D$	0	0	0	0	0
$T_2^\dagger D T_1$	0.02	0.01	0.02	0.02	0.02
$T_2^\dagger D T_2$	-0.06	-0.04	-0.05	-0.04	-0.04

ement between the Slater determinant, and a state, where one orbital is excited to a virtual state, that is, a one hole and one particle excitation in all orders of residual Coulomb interaction. This can be easily seen from the diagrammatic representation of this term, where an electron jumps into a virtual state, and then falls back into its original hole state, after interacting with the PDM operator [8]. When we examine the trends, we observe that the DT_1 term increases monotonically from BeF to BaF. This is strongly tied to the correlation trend in the three heavier molecules. The second most important correlation contribution is from the $T_2^\dagger D T_2$ term, which follows no specific trend, but is always negative. Hence, its effect is to always reduces the PDM. Also, its value is almost the same for all the considered AEMs, that is, it seems to have a rather weak dependence on Z, as compared to the DT_1 term.

The fractional contributions of the correlation effects increase from MgF to BaF, with BaF's contribution being 0.22 D.

Also, the PDM depends on the difference between the nuclear term is from the electronic terms. It was already seen that among the latter, the DF term dominates. Hence, one can say that the DF term's effect is to 'cancel out' a large fraction of the nuclear contribution. The correlation terms can either 'cancel out' or enhance the PDM, as seen from Table IV, for example, they add up to -0.2 for BeF, and 0.75 for BaF). For BeF and MgF, it plays the role of canceling, while for the heavier ones, it adds up.

In the Table below, a quick summary of previous calculations and experiment is presented, and is compared with our results.

Semi-empirical models, on the PDMs of AEMs, and then the experimental measurements' values, shall be discussed first in this section, followed by a detailed comparison of our work with ab initio calculations.

Table 3.5: Comparison of present work with previous calculations and experiment

$Molecule$	$Work$	$Method$	$PDM(D)$
BeF	Langhoff et al [25]	CPF	1.086
	Buckingham et al [29]	MP2	1.197
	Kobus et al [30]	FD-HF	-1.2727
	This work (QZ)		1.10
	Expt	-	-
MgF	Torring et al [23]	Ionic model	3.64
	Langhoff el al [25]	CPF	3.077
	Mestdagh el al [26]	EPM	3.5
	Buckingham el al [29]	MP2	3.186
	Kobus el al [30]	FD-HF	-3.1005
	This work (QZ)		3.06
	Expt	-	-
CaF	Torring et al [23]	Ionic model	3.34
	Rice et al [24]	LFA	3.01
	Langhoff et al [25]	CPF	3.06
	Mestdagh et al [26]	EPM	3.2
	Bundgen et al [27]	MRCI	3.01
	Allouche et al [28]	LFA	3.55
	Buckingham et al [29]	MP2	3.19
	Kobus et al [30]	FD-HF	-2.6450
	This work (QZ)		3.16
	Expt [32]		$3.07(7)$
SrF	Torring et al [23]	Ionic model	3.67
	Langhoff et al [25]	CPF	3.199
	Mestdagh et al [26]	EPM	3.59
	Allouche et al [28]	LFA	3.79
	Kobus et al [30]	FD-HF	-2.5759
	Prasannaa et al [8]	CCSD	3.41
	Sasmal et al [31]	Z-vector	3.4504
	This work (QZ)		3.60
	Expt [45]		$3.4676(1)$
BaF	Torring et al [23]	Ionic model	3.44
	Mestdagh et al [26]	EPM	3.4
	Allouche et al [28]	LFA	3.91
	This work (QZ)		3.40
	Expt [33]		$3.170(3)$

Torring et al [23] performed one of the earliest calculations of the PDMs of the AEMs. They did so by employing an ionic model, and calculated the PDMs of MgF, CaF, SrF and BaF. Their results are then compared with the Rittner model [44], and also with experiment (whatever was then available). The PDM of CaF was experimentally determined to be

3.07(7) D, by Childs et al [32], and that of SrF by Kandler et al [45]. Later that year, the Ligand field approach (LFA) was implemented to obtain 3.01 D for CaF's PDM [24]. Ernst et al [33] measured BaF's PDM to be 3.170(3) D one year later. An electrostatic polarization model (EPM) for calculating the PDMs of MgF, CaF, SrF, BaF, and several other systems was developed by Mestdagh et al [26]. In 1993, the LFA was extended by Allouche et al [28], and the PDMs of Ca, Sr and Ba monohalides were calculated.

Langhoff et al [25] were the first to use an ab initio approach to compute the PDMs of some of the AEMs (and several other molecules), viz., BeF, MgF, CaF, and SrF. They used the experimental values of bond lengths for their calculations (Refer Table III in their work). They used extended STOs (Slater Type Orbitals), and added to them diffuse and polarization functions. Their basis sets were: Be: (6s, 4p, 1d), Mg: (8s, 6p, 4d, 2f), Ca: (10s, 8p, 4d, 2f), Sr: (12s, 10p. 7d, 3f), and F: (6s, 5p, 4d, 2f). The largest basis sets that we used also contain in them diffuse and polarization functions. Also, as seen from Table 3.1, they are larger. They used the CISD and a size extensive version of CISD, called the coupled pair functionals (CPF) method. Since CPF is better than CISD, only their CPF results are used for comparison with our work. However, not all electrons are correlated in their work. Also, their calculations are non-relativistic. Hence, due to a larger basis, a method that can account for higher order correlations, given a level of truncation, and a fully relativistic, all-electron calculation, is an improvement over their results.

The MRCI SD approach was used by Bundgen et al [27], to calculate the ground state PDM of CaF. Their bond length was slightly lesser than the one used by us. Their contracted GTOs were: Ca: [8s, 7p, 3d, 1f] and F: [5s, 4p, 1d], with a total of 17 electrons correlated in their work. In our fully relativistic work, a larger basis set is employed, and all the electrons are correlated. Also, MRCI SD is not size extensive.

To calculate PDMs of BeF, MgF and CaF (and other properties), Buckingham et al [29] used non-relativistic MP2. They calculated the bond lengths first, and then computed the PDMs. They used contracted GTOs: Be: [5s, 3p, 1d], Mg: [6s, 5p, 3d], Ca: [9s, 6p, 3d], and F: [5s, 4p, 2d]. MP2 is size extensive, but their calculations are non-relativistic, and also, MP2 captures single and double excitations, but only to the first order of perturbation in the residual Coulomb interaction.

The work by Kobus et al [30] involved calculating the PDMs by using finite difference HF. However, for heavier AEMs, their results get less accurate, since the correlation effects get important with Z, and HF does not account for them.

Sasmal et al [31] calculated the PDM of SrF to improve upon our earlier result [8], using the Z-vector approach in the RCCM.

3.14 Summary

In this chapter, we discussed the coupled cluster method in great detail. That included the linked cluster theorem, and the diagrammatic representation of CCM. Later, we discussed the application of a relativistic CCSD method to computing the PDMs of AEMs, which are of importance in high precision experiments that probe fundamental physics. We also analyzed the results, and tried to understand the interplay between relativistic and correlation effects. We then compare our results with previous works. Now that we have established the accuracy of our method, and applied it successfully to the PDM of AEMs, we apply it to mercury monohalides in the next chapter, and identify these molecules as promising candidates for future eEDM searches.

BIBLIOGRAPHY

[1] J. Cizek, in Advances in Chemical Physics, Volume XIV: Correlation Effects in Atoms and Molecules, edited by W. C. Lefebvre and C. Moser, Interscience publishers, page 35 (1969).

[2] UTChem 2004: Yanai, T.; Kamiya, M.; Kawashima, Y.; Nakajima, T.; Nakano, H.; Nakao. Y; Sekino, H.; Paulovic, J.; Tsuneda, T.; Yanagisawa, S.; Hirao, K., REL4D: Abe, M.; Iikura, H.; Kamiya, M.; Nakajima, T.; Paulovic, J.; Yanagisawa, S.; Yanai. T.

[3] T. Yanai, R. J. Harrison, T. Nakajima, Y. Ishikawa, and K. Hirao, New implementation of molecular double point-group symmetry in four-component relativistic Gaussian-type spinors, Int. J.. Quantum Chem. **107**, 1382 (2007).

[4] DIRAC, a relativistic ab initio electronic structure program, Release DIRAC08 (2008), written by L. Visscher, H. J. Aa. Jensen, and T. Saue, with new contributions from R. Bast, S. Dubillard, K. G. Dyall, U. Ekstrom, E. Eliav, T. Fleig, A. S. P. Gomes, T. U. Helgaker, J. Henriksson, M. Ilias, Ch. R. Jacob, S. Knecht, P. Norman, J. Olsen, M. Pernpointner, K. Ruud, P. Salek, and J. Sikkema.

[5] T. J. Lee, P. R. Taylor, A diagnostic for determining the quality of single-reference electron correlation methods, Int. J. Quantum Chem., volume 36, issue S23, John Wiley and Sons, Inc., http://dx.doi.org/10.1002/qua.560360824, 199-207 (1989).

[6] W. Klopper and D. P. Tew, Coupled cluster theory: Fundamentals, , C4 Tutorial, Zürich, 2–4 October 2006, URL: http://www.ipc.kit.edu/theochem/download/Kapitel3.pdf.

[7] Wenjian Liu, Advances in relativistic molecular quantum mechanics, Physics Reports, 537(2):59 89 (2014).

[8] V. S. Prasannaa, M. Abe, and B. P. Das, Permanent electric dipole moment of strontium monofluoride as a test of the accuracy of a relativistic coupled-cluster method, Phys. Rev. A **90**, 052507 (2014).

[9] W. E. Ernst, J. Kandler, S. Kindt, and T. Torring, Electric dipole moment of SrF $X^2\Sigma^+$ from high-precision stark effect measurements, Chem Phys Lett **113**, 351 (1985).

[10] E. S. Shuman, S. F. Barry, D. DeMille, Nature **467**, Laser cooling of a diatomic molecule, 820-823 (2010).

[11] C. Trefzger, C. Menotti1, B. Capogrosso-Sansone, M. Lewenstein, Ultracold Dipolar Gases in Optical Lattices, J. Phys. B: At. Mol. Opt. Phys. **44** 193001 (2011).

[12] T. Mishra, R. V. Pai, S. Ramanan, M. Sethi Luthra, B. P. Das, Supersolid and solitonic phases in the one-dimensional extended Bose-Hubbard model, Phys. Rev. A **80** 043614 (2009).

[13] S.C. Mathavan, C. Meinema, J.E. van den Berg, H.L. Bethlem and S. Hoekstra, Deceleration, cooling and trapping of SrF molecules for precision spectroscopy, 46th Conference of the European Groups on Atomic Systems (2014), URL http://egas46.univ-lille1.fr/abstracts/151/151.pdf.

[14] J.E. van den Berg, S.C. Mathavan, C. Meinema, J. Nauta, T.H. Nijbroek, K. Jungmann, H.L. Bethlem, S. Hoekstra, Traveling-wave deceleration of SrF molecules, Journal of Molecular Spectroscopy **300** 22–25 (2014).

[15] J. E. van den Berg, Using cold molecules to detect molecular parity violation, SSP2012, Groningen, URL $https : //www.kvi.nl/ssp2012/material/107 - berg,\_van\_den/slides/107 - 1 - praatjeSSP2012.pdf$.

[16] Ed Hinds, private communication.

[17] M. K. Nayak and B. P. Das, Relativistic configuration-interaction study of the nuclear-spin-dependent parity-nonconserving electron-nucleus interaction constant W_a in BaF, Phys. Rev. A 79, 060502(R) (2009).

[18] D. DeMille, S. B. Cahn, D. Murphree, D. A. Rahmlow, and M. G. Kozlov, Using Molecules to Measure Nuclear Spin-Dependent Parity Violation, Phys. Rev. Lett. 100, 023003 (2008).

[19] M. Abe, G. Gopakumar, M. Hada, B. P. Das, H. Tatewaki, and D. Mukherjee, Application of relativistic coupled-cluster theory to the effective electric field in YbF, Phys. Rev. A 90, 022501 (2014).

[20] L. I. Schiff, Measurability of Nuclear Electric Dipole Moments, Phys. Rev. 132, 2194 (1963).

[21] P. G. H. Sandars, The electric-dipole moments of an atom I. Some general considerations, J. Phys. B: At. Mol. Phys., Volume 1 Number 3, 511 (1968).

[22] B. P. Das, in Aspects of Many-Body Effects in Molecules and Extended Systems, edited by D. Mukherjee (Springer, Berlin, 1989), p. 411.

[23] T. Torring, W. E. Ernst, and S. Kindt, Dipole moments and potential energies of the alkaline earth monohalides from an ionic model, J Chem Phys, **81**, 4614 (1984).

[24] S. F. Rice, H. Martin, and R. W. Field, The electronic structure of the calcium monohalides: A ligand field approach, J Chem Phys **82**, 5023 (1985).

[25] S. R. Langhoff, C. W. Bauschlicher Jr., H. Partridge, and R. Ahlrichs, Theoretical study of the dipole moments of selected alkaline earth halides, J Chem Phys, **84**, 5025 (1986).

[26] J. M. Mestdagh and J. P. Visticot, Semiempirical electrostatic polarization model of the ionic bonding in alkali and alkaline earth hydroxides and halides, Chem Phys, **155**, 79-89 (1991).

[27] P. Bundgen, B. Engels, and S. D. Peyerimhoff, An MRD-CI study of low-lying electronic states in CaF, Chem Phys Lett, Volume 176, number 5, pages 407-412 (1991).

[28] A. R. Allouche, G Wannous and M. Aubert-Frecon, A ligand-field approach for the low-lying states of Ca, Sr and Ba monohalides, Chem Phys, **170**, 11-22 (1993).

[29] A. D. Buckingham, and R. M. Olegario, Hyperfine coupling in alkaline earth monofluorides. Limitations of the ionic model, Chem Phys Lett, Volume 212, issue 3-4, pages 253-259 (1993).

[30] J. Kobus, D. Moncrieff, S. Wilson, Comparison of the electric moments obtained from finite basis set and finite-difference Hartree-Fock calculations for diatomic molecules, Physical Review A, Volume 62, 062503 (2000).

[31] S. Sasmal, H. Pathak, M. K. Nayak, N. Vaval, and S. Pal, Implementation of the Z-vector method in the relativistic-coupled-cluster framework to calculate first-order energy derivatives: Application to the SrF molecule, Phys. Rev. A 91, 030503(R) (2015).

[32] W. J. Childs, L. S. Goodman, U. Nielsen, and V. Pfeufer, Electric dipole moment of CaF ($X^2\Sigma^+$) by molecular beam, laser rf, double resonance study of Stark splittings, J. Chem. Phys. **80**, 2283-2287 (1984).

[33] W. E. Ernst, J. Kandler and T. Torring, Hyperfine structure and electric dipole moment of BaF $X^2\Sigma^+$, J. Chem. Phys. 84, 4769 (1986).

[34] V.S. Prasannaa, A.C. Vutha, M. Abe, and B.P. Das, Mercury Monohalides: Suitability for Electron Electric Dipole Moment Searches, Phys. Rev. Lett. 114, 183001 (2015).

[35] Molecular Spectra and Molecular Structure, IV. Constants of Diatomic Molecules, edited by K. P. Huber and G. Herzberg (Van Nostrand Reinhold, New York, 1979).

[36] Ch. Ryzlewicz and Torring, Formation and microwave spectrum of the 2.SIGMA. radical barium monofluoride, Chem Phys 51, 329 (1980).

[37] K. G. Dyall, Relativistic double-zeta, triple-zeta, and quadruple-zeta basis sets for the 4s, 5s, 6s, and 7s elements, J. Phys. Chem. A, 113, 12638 (2009).

[38] T. Noro, M. Sekiya, and T. Koga, Segmented contracted basis sets for atoms H through Xe: Sapporo-(DK)-nZP sets ($n = D, T, Q$), Theor. Chem. Acc., 131, 1124 (2012).

[39] Schuchardt, K.L., Didier, B.T., Elsethagen, T., Sun, L., Gurumoorthi, V., Chase, J., Li, J., and Windus, T.L., Basis Set Exchange: A Community Database for Computational Sciences, , J. Chem. Inf. Model., 47(3), 1045-1052 (2007), doi:10.1021/ci600510j.

[40] Feller, D., The Role of Databases in Support of Computational Chemistry Calculations, J. Comp. Chem., 17(13), 1571-1586 (1996).

[41] C. David Sherrill, Basis Sets in Quantum Chemistry, URL: http://vergil.chemistry.gatech.edu/courses/chem6485/pdf/basis-sets.pdf.

[42] V. S. Prasannaa, M. Abe, and B. P. Das, Permanent Electric Dipole Moment of Strontium Monoflouride in its ground State Using a Relativistic Coupled Cluster Method: Basis Set Dependence (manuscript under preparation).

[43] E. Eliav, U. Kaldor, and Y. Ishikawa, Relativistic coupled cluster theory based on the no-pair dirac–coulomb–breit hamiltonian: Relativistic pair correlation energies of the xe atom, Int. J. Quantum Chem. 52, 205 (1994).

[44] E. S. Rittner, Binding Energy and Dipole Moment of Alkali Halide Molecules, J. Chem. Phys., 19, 1030 (1951).

[45] W. E. Ernst, J. Kandler, and T. Torring, Hyperfine structure and electric dipole moment of BaF $X^2\Sigma^+$, J. Chem. Phys. 84, 4769 (1986).

4

EFFECTIVE ELECTRIC FIELDS IN MERCURY MONOHALIDES USING THE RELATIVISTIC COUPLED CLUSTER METHOD

4.1 Introduction

This chapter, and the next, are the most important ones in the thesis. In this chapter, we identify mercury monohalides as promising future candidates for eEDM measurements, using our fully relativistic coupled cluster approach.
. We shall first address the question of how and why we chose mercury monohalides (HgX). We recall the figure of merit for an eEDM experiment:

$$\delta d_e \sim \frac{1}{2\pi E_{eff}\sqrt{NT\tau}\eta} \tag{4.1}$$

We need a molecule, in some state, with a large E_{eff}, and if possible, a large polarization factor. Long coherence times and a large number of molecules are experimental factors. Note that all of these conditions are not usually satisfied! The goal is to find a molecule (or molecules), in some state (s), which can give us high experimental sensitivity.

4.1.1 Why HgX?

Taking these factors into account, we have chosen mercury halides (HgF, HgCl, HgBr and HgI; the latter two may be suitable for experiment). Two factors point towards large values of E_{eff} for HgX:
1. It is believed that E_{eff} scales as Z^3, with Z being the atomic number of the heavier atom. This indicates that a heavy system like HgX may give a large E_{eff},
2. Also, there has been some previous works that identified HgF as promising (for example, [1]); however, since computational resources and many-body techniques were not as advanced, the results were not usually in agreement with one another. Also, in the diamagnetic sector, Hg atom is among the leading candidates to probe hadronic sources of P and T violating interactions, and has provided very good bounds on such interactions [2]. This motivates us to try if a diamagnetic system containing Hg can give us promising results for eEDM. Finally, we note that the properties of these type of systems (with a single unpaired valence electron) can be computed accurately, using single reference methods. Also, they are sensitive to eEDM in their ground states itself, unlike systems in some metastable state having two valence electrons. The latter class of systems require a more complicated description [3]. Experimentally, the heavier HgX molecules are more electrically polarizable than HgF, and this in turn leads to better control over systematic effects. In this chapter, we provide the results for the E_{eff}s of HgX, followed by a very brief discussion on the experimental aspects. Before proceeding to discuss these, we shall take a look at some of the theoretical aspects of E_{eff}.

4.1.2 Only the SOMO survives in E_{eff}

In the expression for E_{eff}^{DF}, we can show that only the singly occupied molecular orbital (SOMO) survives. This is because the rest of the terms cancel out. This can be understood as follows:

$$\begin{aligned}\sum_{i}^{MO}\langle\varphi_i|\boldsymbol{h}_{\boldsymbol{eEDM}}^{\boldsymbol{eff}}|\varphi_i\rangle &= \sum_{i'}^{(MO-1)/2}[\langle\varphi_{i'}|\boldsymbol{h}_{\boldsymbol{eEDM}}^{\boldsymbol{eff}}|\varphi_{i'}\rangle \\ &+ \sum_{\bar{i}'}^{(MO-1)/2}\langle\varphi_{\bar{i}'}|\boldsymbol{h}_{\boldsymbol{eEDM}}^{\boldsymbol{eff}}|\varphi_{\bar{i}'}\rangle] \\ &+ \langle\varphi_v|\boldsymbol{h}_{\boldsymbol{eEDM}}^{\boldsymbol{eff}}|\varphi_v\rangle \end{aligned} \tag{4.2}$$

Here, we have decomposed the left hand side of the equation into three terms. The first

and the second summations in the right hand side are the contributions from the doubly occupied orbitals in the Kramer's pairs, $\varphi_{i'}$ and $\varphi_{\bar{i}'}$. The last term is the contribution from SOMO. The Kramer's pair orbitals are related to each other by the time reversal operator ($\boldsymbol{\tau}$) [4]:

$$|\varphi_{\bar{i}'}\rangle = \boldsymbol{\tau}|\varphi_{i'}\rangle \tag{4.3}$$

$$-|\varphi_{i'}\rangle = \boldsymbol{\tau}|\varphi_{\bar{i}'}\rangle \tag{4.4}$$

Therefore,

$$\begin{aligned}\langle\varphi_{\bar{i}'}|\boldsymbol{h}^{\boldsymbol{eff}}_{\boldsymbol{eEDM}}|\varphi_{\bar{i}'}\rangle &= \langle\varphi_{i'}|\tau^{\dagger}\boldsymbol{h}^{\boldsymbol{eff}}_{\boldsymbol{eEDM}}\tau|\varphi_{i'}\rangle \\ &= -\langle\varphi_{i'}|\boldsymbol{h}^{\boldsymbol{eff}}_{\boldsymbol{eEDM}}|\varphi_{i'}\rangle \end{aligned} \tag{4.5}$$

From here, we can see that all terms, except the SOMO term, cancel pairwise.

The last step can be understood in the following way:

$$\boldsymbol{\tau}^{\dagger}\boldsymbol{h}\boldsymbol{\tau} = (-i\boldsymbol{\sigma_y}\boldsymbol{\tau_o})^{\dagger}\boldsymbol{h}(-i\boldsymbol{\sigma_y}\boldsymbol{\tau_o}) \tag{4.6}$$

Here, a shorthand notation for $\boldsymbol{h}^{\boldsymbol{eff}}_{\boldsymbol{eEDM}}$, which is just '$\boldsymbol{h}$', is used. The relation $\boldsymbol{\tau} = -i\boldsymbol{\sigma_y}\boldsymbol{\tau_o}$ is true for spin-1/2 particles, such as the electron [4]. $\boldsymbol{\tau_o}$ is the complex conjugation operator, and $\boldsymbol{\sigma_y}$ is one of the Pauli matrices (in our specific case, it is its 4×4 version).

Let us first evaluate $(-i\boldsymbol{\sigma_y}\boldsymbol{\tau_o})$, and define it as, say, $\boldsymbol{M}$. We do this, since this is a real quantity, and it simplifies things. It is:

$$\boldsymbol{M} = \begin{pmatrix} 0 & -1 & 0 & 0 \\ 1 & 0 & 0 & 0 \\ 0 & 0 & 0 & -1 \\ 0 & 0 & 1 & 0 \end{pmatrix} \tag{4.7}$$

Using the relation $(\boldsymbol{AB})^{\dagger} = \boldsymbol{B}^{\dagger}\boldsymbol{A}^{\dagger}$, one obtains:

$$\boldsymbol{\tau}^{\dagger}\boldsymbol{h}\boldsymbol{\tau} = \boldsymbol{\tau}_{\boldsymbol{o}}^{\dagger}\boldsymbol{M}^{\dagger}\boldsymbol{h}\boldsymbol{M}\boldsymbol{\tau}_{\boldsymbol{o}} \tag{4.8}$$

$$= \boldsymbol{\tau_o^\dagger h \tau_o} \tag{4.9}$$

Using the fact that $\boldsymbol{\tau_o}|\varphi\rangle = |\varphi^*\rangle$, and $\langle\varphi|\boldsymbol{\tau_o^\dagger} = \langle\varphi|$ (where φ is some MO), one obtains:

$$\begin{aligned}
\langle\varphi|\boldsymbol{\tau_o^\dagger h \tau_o}|\varphi\rangle &= \begin{pmatrix} \varphi_\alpha^L & \varphi_\beta^L & \varphi_\alpha^S & \varphi_\beta^S \end{pmatrix} \begin{pmatrix} 0 & 0 & p^2 & 0 \\ 0 & 0 & 0 & p^2 \\ -p^2 & 0 & 0 & 0 \\ 0 & -p^2 & 0 & 0 \end{pmatrix} \begin{pmatrix} \varphi_\alpha^{L*} \\ \varphi_\beta^{L*} \\ \varphi_\alpha^{S*} \\ \varphi_\beta^{S*} \end{pmatrix} \\
&= -\langle\varphi_\alpha^L|\boldsymbol{p^2}|\varphi_\alpha^{S*}\rangle - \langle\varphi_\beta^L|\boldsymbol{p^2}|\varphi_\beta^{S*}\rangle \\
&+ \langle\varphi_\alpha^S|\boldsymbol{p^2}|\varphi_\alpha^{L*}\rangle + \langle\varphi_\beta^S|\boldsymbol{p^2}|\varphi_\beta^{L*}\rangle
\end{aligned} \tag{4.10}$$

The matrices above use the fact that $\boldsymbol{h} = \frac{2icd_e}{e}\boldsymbol{\beta\gamma_5 p^2}$. The factor $\frac{2icd_e}{e}$ does not affect our analysis, so it is ignored. Also, $\boldsymbol{\beta\gamma_5} = \begin{pmatrix} 0 & 0 & 1 & 0 \\ 0 & 0 & 0 & 1 \\ -1 & 0 & 0 & 0 \\ 0 & -1 & 0 & 0 \end{pmatrix}$, in the Dirac basis, which is what we use throughout. Now, when $-\langle\varphi|\boldsymbol{h}|\varphi\rangle$ is evaluated independently, it gives the same result as $\langle\varphi|\boldsymbol{\tau_o^\dagger h \tau_o}|\varphi\rangle$. Therefore, $\boldsymbol{\tau_o^\dagger h \tau_o} = -\boldsymbol{h}$.

In the next subsection, we shall decompose the expression for E_{eff} in a way that makes it suitable for analysis.

4.1.3 What does E_{eff} simplify into?

Let us evaluate the expression for E_{eff}, not at the DF level, but for, say, the Dirac-Coulomb Hamiltonian. The expression we need to evaluate is $2ic\langle\psi|\boldsymbol{\beta\gamma_5 p^2}|\psi\rangle$. Only the SOMO survives, as seen in the earlier section, so we need to solve for $2ic\langle\varphi|\boldsymbol{\beta\gamma_5 p^2}|\varphi\rangle$. φ is the SOMO. We obtain:

$$2ic\langle\varphi|\boldsymbol{\beta\gamma_5 p^2}|\varphi\rangle = 2ic \begin{pmatrix} \varphi^{L\dagger} \\ \varphi^{S\dagger} \end{pmatrix} \begin{pmatrix} 0 & p^2 \\ -p^2 & 0 \end{pmatrix} \begin{pmatrix} \varphi^L \\ \varphi^S \end{pmatrix} \tag{4.11}$$

$$= 2ic(-\langle\varphi^L|\boldsymbol{p^2}|\varphi^S\rangle - \langle\varphi^S|\boldsymbol{p^2}|\varphi^L\rangle) \tag{4.12}$$

$$= -4ic\langle\varphi^L|\boldsymbol{p^2}|\varphi^S\rangle \tag{4.13}$$

Note that two points have been used here. The first is that the two terms do not cancel out, because of the subtle fact that the small component has an i in it. Because of that,

its conjugate transpose does not give back the small component, but the minus of it! The second is that p^2 is Hermitian. Also, note that the final E_{eff} is real, because of the i in the small component.

4.1.4 DF effective electric field in terms of basis sets

Consider the expression given above, but replace the general wave function by the DF one. For example, φ^L is the large component of the DF 4-component spinor. In practice, what we solve for are actually the coefficients accompanying a known basis set. Therefore, expanding the large component gives us: $\varphi^L = \sum_k C_k^L |\chi_k^L\rangle$. Here, C_k^L is the coefficient that we obtain after self consistently solving the DF equations, and χ_k is a basis function. When this is done for the bra and the ket, one obtains:

$\sum_{k=1}^{q} \sum_{l=q+1}^{2q} C_k^{*S} C_l^L \langle \chi_{v,k}^S | \boldsymbol{p^2} | \chi_{v,l}^L \rangle$

This is very similar to the expression for the DF PDM in chapter 4, which we analyzed, except that L and S do not mix in a given matrix element. Note that in the above expression, the factor of 2c is not explicitly mentioned.

4.2 Results

Table I gives the results of our calculations, both at the DF and the CCSD levels. It also gives the details of the basis sets chosen (cc-pV DZ for F, Cl and Br [5], and Dyall's c2v for Hg and I [6]). As in the case of the AEMs, none of the core orbitals were frozen. The bond lengths used were (in nm): HgF (0.200686) [7], HgCl (0.242), HgBr (0.262), HgI (0.281) [8]. The values of E_{eff} are extremely large for all the HgX candidates; they are about one and a half times larger than ThO's effective field [3], and five times that of YbF [9]. Also, the T_1 diagnostics indicate that the CCSD calculations were reliable.

Molecule	Method	Basis	$T_{1,dia}$	E_{eff} (GV/cm)
HgF	DF	Hg:22s,19p,12d,9f,1g F:9s,4p,1d	-	104.25
HgCl	DF	Hg:22s,19p,12d,9f,1g Cl:12s,8p,1d	-	103.57
HgBr	DF	Hg:22s,19p,12d,9f,1g Br:14s,11p,6d	-	97.89
HgI	DF	Hg:22s,19p,12d,9f,1g I:21s,15p,11d	-	96.85
HgF	CCSD	Hg:22s,19p,12d,9f,1g F:9s,4p,1d	0.0268	115.42
HgCl	CCSD	Hg:22s,19p,12d,9f,1g Cl:12s,8p,1d	0.0239	113.56
HgBr	CCSD	Hg:22s,19p,12d,9f,1g Br:14s,11p,6d	0.0255	109.29
HgI	CCSD	Hg:22s,19p,12d,9f,1g I:21s,15p,11d	0.0206	109.30

Table 4.1: Summary of the calculated results (E_{eff}) of the present work.

The table given below compares our result for E_{eff} in HgF with previous calculations. No previous calculations are available for the other HgX candidates.

Work	E_{eff} (GV/cm)
Y Y Dmitriev *et al.* [1]	99.26
Meyer *et al.*[10]	68
Meyer *et al.*[11]	95
This work	115.42

Table 4.2: Effective electric field, E_{eff}, in the HgF molecule.

Dmitriev *et al.* made use of relativistic effective core potentials (ECP) to obtain the value of E_{eff} in HgF. The minimal atomic basis set for F, and five relativistic valence

orbitals $5d_{3/2}$, $5d_{1/2}$, $6s_{1/2}$, $6p_{1/2}$, and $6p_{3/2}$ for Hg, were used. Meyer *et al.* obtained E_{eff} for the same molecule, using a non-relativistic software,in order to compare the results of their method with those from other approaches.

Correlation effects contribute $\sim 10\%$, with cancellations between the eight terms that constitute them. Table III illustrates this by showing their contributions, in HgF.

Term	Contribution (GV/cm)
DF	104.25
$H^{\rm eff}_{\rm EDM}T_1$	10.08
$H^{\rm eff}_{\rm EDM}T_2$	0
$T_1^\dagger H^{\rm eff}_{\rm EDM}$	10.08
$T_1^\dagger H^{\rm eff}_{\rm EDM}T_1$	-3.91
$T_1^\dagger H^{\rm eff}_{\rm EDM}T_2$	0.22
$T_2^\dagger H^{\rm eff}_{\rm EDM}$	0
$T_2^\dagger H^{\rm eff}_{\rm EDM}T_1$	0.22
$T_2^\dagger H^{\rm eff}_{\rm EDM}T_2$	-5.52

Table 4.3: Contributions from the individual terms to the effective electric field of HgF.

Since the sensitivity of an eEDM experiment is $\propto \mathcal{E}_{\rm eff}\sqrt{N}$, where N is the number of molecules whose spin precession is detected, one can look at how the HgX molecules fare in this regard. There is a possibility that large quantities of these molecules can be produced in at ultracold temperatures, for example, by photo-associating laser-cooled mercury and magnetically trapped halogen atoms [12]. The sensitivity of an eEDM experiment also depends on coherence time. This can possibly be taken care of by using an intense and slow beam or fountain of these molecules, which may lead to a coherence time of about $\sim$1 s. These molecules can be detected efficiently too: a repulsive $A^2\Pi$ state above their $X^2\Sigma$ state (the ground state) can dissociate into Hg (^1S) and X (^2P) atoms. One can, hence, state-selectively photodissociate HgX, and use the idea of laser-induced cycling fluorescence on the resulting Hg atom. This can lead to highly efficient detection. Finally, one must be able to polarize eEDM candidate molecules as much as possible by lab electric fields (kV/cm), to take full advantage of their effective electric fields. The relevant quantity that decides the required lab field is $\mathcal{E}_{\rm pol} = 2B_e/D$, where D is the molecular dipole moment (PDM) and B_e is the rotational constant of the molecule. On these grounds, HgBr and HgI are attractive eEDM candidates, because of their large $\mathcal{E}_{\rm eff}$ and low $\mathcal{E}_{\rm pol}$. This shall be discussed in detail, in the next chapter.

4.3 Summary

In this chapter, we have established HgX as potential candidates for future eEDM experiments. In the next chapter, we shall perform a detailed theoretical analysis of the E_{eff} of these molecules.

BIBLIOGRAPHY

[1] Y. Y. Dmitriev and Y. G. Khait and M. G. Kozlov, Calculation of the spin-rotational Hamiltonian including P- and P, T-odd weak interaction terms for HgF and PbF molecules, Phys. Lett. A, 167, 280-286 (1992).

[2] R. Vaidya, Electric Dipole Moment of Neutron, Deuteron and Mercury in Supersymmetry w/o R-parity, talk in PCPV 2013, url: $https$: $//www.prl.res.in/\ bijaya/PCPV - Rishi.pdf$.

[3] T. Fleig and M. K. Nayak,Electron electric dipole moment and hyperfine interaction constants for ThO, J. Mol. Spectrosc., 300,16-21 (2014).

[4] K.G. Dyall and K. Faegri, Jr., Introduction to Relativistic Quantum Chemistry (Oxford University Press,New York,2006).

[5] Schuchardt, K.L. and Didier, B.T. and Elsetha- gen, T. and Sun, L. and Gurumoorthi, V. and Chase, J. and Li, J. and Windus, T.L., Basis Set Exchange: A Community Database for Computational Sciences, J. Chem. Inf. Model., 47(3), 1045-1052 (2007).

[6] K.G. Dyall, Theor. Chem. Acc., Relativistic and nonrelativistic finite nucleus optimized double zeta basis sets for the 4p, 5p and 6p elements (Theor Chem Acc (1998) 99:366-371): addendum, vol 108, issue 6, pages 365 (2002).

[7] S. Knecht and S. Fux and R. van Meer and L. Visscher and M. Reiher and T. Saue, Mössbauer spectroscopy for heavy elements: a relativistic benchmark study of mercury, Theor. Chem. Acc., 129, 631-650 (2011).

[8] Cheung, Nai-ho and Cool, TA, Franck-Condon factors and r-centroids for the $B^2\Sigma - X^2\Sigma$ systems of HgCl, HgBr, and HgI, J. Quant. Spectrosc. Radiat. Transf., 21, issue 5, 397-432 (1979).

[9] Abe, M. and Gopakumar, G. and Hada, M. and Das, B. P. and Tatewaki, H. and Mukherjee, D., Application of relativistic coupled-cluster theory to the effective electric field in YbF, Phys. Rev. A, 90, 022501 (2014).

[10] E. R. Meyer, J. L. Bohn, M. P. Deskevich, Candidate molecular ions for an electron electric dipole moment experiment, Phys. Rev. A, 73, 062108 (2006).

[11] E. R. Meyer and J. L. Bohn, Prospects for an electron electric dipole moment search in metastable ThO and ThF+, Phys. Rev. A 78, 010502(R) (2008).

[12] Rennick, C. J. and Lam, J. and Doherty, W. G. and Softley, T. P., Magnetic Trapping of Cold Bromine Atoms, Phys. Rev. Lett., 112, 023002 (2014).

5

HgX: Analysis of Effective Electric Fields

5.1 Introduction

Previously, the effective electric fields of HgX were computed, and the molecules were identified as promising candidates for eEDM experiments in the future [1]. In this chapter, we shall elaborate on the previous work, in great detail. Particularly, the different contributions to E_{eff} are analyzed, at both the Dirac-Fock and CCSD levels.

5.2 Results and discussions

The bond lengths and the basis sets we used are the same as those in the previous chapter. For the TZ calculations, we again used Dyall's basis and cc-pvTZ basis. Presented below are the results that we obtained:

Term	HgF	HgCl	HgBr	HgI
DF	104.25	103.57	97.89	96.85
$H^{\text{eff}}_{\text{EDM}}T_1$+ cc	20.16	19.34	22.18	24.78
$T_1^\dagger H^{\text{eff}}_{\text{EDM}}T_1$	-3.91	-3.58	-4.07	-4.77
$T_1^\dagger H^{\text{eff}}_{\text{EDM}}T_2$+ cc	0.44	0.194	-0.2	-0.30
$T_2^\dagger H^{\text{eff}}_{\text{EDM}}T_2$	-5.52	-5.96	-6.5	-7.26
Total	115.42	113.56	109.29	109.30

Table 5.1: Contributions, from the individual terms, to the effective electric field of HgX. cc refers to complex conjugate, of the term that it accompanies.

The terms that we obtain from the linear expectation value expression, as well as the total E_{eff} are shown in Table I. Extending this computation from HgF (as in our previous work) to all HgX enables us to study the trends in E_{eff}. Moreover, we had identified HgBr as promising, in our earlier work. Therefore, theoretical details about the HgX molecules other than HgF also become useful.

The DF contribution is the largest, and we observe that it decreases from HgF to HgI. Electron correlation accounts for about 9 percent of the total E_{eff}. From this, we can conclude that for these molecules, both E_{eff} as well as the amount of correlation does not strongly change with Z of the lighter atom. Among the correlation terms, the largest is the $H^{\text{eff}}_{\text{eEDM}}T_1$ term, while the second and the third most important contributions are from the $T_2^\dagger H^{\text{eff}}_{\text{eEDM}}T_2$, and the $T_1^\dagger H^{\text{eff}}_{\text{eEDM}}T_1$ terms, respectively. We also observe that they have a reducing effect on E_{eff}. As we go from HgF to HgBr, the overall values of E_{eff} drop. Note that HgBr and HgI have almost the same values of E_{eff}, even though the DF value of the latter is smaller than the former. We can explain this observation, from the fact that the difference between $H^{\text{eff}}_{\text{eEDM}}T_1$, and the combined $T_1^\dagger H^{\text{eff}}_{\text{eEDM}}T_1 + T_2^\dagger H^{\text{eff}}_{\text{eEDM}}T_2$ terms is larger, in the case of HgI.

We shall now try to understand how the correlation trends vary in the E_{eff}s of HgX, when compared with those in our previous and ongoing works. We had performed the same analysis, both in our earlier work on the PDM of SrF [2], as well as the PDMs of the other alkaline earth monofluorides (AEMs) [3]. Although E_{eff} and PDM appear to be completely different properties, they share similarities, for example, both depend on the

mixing of opposite parity orbitals. Therefore, it becomes worthwhile to see if there are any similarities in their correlation trends. We begin by comparing the correlation trends between the E_{eff} of HgX and the PDMs of the AEMs. Although both are systems with one outer, unpaired electron, we observe that in AEMs, electron correlation can reduce (for example, BeF, by around 20 percent) or increase (for example, BaF, by around 20 percent) the PDM, whereas the effect of correlations on the E_{eff}s of HgX is almost constant. We further notice that the PDMs of HgX follow a completely different trend; correlations decrease the PDM very significantly [4]. Next, we compare the correlations between the E_{eff}s of HgX and YbF, and also RaF. As seen earlier, YbF sets among the best limits for eEDM, while RaF is a promising eEDM candidate. For HgX, correlations come to about nine percent, while for YbF, it is about twenty percent [5]. In the case of RaF [6], it is around thirty percent. All of these are systems with one unpaired electron, and their heavier atoms' atomic numbers are similar, but their effective fields and their correlation effects are vastly different. Let us compare the correlations in HgI and RaF, for example. The correlation effects are around nine percent in HgI, due to nearly half of the $H^{\rm eff}_{\rm eEDM}T_1$ term being cancelled out by the other correlation terms. In RaF, the $H^{\rm eff}_{\rm eEDM}T_1$ term accounts for around 20 GV/cm, while the rest only to -0.5 GV/cm. That is, the values that we finally obtain are due to several cancellations at work, both at DF and the correlation levels. We shall now attempt to understand further how these cancellations are, for HgX. Also, the above mentioned brief discussion points towards the requirement of detailed theoretical studies, in order to understand better the correlation effects as well as the trends, of these class of polar molecules.

Figure I shows some of the Goldstone diagrams from the expectation value expression, given by equation (3.116). The diagrams given are those that correspond to the DF term, $H^{\rm eff}_{\rm eEDM}T_1$, $T_1^\dagger H^{\rm eff}_{\rm eEDM}T_1$, the direct counterparts of the $T_1^\dagger H^{\rm eff}_{\rm EDM}T_2$, and the $T_2^\dagger H^{\rm eff}_{\rm eEDM}T_2$ terms. We do not give the conjugate diagrams, since they give the same result.

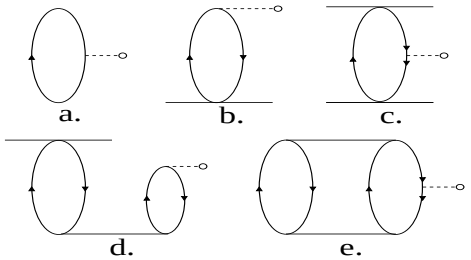

Figure 5.1: Goldstone diagrams for E_{eff}: a. DF term, b. $H^{\rm eff}_{\rm eEDM}T_1$, c. the $T_1^\dagger H^{\rm eff}_{\rm eEDM}T_1$ term, d. Direct diagrams of the $T_1^\dagger H^{\rm eff}_{\rm eEDM}T_2$ term and the $T_2^\dagger H^{\rm eff}_{\rm eEDM}T_2$ term, respectively.

We shall only consider the $H^{\rm eff}_{\rm eEDM}T_1$ diagram (just for illustration), since it contributes

the most to the effective electric field. This term is expanded as

$$\sum_{i,a}[\langle\varphi_i|\{\boldsymbol{h}^{\boldsymbol{eff}}_{\boldsymbol{eEDM}}\}|\varphi_a\rangle\langle\varphi_a|\boldsymbol{t}|\varphi_i\rangle]_C \tag{5.1}$$

The summation is over i and a, with 'i' referring to the occupied orbitals (holes), and 'a' to the virtual orbitals (particles). The above expression is obtained by applying the Slater-Condon rules to the original expression, $\langle\Phi_0|\{\boldsymbol{H}^{\boldsymbol{eff}}_{\boldsymbol{eEDM}}\}\boldsymbol{T_1}|\Phi_0\rangle_C$. Mathematically, $H^{\rm eff}_{\rm eEDM}T_1$ is an all-order residual Coulomb interaction, which leads to an electron from an occupied orbital, 'i', jumping into a virtual orbital, 'a', and then falling back into the same state, 'i', after the interaction of the particle with the eEDM. This diagram represents several correlation effects, like the Brueckner pair correlation (BPC) [7], among others, but is not at all obvious from the Goldstone diagram, because the T_1 part embodies in it the residual Coulomb interaction, to all orders of perturbation. For greater clarity, we consider a prototypical second order BPC (See Figure 2), as one example of the several physical effects contained in a coupled cluster diagram. The figure is a many-body perturbation theory (MBPT) diagram, and it represents a valence orbital, denoted by v, interacting with a core orbital, i, through one order of Coulomb interaction, so that i is excited to a virtual orbital, a, and v to b. Then, a and b interact through an order of Coulomb interaction (and hence a total of two orders of Coulomb interaction), so that a returns to the orbital i, and b to c. Then, c interacts with a single particle's eEDM (denoted by O), and de-excites to v. This diagram is equivalent to $H^{\rm eff}_{\rm eEDM}T_1^{(2),BPC}$, where the superscript denotes a perturbation that is second order in the residual Coulomb interaction, due to BPC. We can extend these BPC effects to higher orders in the Coulomb interaction, for example, figure 3, which shows a third order BPC. As mentioned earlier, the $H^{\rm eff}_{\rm eEDM}T_1$ term accounts for all orders of this effect, as well as many other such physical effects. This example is a testament of the power of a coupled cluster theory.

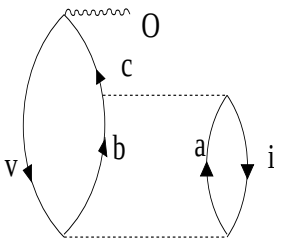

Figure 5.2: A MBPT diagram, representing 2^{nd} order Brueckner pair correlation

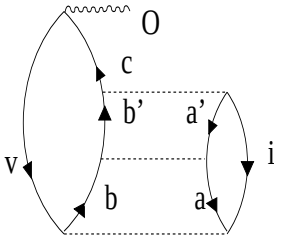

Figure 5.3: A MBPT diagram, representing 3^{rd} order Brueckner pair correlation

Table II gives the contributions to E_{eff}, at the DF level, with TZ basis sets. The same analysis with the DZ basis sets isn't presented, since TZ is closer to the actual wave function than DZ, and also, the results using both the basis sets display the same trend. Before we start the discussion on the results, we shall quickly comment on the notation. In the second column, for example, $s - p_{1/2}$, refers to $\sum_s \sum_{p_{1/2}} C_s^{*S} C_{p_{1/2}}^L \langle \chi_{v,s}^S | \boldsymbol{p^2} | \chi_{v,p_{1/2}}^L \rangle$. The first and the second summations are over all the small component basis sets, and the large component basis sets of the s and $p_{1/2}$ angular momentum functions, respectively. We recall that the mixing between orbitals of same parity is zero, and therefore, terms that mix s and d, for example, vanish. We have only given s, $p_{1/2}$, $p_{3/2}$, $d_{3/2}$, $d_{5/2}$, and $f_{5/2}$ orbitals for Hg, and s and $p_{1/2}$ for X, in the Table, since the other terms contribute negligibly to E_{eff}^{DF}. We can also observe this in the Table, by looking at the difference between the rows labelled, 'Total', which is the sum of the mixings associated with the orbitals considered, and 'DF', which is the total contribution at the DF level. This difference decreases from F to Br. The combined $s - p_{1/2}$ and $p_{1/2} - s$ contribution from Hg dominates, accounting for over hundred percent of the total DF value of E_{eff} for HgF, HgCl, and HgBr. In the case of HgI, the halide atom's contribution becomes important, and hence we do not see such overwhelming dominance of the term from the heavy atom.

We also see that for all of the terms, the absolute magnitude for Hg drops, as we go from from F to I. In X, however, we observe the opposite trend, especially in the case of HgI, where the contribution increases E_{eff} by more than 2.5 GV/cm.

Since the he angular momentum functions are, in a strict sense, not atomic orbitals, but actually terms from the basis sets that we choose, we cannot narrow down on the principal quantum numbers of the orbitals that contribute significantly. What we can do, however, is intuitively guess that the major contribution is from the 6s and the $6p_{1/2}$ (virtual) orbitals of the Hg atom, since they lie close in energy. Also, their radial overlap is large. Moreover, we can also expect that the matrix elements of the eEDM operator between these two orbitals of opposite party be large.

That the $s - p_{1/2}$ and $p_{1/2} - s$ mixing in the heavier atom is important in the E_{eff} of HgF has been pointed out in the past, for example, Ref.s [8]. We shall compare the results

that we obtained with the previous works a little later in this chapter. We have, in our work, accounted for not only the $s - p_{1/2}$ and $p_{1/2} - s$ mixing, but also that of the other orbitals, and for both the atoms in HgX. We then see that the $s - p_{1/2}$ mixing of the heavier atom that dominates, among all other terms. In the Table, we have only shown the result for $s - p_{1/2}$ and $p_{1/2} - s$ mixing in the halide atom. This is because we found that the other contributions from the lighter atom are negligible. Also, note that in HgI, for example, the 'lighter' atom is heavy enough for relativistic effects to become pronounced. However, it is surprising to see that even so, the $s - p_{1/2}$ and $p_{1/2} - s$ mixing from I is very small.

Finally, we see that it is not just the large values of the $s - p_{1/2}$ and the $p_{1/2} - s$ mixings (of the heavier atom) that matter, but what remains when they cancel each other's contributions. This illustrates the important idea of cancellations, which occur in these kind of ab initio calculations. In the case of iodine (for HgI), the two terms by themselves cannot be neglected, but since they cancel each other out almost completely, they leave behind a very small contribution to the DF E_{eff}.

Atom	Mixing	HgF	HgCl	HgBr	HgI
Hg	$s - p_{1/2}$	-266.29	-262.07	-249.39	-242.34
Hg	$p_{1/2} - s$	373.37	367.74	349.42	339.56
Hg	$p_{3/2} - d_{3/2}$	31.22	25.22	21.84	20.99
Hg	$d_{3/2} - p_{3/2}$	-32.26	-26.35	-22.48	-21.84
Hg	$d_{5/2} - f_{5/2}$	-0.91	-0.51	-0.39	-0.33
Hg	$f_{5/2} - d_{5/2}$	0.92	0.52	0.4	0.33
X	$s - p_{1/2}$	-2.78	-4.85	-10.58	-17.19
X	$p_{1/2} - s$	2.79	4.92	11.17	19.87
Total:		106.06	104.62	99.99	99.05
DF		105.47	104.03	99.55	98.99
	$s - p_{1/2}$ and $p_{1/2} - s$	107.08	105.67	100.03	97.22

Table 5.2: Summary of the DF results, of the contributions from various orbitals' mixings, at the TZ level

We shall now try to expound why the $H_{\mathrm{eEDM}}^{\mathrm{eff}} T_1$ term (and its complex conjugate) is large, among the seven non-zero correlation terms. We already observed that the DF contribution is the leading one among others, and this is because of the large difference between the large $s - p_{1/2}$ and $p_{1/2} - s$ terms, of Hg (the notation is same as that in Table II). We recall that s is an occupied orbital, and that $p_{1/2}$ is a virtual. If we only focus only on the matrix elements (their values are several orders larger than their corresponding coefficients), we see that those of the form,$\langle o|\boldsymbol{h}_{\boldsymbol{eEDM}}^{\boldsymbol{eff}}|v\rangle$ (denoting occupied orbitals as, 'o', and virtual as, 'v'), occur not only in the DF term, but also in the expression for $H_{\mathrm{eEDM}}^{\mathrm{eff}} T_1$ (which means that it also contains matrix elements between s and $p_{1/2}$). The difference

is that $H^{\rm eff}_{\rm eEDM}T_1$ also has a t_1 amplitude, which is an indicator of the "weight" associated with a given one-hole one-particle excitation. The t amplitudes are like probability amplitudes, and are therefore lesser than one. This means that we can see the amplitude as having a "reducing" effect on the $H^{\rm eff}_{\rm eEDM}T_1$ term, for every combination of i and a. This is presumably why $H^{\rm eff}_{\rm eEDM}T_1$ is not as large as the DF contribution; the large matrix elements come with the smaller values of the t_1 amplitudes. This is, of course, not the only reason why the DF term is much larger than the other terms. It is because the term also contains matrix elements of the type $\langle o|\boldsymbol{h}^{\boldsymbol{eff}}_{\boldsymbol{eEDM}}|o\rangle$ and $\langle v|\boldsymbol{h}^{\boldsymbol{eff}}_{\boldsymbol{eEDM}}|v\rangle$, and their net cancellation also contributes in the final value of the DF term. Also, there are cancellations between several terms that make $H^{\rm eff}_{\rm eEDM}T_1$, recalling that not all matrix elements or the t_1 amplitudes are positive.

Let us now examine the matrix elements, of the form $\langle o|\boldsymbol{h}^{\boldsymbol{eff}}_{\boldsymbol{eEDM}}|v\rangle$. They appear only in $H^{\rm eff}_{\rm eEDM}T_1$ and $T_2^\dagger H^{\rm eff}_{\rm eEDM}T_1$ (and its complex conjugate). But, we observe that the latter is, in fact, very small, compared to the former. This is probably because to two reasons, the first being the nature of the cancellations that occur among the four terms that make $T_2^\dagger H^{\rm eff}_{\rm eEDM}T_1$:

$$\sum_{i>j,a>b}[t^{ab*}_{ij}t^a_i\langle b|\boldsymbol{h}^{\boldsymbol{eff}}_{\boldsymbol{eEDM}}|j\rangle + t^{ab*}_{ij}t^b_j\langle a|\boldsymbol{h}^{\boldsymbol{eff}}_{\boldsymbol{eEDM}}|i\rangle - t^{ab*}_{ij}t^a_j\langle b|\boldsymbol{h}^{\boldsymbol{eff}}_{\boldsymbol{eEDM}}|i\rangle - t^{ab*}_{ij}t^b_i\langle a|\boldsymbol{h}^{\boldsymbol{eff}}_{\boldsymbol{eEDM}}|j\rangle] \tag{5.2}$$

We have neither mentioned explicitly that the operator is normal ordered, nor that each term is connected. These four terms, respectively, are 0.72, 0.24, -0.03, and 0.77, for HgF, the representative case (this is because we expect the trends to be similar for the other HgX). All these four terms have matrix elements of the form, $\langle o|\boldsymbol{h}^{\boldsymbol{eff}}_{\boldsymbol{eEDM}}|v\rangle$. Among those, two are dominant, but they almost cancel each other out. The second reason can be attributed to the presence of another t amplitude, t_2, which is also less than one, and this "reduces" the net contribution even more.

The $T_1^\dagger H^{\rm eff}_{\rm eEDM}T_1$ term is made of matrix elements of types $\langle o|\boldsymbol{h}^{\boldsymbol{eff}}_{\boldsymbol{eEDM}}|o\rangle$ and $\langle v|\boldsymbol{h}^{\boldsymbol{eff}}_{\boldsymbol{eEDM}}|v\rangle$. To see their contribution, we expand $T_1^\dagger H^{\rm eff}_{\rm eEDM}T_1$:

$$\begin{aligned} &- \sum_{i,j,a} t^{a*}_i t^a_j\langle j|\boldsymbol{h}^{\boldsymbol{eff}}_{\boldsymbol{eEDM}}|i\rangle + \sum_{i,a,b} t^{a*}_i t^b_i\langle a|\boldsymbol{h}^{\boldsymbol{eff}}_{\boldsymbol{eEDM}}|b\rangle \\ &- \sum_{i,a} t^{a*}_i t^a_i\langle i|\boldsymbol{h}^{\boldsymbol{eff}}_{\boldsymbol{eEDM}}|i\rangle + \sum_{i,a} t^{a*}_i t^a_i\langle a|\boldsymbol{h}^{\boldsymbol{eff}}_{\boldsymbol{eEDM}}|a\rangle \end{aligned} \tag{5.3}$$

$$= \quad I + II + III + IV \tag{5.4}$$

The first term corresponds to Figure 1. c, while the second is similar to the figure, except that the eEDM vertex occurs not between two holes, but between two particles. The third term is same as the first again, except that both the holes are the same orbitals, that is, the interaction of the hole with the eEDM leaves the particle unchanged. The fourth is once again, same as the second, but with the two particles being the same orbital, instead of two holes. We have expanded $T_1^\dagger H_{\rm eEDM}^{\rm eff} T_1$ in this particular fashion, so that we can discern which type of matrix elements contribute to it significantly. Table III summarizes the contributions to this term.

Term	Contribution (GV/cm)
I	10^{-3}
II	2.94
III	-4.44
IV	2.4

Table 5.3: The terms that contribute to $T_1^\dagger H_{\rm eEDM}^{\rm eff} T_1$

From the Table, we observe that a significant contribution to the magnitude of these terms come from those that contain the eEDM operator between the same orbitals (terms II and III). These matrix elements are non-zero, even though $\boldsymbol{h_{eEDM}^{eff}}$ is P-odd. This is due to the fact that the orbitals are actually MOs, and each MO is a linear combination of basis functions, of different angular momenta. In fact, in $T_2^\dagger H_{\rm eEDM}^{\rm eff} T_2$ term, the major contribution is also from matrix elements between the same orbitals (-4.7 GV/cm).

Table IV presents a summary of the results obtained from previous works. Since the results are available for HgF only, we briefly discuss those, and compare them with our result. The very first work on HgF's E_{eff} was by Kozlov [9]. They adopted a relativistic, and semi-empirical calculation. The main theme of the paper was the nuclear anapole moment, and electron-nucleus P and T violating interactions. Because it is a semi-empirical calculation, it cannot break the final value of E_{eff} into its constituent DF and correlation parts. Therefore, their Table only gives the final result.

In a later work, Dmitriev et al [10] calculated the E_{eff} of HgF. They used their calculated bond length, of 2.11 Angstrom, and employed a minimal atomic basis set for F. For Hg, they used five relativistic valence orbitals, $5d_{3/2}$, $5d_{5/2}$, $6s_{1/2}$. $6p_{1/2}$, and $6p_{3/2}$. Their final result for E_{eff} was about 100 GV/cm. We can describe their computation as quasi relativistic, because it requires the addition of the spin-orbit interaction to a non-relativistic Hamiltonian, whereas our work is fully relativistic, in that we use a Dirac-Coulomb Hamil-

tonian, instead of an effective one. This approach has the spin-orbit interaction as well as other effects built into it. Dmitriev et al also did not account for orbital mixing beyond $d_{5/2}$. Also, the effect of F was not taken into account, and only the principal quantum numbers 5 and 6 were considered. Our work makes no such restrictions. Finally, they had used CI, with only three outer electrons excited. We do not freeze any of the occupied orbitals, and therefore, the Hilbert space that we have considered, in order to accurately capture the correlation effects, is larger than that that they used. We also note that our error estimate of 5 percent is better than theirs, which is 20 percent. Also, their estimate of E_{eff} does not separate the DF and correlation contributions, while we have provided a detailed description of both, in our work. Finally, fortuitous cancellations may be why their HgF E_{eff} closely agree with ours. For example, in their work, they also calculated the PDM of HgF to be 4.15 D. But, we obtain 2.61 D, at the CCSD level!

Meyer et al [8] calculated E_{eff} of several molecules, including HgF. They used their non-relativistic software for this, to compare it with the accuracy of their method. In a later work, they improved their result to 95 GV/cm [11].

In our previous work on HgX [1], we had used the relativistic coupled cluster method, and shown that E_{eff}, for all the HgX molecules, is much larger than the rest of the current eEDM candidates. In this work, we have performed a detailed analysis of the physical effects involved at the DF as well as the correlation levels. We wish to emphasize that we also decompose the final value of E_{eff}, into its DF and correlation contributions, in order to analyze them.

Work	$\mathcal{E}_{\text{eff}}$ (GV/cm)
Y Y Dmitriev *et al.* [10]	99.26
Meyer *et al.*[8]	68
Meyer *et al.*[11]	95
This work	115.42

Table 5.4: Effective electric field, $\mathcal{E}_{\text{eff}}$, in the HgF molecule, calculated in earlier literature

The error estimates are the same as that in our previous work, since we are only expounding the theoretical aspects of the earlier work, here(Refer [1]). However, in our latest ongoing work, we have improved upon the E_{eff}s of HgX, using a finite field approach [12]. The non-linear terms in the expectation value expression, in fact, contribute much lesser than our earlier estimate, which is 3.5 percent.

5.3 Summary

We have computed the effective electric fields of mercury monohalides, without freezing any of the occupied orbitals. We used Dyall's basis for Hg and I, whereas for the other halides, we used the cc-pV basis. We show that the DF term contributes the most to E_{eff} (about ninety percent). Also, we report the trends in some of the correlation terms, at the DZ level. We observe that the one hole-one particle excitation contributes the most, at the coupled cluster level. We also present an example of a physical effect (which can be seen explicitly in MBPT) that this diagram subsumes. Also, we study the mixings of those atomic orbitals that significantly contribute to the DF value of E_{eff}. We also observe their trends, at the TZ level. The $s - p_{1/2}$ mixing in Hg is found to contributes the most to E_{eff}^{DF}. In the next chapter, we shall compute the PDMs of HgX molecules, since the PDM plays an important role in the sensitivity of an eEDM experiment.

BIBLIOGRAPHY

[1] V.S. Prasannaa, A.C. Vutha, M. Abe, and B.P. Das, Mercury Monohalides: Suitability for Electron Electric Dipole Moment Searches, Phys. Rev. Lett. 114, 183001 (2015).

[2] V. S. Prasannaa, M. Abe, and B. P. Das, Permanent electric dipole moment of strontium monofluoride as a test of the accuracy of a relativistic coupled-cluster method, Phys. Rev. A 90, 052507 (2014).

[3] V. S. Prasannaa, S. Sreerekha, M. Abe, V. M. Bannur, and B. P. Das, Permanent electric dipole moments of alkaline-earth-metal monofluorides: Interplay of relativistic and correlation effects, Phys. Rev. A 93, 042504 (2016).

[4] V. S. Prasannaa, M. Abe, B. P. Das, Asian Journal of Physics, in the issue, 'Advances in High Precision Spectroscopy and Tests of Fundamental Physics', Vol. 25, No 10 , page 1259 (2016).

[5] M. Abe, G. Gopakumar, M. Hada, B. P. Das, H. Tatewaki, and D. Mukherjee, Application of a Relativistic Coupled-Cluster Theory to the Effective Electric Field in YbF, Phys. Rev. A 90, 022501 (2014).

[6] V. S. Prasannaa et al, unpublished.

[7] I. Lindgren and J. Morrison, Atomic Many-Body Theory, 2nd ed. (Springer-Verlag, Berlin, 1986).

[8] E. R. Meyer, J. L. Bohn, and M. P. Deskevich, Candidate molecular ions for an electron electric dipole moment experiment, Phys. Rev. A 73, 062108 (2006).

[9] M. G. Kozlov, Semiempirical calculations of P and P,T odd effects in diatomic molecule radicals, Zh. Eksp. Teor. Fiz, 89, 1933 (1985).

[10] Y. Y. Dmitriev, Y. G. Khait, M. G. Kozlov, L. N. Labzovsky, A. O. Mitrushenkov, A. V. Shtoff, and A. V. Titov, Calculation of the spin rotational Hamiltonian including P and P, T odd weak interaction terms for HgF and PbF , Phys. Lett. A 167, 280 (1992).

[11] E. R. Meyer and J. L. Bohn, Prospects for an electron electric dipole moment search in metastable ThO and ThF+, Phys. Rev. A 78, 010502(R) (2008).

[12] V. S. Prasannaa, M. Abe, V. M. Bannur, B. P. Das, to be submitted (2017).

6

PERMANENT DIPOLE MOMENTS OF HGX

6.1 Introduction

As seen in the previous chapters, PDMs play a role in estimating the sensitivity of an eEDM experiment. One needs to take into account the extent to which a molecule can be polarized, by an external lab field. A molecule with as high an E_{eff} as possible, and in which one can polarize it with as low a lab field as possible, is a good option for eEDM search experiment, besides other experimental features. The latter is quantified by the polarizing electric field, $E_{pol} = 2B/D$, where B is the rotational constant, and D the PDM. In this chapter, the PDMs of HgX and their correlation trends shall be discussed.

From our earlier work [1] as well as that of others [2], we have observed that correlation effects for the PDM of a one valence electron diatomic seems to be around ten percent. However, the HgX molecules' PDMs show an entirely different trend! This illustrates the importance of accurate many-body calculations of not just quantities like effective electric fields, but also those such as PDMs, where experimental data is not yet available.

6.2 Results

The same bond lengths from our earlier work on HgX were used. We also used the same basis sets, for consistency in the calculations.

Table I gives the details of the DF and the CCSD contributions to the PDMs.

Table 6.1: Summary of the calculated results of the present work; the basis set for Hg: 22s,19p,12d,9f,1g

Molecule	$Method$	$PDM(D)$
HgF	DF	3.959
HgCl	DF	4.23
HgBr	DF	4.40
HgI	DF	3.915
HgF	CCSD	2.609
HgCl	CCSD	2.721
HgBr	CCSD	2.364
HgI	CCSD	1.644

The DF values of PDM increase from HgF to HgBr, and reduces slightly for HgI. The same trend is observed in the effective fields too, of these molecules. However, the similarities end there, since unlike the HgX E_{eff}s, which had almost the same amount of correlation, HgX PDMs' correlation effects are drastically different. In fact, HgI's correlation terms account for over hundred percent of the DF value! This would mean that the sensitivity of the HgI eEDM experiment would be almost twice as high, if one were to only use the DF value. This illustrates the kind of scenarios, where accurate computation of properties are necessary, when experimental values aren't available. Most other eEDM candidates do not appear to have such large correlation contributions, for example, the PDM of YbF at the DF level is 3.21 D, and is 3.6 D at the CCSD level [2]. As the lighter element's Z increases, so does the correlation contribution. In the work on AEMs' PDMs, it was observed that the quantity's correlation part increases with Z of the heavier atom. However, in this case, the heavier atom is always Hg. Also, for HgX, correlations reduce the PDM, like in the case of BeF, MgF, and CaF. However, the correlations increase the PDMs of SrF, and BaF. YbF's PDM also increases when correlations are taken into account [2].

Let us now discuss the electronegativity aspect. Usually, if there is a large difference in electronegativity of the two atoms that bond, then a large value of the PDM is expected (since the separation of charges is larger). However, for HgX, the CCSD results show that HgCl has the highest PDM.

Table II gives a summary of the results for the PDM of HgF obtained earlier by other

many-body techniques and experiment.

Table 6.2: Summary of the PDMs of HgX from previous works and the present one

Molecule	$Method$	$Reference$	$PDM(D)$
HgF	CI	Yu Yu Dmitriev et al	4.15
	DF	This work	3.959
	CCSD	This work	2.609
HgCl	CI	Wadt	3.28
	DF	This work	4.23
	CCSD	This work	2.721
HgBr	CI	Wadt	2.62
	DF	This work	4.40
	CCSD	This work	2.364
HgI	DF	This work	3.915
	CCSD	This work	1.644

Yu Yu Dmitriev et al [3] computed the PDM of HgF to be 4.15 D, using a bond length of 2.11 Angstrom. Their CI study used a Complete Active Space Self Consistent Field (CASSCF) program, with their active space including three outer electrons. Wadt [4] calculated the PDMs for HgCl and HgBr using CI (with effective core potentials (ECPs)), while calculating some quantities that he felt would be of use, for experimentalists trying to design efficient high-power visible-ultraviolet lasers, using the two molecules. He employed non-relativistic ECPs for Cl and Br, but relativistic ones for Hg. The basis sets were of the DZ type, with polarization functions.

Table 6.3: Electronic (at the CCSD level) and nuclear contributions to the PDM

Molecule	Electronic terms	Nuclear term
HgF	-768.599	771.208
HgCl	-919.565	922.286
HgBr	-1004.465	1006.829
HgI	-1078.199	1079.843

Table III gives the electronic and nuclear terms, just as in the AEM work. Their ratio differ from one another only in the third decimal place. However, it increases monotonically, with increase in Z. The electronic term, hence, 'grows' faster than the nuclear term, that is, it is slightly more sensitive to Z, than the latter.

The terms in Table IV show that the DF term is the largest, just as in the AEMs. It is at least three magnitudes larger than the DT_1 term, which is the largest correlation term. But, since the large DF value is almost cancelled out by the nuclear term, each of the correlation

Table 6.4: Contributions from the individual terms to the PDM

Term	HgF	HgCl	HgBr	HgI
DF	-767.249	-918.056	-1002.430	-1075.929
DT_1	-0.504	-0.619	-0.867	-1.033
DT_2	0	0	0	0
$T_1^\dagger D$	-0.504	-0.619	-0.867	-1.033
$T_1^\dagger D T_1$	-0.343	-0.277	-0.349	-0.299
$T_1^\dagger D T_2$	0.110	0.111	0.151	0.176
$T_2^\dagger D$	0	0	0	0
$T_2^\dagger D T_1$	0.110	0.111	0.151	0.176
$T_2^\dagger D T_2$	-0.219	-0.216	-0.254	-0.257

terms become very important. Both the DF and the DT_1 terms increase as we go from HgF to HgI. The $T_1^\dagger D T_1$ term, along with the DF and the DT_1 terms, reduce the PDM.

Table 6.5: Contributions from the SOMO to the DF PDM

Molecule	SOMO	%Fraction
HgF	-11.958	1.56
HgCl	-13.028	1.42
HgBr	-13.040	1.3
HgI	-12.690	1.18

As seen earlier, only the SOMO contributes to E_{eff}. This is not so for the PDM. All of the MOs contribute. Table V shows that if the DF PDM is decomposed as being comprised of SOMO and the rest of the orbitals, the former contributes to only about 1.5 percent of the total PDM.

The values of E_{eff}/E_{pol}, for the HgX molecules, are presented in Table VI. The quantity is related to the sensitivity of an eEDM experiment by the relation: $E_{pol} \equiv 2B/D$. This tells us that this quantity is dictated predominantly by how heavy a molecule is. But, if the PDM were to be an order or two lesser, it can compensate for Z.

Table 6.6: Enhancement factor for an eEDM experiment, due to E_{eff} and the PDM

Molecule	E_{eff} (GV/cm)	E_{pol} (kV/cm)	E_{eff}/E_{pol} ($\times 10^7$)
HgF	115.42	4.29	2.69
HgCl	113.56	1.63	6.97
HgBr	109.29	0.85	12.86
HgI	109.30	0.77	14.19

In our earlier work, the PDMs used were from Dmitriev and Wadt's work, to evaluate E_{pol}. Here, this is improved upon, where our RCCM values of the PDM are used. We see

that the polarizing field changes from about 2 kV/cm, to about a kV/cm, for HgBr. This again reinforces the need for accurate many-body calculations, when experimental data is not available.

Only the equilibrium bond length is not computed using our CCSD method, in this work. This is under the assumption that both E_{eff} and the PDM do not vary strongly near the equilibrium separation.

6.3 Summary

In this chapter, we calculated the PDMs of the HgX molecules. We decomposed the property in terms of its constituent terms, just as in the previous chapters. An important difference between the PDM and E_{eff} is illustrated, by looking at the SOMO contribution to the PDM. We compare our results with earlier calculations on the PDM of HgF. Finally, we now compute the new value of E_{eff}/E_{pol}, using our PDM results.

In the next chapter, we shall discuss about possible future directions of the work carried out in this thesis.

BIBLIOGRAPHY

[1] V. S. Prasannaa, S. Sreerekha, M. Abe, V. M. Bannur, and B. P. Das, Permanent electric dipole moments of alkaline earth metal monofluorides: Interplay of relativistic and correlation effects, Phys. Rev. A 93, 042504 (2016).

[2] M. Abe, G. Gopakumar, M. Hada, B. P. Das, H. Tatewaki, D. Mukherjee, Application of relativistic coupled-cluster theory to the effective electric field in YbF, Phys. Rev. A 90, 022501 (2014).

[3] Y. Y. Dmitriev, Y. G. Khait, M. G. Kozlov, L. N. Labzovsky, A. O. Mitrushenkov, A. V. Shtoff, and A. V. Titov, Calculation of the spin rotational Hamiltonian including P and P, T odd weak interaction terms for HgF and PbF , Phys. Lett. A 167, 280 (1992).

[4] W. R. Wadt, The electronic structure of HgCl and HgBr, Appl. Phys. Lett. 34, 658 (1979).

7

FUTURE WORK

7.1 Introduction

We plan on working in three broad directions. The first is to improve the existing results, by employing better basis sets, for example. For this, we are carrying out work on understanding the basis set dependence of properties. The second is to improve the results by using a better many-body technique. For example, we saw in Chapter 3 that NCCM is better than CCM, in that we do not need to truncate the expectation value expression. Another alternative is to not use the expectation value approach at all for evaluating properties, but rather use an energy derivative approach, called the finite field coupled cluster method (FFCC). The third direction for future work is to search for possibly better eEDM candidates. We shall elaborate on these three aspects in this Chapter.

7.2 Basis set dependence

In this section, we shall discuss some preliminary results from our calculations of PDMs of SrF, with various basis sets, and observe how it changes. We use three basis sets for each atom. For Sr, we use Dyall's basis, which does not contain in it diffuse and polarization functions. Then, we append to the Dyall basis diffuse and polarization functions taken from Sapporro's basis. We finally use the full Sapporro basis sets. For F, we use cc-pVNZ basis, and then the ccpcV-NZ basis, which take into account the core-core effects [1, 2]. Finally, we use aug-ccpV-NZ basis, which adds to the cc-pV basis sets diffuse functions. This gives an estimate of the sensitivity of the property in the far-nuclear regions.

In the table given below, the first column gives the basis sets used for Sr, while the first row mentions the basis used for F. The first number in a cell is the CCSD PDM, while the number in parenthesis is the percentage fraction difference of the value obtained with respect to experiment ($\%$ frac.), that is, (calculated value-experiment)/experiment.

Table 7.1: Summary of the calculated results of SrF at the CCSD level

CCSD	n	cc-pVNZ	cc-pCVNZ	aug cc-pVNZ
Dyall	DZ	3.20 (-7.72)	3.21 (-7.43)	3.79 (9.30)
Dyall	TZ	3.34 (-3.68)	3.40 (-1.95)	3.63 (4.68)
Dyall	QZ	3.38 (-2.53)	3.39 (-2.24)	3.57 (2.95)
Dyall+Sapporo	DZ	2.96 (-14.64)	2.96 (-14.64)	3.51 (1.22)
Dyall+Sapporo	TZ	3.41 (-1.66)	3.43 (-1.08)	3.56 (2.66)
Dyall+Sapporo	QZ	3.60 (3.82)	3.60 (3.82)	3.58 (3.24)
Sapporo+diff	DZ	2.96 (-14.64)	2.97 (-14.35)	3.58 (3.24)
Sapporo+diff	TZ	3.42 (-1.37)	3.43 (-1.08)	3.56 (2.66)
Sapporo+diff	QZ	3.57 (2.95)	3.57 (2.95)	3.58 (3.24)

From the Table, we observe that core-core correlations are not so important, but the diffuse functions are. That is, the PDM can be thought of as a property that is sensitive to the far-nuclear region. Note that Sr is very heavy, as compared to F. We plan on extending the work to BeF, where BeF is much lighter with respect to F, and MgF, where the masses of the atoms are comparable. This will provide us with a better perspective on the dependence of PDM on the choice of basis sets. In the end, we plan on applying our knowledge of basis set dependence to the mercury halides' PDMs as well as E_{eff}. These results are not only aimed at improving the accuracy of our earlier results by including those physical effects that may be more important, but also be extremely useful in evaluating accurately E_{eff} of molecules like YbF, whose experimental results are already available.

7.3 The finite field coupled cluster method

Since we have established that HgX are excellent candidates for eEDM search, we need to perform precise calculations of their effective electric fields (higher quality basis sets). We can also improve the result by using a different/modified many-body technique: the finite field method. In the finite field coupled cluster method (FFCC), a property is expressed as an energy derivative, instead of an expectation value problem.

Consider an unperturbed Hamiltonian, $\boldsymbol{H_0}$. It satisfies the equation:

$$\boldsymbol{H_0}|\psi_0\rangle = E_0|\psi_0\rangle$$

If we apply a perturbation, $\boldsymbol{H'}$, to it, then:

$$\begin{aligned} \boldsymbol{H}(\lambda) &= \boldsymbol{H_0} + \boldsymbol{H'} && (7.1)\\ \boldsymbol{H}(\lambda)|\psi(\lambda)\rangle &= E(\lambda)|\psi(\lambda)\rangle \\ E(\lambda) &= E_0 + \lambda E_1 + \cdots && (7.2)\\ E_1 &= \langle\psi_0|\boldsymbol{H'}|\psi_0\rangle && (7.3) \end{aligned}$$

But, $E(\lambda)$ is also:

$$E(\lambda) = E_0 + \lambda\frac{\partial E}{\partial\lambda}|_{\lambda=0} + \cdots \quad (7.4)$$

In the CCM, $|\psi_0\rangle = e^{\boldsymbol{T}}|\Phi_0\rangle$. Since the CCM is non-variational, the energy derivative is actually equal to the expectation value expression and a correction term [3].

$$\therefore \frac{\partial E}{\partial\lambda}|_{\lambda=0} \approx \langle\psi_0|\boldsymbol{H'}|\psi_0\rangle \quad (7.5)$$

Any first order property can now be defined as an energy derivative, instead of solving the expectation value expression. If we compute a property using the energy derivative approach, we account for both the non-linear terms in the expectation value expression, which we had neglected, as well as this coupled cluster correction term.

Now, let us derive an expression for the derivative:

Consider a molecule, described by the Dirac-Coulomb Hamiltonian, $\boldsymbol{H_0}$. Its total en-

ergy, E, is given by the sum of its Dirac-Fock (DF) energy, E^{DF}, and the correlation energy, ΔE.

$$E = E^{DF} + \Delta E \tag{7.6}$$

If the system is perturbed by $\lambda \boldsymbol{H'}$, where λ is the perturbation parameter, and $\boldsymbol{H'}$ is the perturbation operator, then the total energy is

$$E(\lambda) = E^{DF}(\lambda) + \Delta E(\lambda) \tag{7.7}$$

Now,

$$\begin{aligned} E^{DF}(\lambda) &= \langle \Phi_0 | \boldsymbol{H}(\lambda) | \Phi_0 \rangle & (7.8) \\ &= \langle \Phi_0 | \boldsymbol{H_0} | \Phi_0 \rangle + \lambda \langle \Phi_0 | \boldsymbol{H'} | \Phi_0 \rangle & (7.9) \end{aligned}$$

Here, $|\Phi_0\rangle$ is the DF wave function of the unperturbed system. Therefore,

$$\frac{E(\lambda) - E}{\lambda} = \frac{\Delta E(\lambda) - \Delta E}{\lambda} + \langle \Phi_0 | \boldsymbol{H'} | \Phi_0 \rangle \tag{7.10}$$

The left hand side of the above equation is the familiar forward difference formula, for calculating a first derivative.

If $\boldsymbol{H'}$ is the eEDM Hamiltonian, and if λ can be thought of as -d_e, then the above expression, is actually the effective electric field, E_{eff}. We can extend this to a central difference version:

$$\begin{aligned} \frac{E(\lambda/2) - E(-\lambda/2)}{\lambda} &= \frac{\Delta E(\lambda/2) - \Delta E(-\lambda/2)}{\lambda} \\ &+ \langle \Phi_0 | \boldsymbol{H'} | \Phi_0 \rangle & (7.11) \end{aligned}$$

And:

$$\begin{aligned} \frac{\partial E}{\partial d_e} &= E_{eff} & (7.12) \\ \frac{\partial E}{\partial \epsilon} &= D & (7.13) \end{aligned}$$

This method removes the issue of having to truncate higher order terms in the CCSD expectation value expression, because the correlation energy requires no truncation! The conversion factors for the PDM and E_{eff} are 2.541 and 5.142 respectively. The former is because 1 atomic unit (for electric dipole moment) corresponds to 2.541 Debye. The latter is because 1 atomic unit (for the electric field) corresponds to 5.142×10^{11} V/m, which is 5.142GV/cm. A six-point central difference version of the energy derivative is:

$$\begin{aligned} E_{eff} &= \frac{45(\Delta E_{\lambda/4} - \Delta E_{-\lambda/4}) - 9(\Delta E_{\lambda/2} - \Delta E_{-\lambda/2}) + (\Delta E_{3\lambda/4} - \Delta E_{-3\lambda/4})}{60(\lambda/4)} \\ &+ O((\lambda/4)^6) \end{aligned} \tag{7.14}$$

Our goal is to apply both two and six point formulae to AEMs, and HgX, and understand the importance of the non-linear terms in the expectation value expression. We have carried out preliminary calculations on these molecules, and as of now, it appears that for the AEMs, results from the linear expectation value is not very different from that obtained using the energy derivative, for both the PDMs and E_{eff}s.

Table 7.2: FFCC results for AEMs

Molecule	Quantity	CCSD	2 pt FFCC
BeF DZ	PDM	0.93	1.01
	E_{eff}	0.003	0.003
BeF TZ	PDM	1.06	1.12
	E_{eff}	0.004	0.004
BeF QZ	PDM	1.10	1.15
	E_{eff}	0.005	0.005
MgF DZ	PDM	2.84	2.91
	E_{eff}	0.06	0.06
MgF TZ	PDM	3.02	3.08
	E_{eff}	0.06	0.06
MgF QZ	PDM	3.07	3.13
	E_{eff}	0.07	0.07
CaF DZ	PDM	3.01	3.07
	E_{eff}	0.23	0.23
CaF TZ	PDM	3.13	3.17
	E_{eff}	0.27	0.27
CaF QZ	PDM	3.16	3.19
	E_{eff}	0.28	0.28
SrF DZ	PDM	2.95	3.02
	E_{eff}	1.91	1.99
SrF TZ	PDM	3.42	3.46
	E_{eff}	2.14	2.12
SrF QZ	PDM	3.6	3.62
	E_{eff}	2.17	2.16
BaF DZ	PDM	2.69	2.77
	E_{eff}	6.48	6.42
BaF TZ	PDM	3	2.96
	E_{eff}	6.65	6.60
BaF QZ	PDM	3.4	3.41
	E_{eff}	7.41	6.46

7.4 Better eEDM candidates?

We had identified HgX as promising candidates for eEDM experiments. The next question is if there are other candidates that are as promising, or maybe even better candidates. From an experimental viewpoint, alkali atoms can be produced in larger numbers, than the halides. If so, would mercury alkalis be suitable candidates? We are currently working on the effective fields and the PDMs of these molecules. Since the bond lengths of these molecules, the mercury alkalis (HgH, HgNa, HgK, HgRb, and HgCs) is not very well known, we need to obtain the bond length of each of these molecules, by plotting the potential energy curve, at the CCSD level. Preliminary calculations on HgH has shown that its PDM is too small to provide good sensitivity for an eEDM experiment, although its $E_{eff} \approx 100GV/cm$. We expect that HgLi and HgNa will have larger PDMs, and reasonable effective fields, making them potential candidates.

7.5 Summary

In this chapter, we explored possibilities for future work in various directions. Preliminary work on basis set dependence of a property like PDM on SrF using the CCSD method, and at QZ level of basis, indicates that diffuse functions are important in moderately heavy systems like SeF, while core-core correlations can be completely ignored. Further work in this direction, and on more molecules, shall be carried out in the future. Our initial set of results using FFCC indicates that the linear expectation value approach may be accurate. We will extend the work for HgX, as well as a few other systems of interest in fundamental physics. We have started work on the HgA molecules as potential candidates for eEDM search experiments.

BIBLIOGRAPHY

[1] B. Temelso , E. F. Valeev , and C. D. Sherrill, A Comparison of One Particle Basis Set Completeness, Higher Order Electron Correlation, Relativistic Effects, and Adiabatic Corrections for Spectroscopic Constants of BH, CH+, and NH, J. Phys. Chem. A, 108, 3068-3075 (2004).

[2] T. H. Dunning Jr., Gaussian basis sets for use in correlated molecular calculations. I. The atoms boron through neon and hydrogen, J. Chem. Phys. 90, 1007 (1989).

[3] J. Noga, M. Urban, On expectation value calculations of one-electron properties using the coupled cluster wave functions, Theoretica chimica acta, Volume 73, Issue 4, pp 291–306 (1998).

i Appendix

i.1 Appendix A: The eEDM Hamiltonian

The correct relativistic form of the eEDM Hamiltonian is derived here. We start with the magnetic dipole interacting with a spin $1/2$ particle. It takes the form:

$$H_{M1} = \frac{\kappa\mu}{2}\sigma_{\mu\nu}F^{\mu\nu} \tag{15}$$

Here, κ is some constant, $\sigma_{\mu\nu} = \frac{i}{2}[\gamma^{\mu}, \gamma^{\nu}]$, and $F^{\mu\nu}$ is the electromagnetic field tensor, given by $\partial^{\mu}A^{\nu} - \partial^{\nu}A^{\mu}$. In matrix form, it is given by:

$$\begin{bmatrix} 0 & -E_x & -E_y & -E_z \\ E_x & 0 & -B_z & B_y \\ E_y & B_z & 0 & -B_x \\ E_z & -B_y & B_x & 0 \end{bmatrix} \tag{16}$$

There is no factor of 1/c for the components of the electric field, since we use natural units, in particle physics.

Now, using the approach by Salpeter, an EDM can be considered as an odd-parity counterpart of the MDM, that is, $H_{E1} = \gamma^5 H_{M1}$. Also, $\kappa\mu$ is replaced by $-id_e$, where the 'i' is to ensure that the resulting Hamiltonian is Hermitian. That leads us to

$$H_{E1} = \frac{id_e}{2}\gamma^5\sigma_{\mu\nu}F^{\mu\nu} \tag{17}$$

$$= -d_e\beta(\vec{\sigma}\cdot\vec{E} - i\vec{\alpha}\cdot\vec{B}) \tag{18}$$

An outline of the derivation to obtain the final expression is given below:

Let us first examine the structure of $F^{\mu\nu}$, to simplify the algebra involved. If $\mu = \nu$, then $F^{\mu\nu} = 0$, and therefore that part of H_{E1}. The second step is to separate out the terms with the electric and magnetic fields. This is straightforward, since from the matrix form of $F_{\mu\nu}$, we see that the first row and the first column contain only the electric fields, and the rest the magnetic fields. Armed with this information, we rewrite H_{E1} as:

$$H_{E1} = \frac{id_e}{2}\gamma^5(\sigma_{0j}F^{0j} + \sigma_{i0}F^{i0} + \sigma_{ij}F^{ij}) \tag{19}$$

The third step is to examine the properties of the matrix elements of $F^{\mu\nu}$ and $\sigma_{\mu\nu}$. The relevant properties are that $F^{\mu\nu} = -F^{\nu\mu}$, and $\sigma_{\mu\nu} = -\sigma_{\nu\mu}$. The former is a well known property, and can be found in many text books on electrodynamics, while the latter can be seen in the following way:

$$\begin{aligned}
\sigma_{\mu\nu} &= \frac{i}{2}[\gamma^\mu, \gamma^\nu] && (20)\\
&= \frac{i}{2}(\gamma^\mu\gamma^\nu - \gamma^\nu\gamma^\mu) && (21)\\
&= -\frac{i}{2}(\gamma^\nu\gamma^\mu - \gamma^\mu\gamma^\nu) && (22)\\
&= -\sigma_{\nu\mu} && (23)
\end{aligned}$$

Because of this, $\sigma_{0j}F^{0j} = \sigma_{i0}F^{i0}$. Therefore,

$$H_{E1} = \frac{id_e}{2}\gamma^5(2\sigma_{0j}F^{0j} + \sigma_{ij}F^{ij}) \tag{24}$$

Now, let us evaluate the first term:

$$\begin{aligned}
id_e\gamma^5\sigma_{0j}F^{0j} &= id_e\gamma^5(\sigma_{01}F^{01} + \sigma_{02}F^{02} + \sigma_{03}F^{03}) && (25)\\
&= id_e\gamma^5(\sigma_{01}E^1 + \sigma_{02}E^2 + \sigma_{03}E^3) && (26)
\end{aligned}$$

Here, E^i refers to the i^{th} component of the electric field. Consider only the first term:

$$\begin{aligned}
id_e\gamma^5\sigma_{01}E^1 &= id_e\gamma^5\frac{i}{2}[\gamma^0, \gamma^1]E^1 && (27)\\
&= id_e\frac{i}{2}(\gamma^5\gamma^0\gamma^1 - \gamma^5\gamma^1\gamma^0)E^1 && (28)\\
&= id_e\frac{i}{2}(-\gamma^0\gamma^5\gamma^1 - \gamma^0\gamma^5\gamma^1)E^1(\because \{\gamma^0, \gamma^5\} = 0, \{\gamma^0, \gamma^1\} = 0) && (29)\\
&= id_e\frac{i}{2}(2\beta\Sigma^1)E^1(\because \gamma^0\ is\ \beta,\ \gamma^1\ is\ \alpha^1,\ and\ \gamma^5\gamma^1 = -\Sigma^1) && (30)\\
&= -d_e\beta\Sigma^1E^1 && (31)
\end{aligned}$$

Repeating this for the other two terms, we obtain:

$id_e\gamma^5\sigma_{0j}F^{0j} = -d_e\beta\vec{\Sigma}\cdot\vec{E}$

Now, let us evaluate the second term of H_{E1}:

Expanding $\sigma_{ij}F^{ij}$, recalling that those terms where $i = j$ vanish, and also using the facts that $F_{ij} = -F_{ji}$and $\sigma^{ij} = -\sigma^{ji}$, we obtain:

$$\frac{id_e}{2}\gamma^5\sigma_{ij}F^{ij} \quad = \quad id_e\gamma^5(\sigma_{12}F^{12} + \sigma_{13}F^{13} + \sigma_{23}F^{23}) \tag{32}$$

From the matrix form of $F^{\mu\nu}$, we read off F^{12} as -B^3, F^{13} as B^2, and F^{23} as -B^1.

Using the facts that $\gamma^5 = i\gamma^0\gamma^1\gamma^2\gamma^3$, and also the fact that the α matrices (or γ^i; i=1, 2, and 3) anti-commute in each of the terms, we obtain:

$id\beta\alpha\cdot\vec{B}$

A quick sample calculation for only $id\gamma^5\sigma_{12}F^{12}$ is provided below, for illustration purposes:

$$\begin{aligned} id\gamma^5\sigma_{12}F^{12} &= idi\gamma^0\gamma^1\gamma^2\gamma^3(\frac{i}{2}(\gamma^1\gamma^2 - \gamma^2\gamma^1))(-B^3) && (33)\\ &= -\frac{id}{2}\gamma^0(\gamma^1\gamma^2\gamma^3\gamma^1\gamma^2 - \gamma^1\gamma^2\gamma^3\gamma^2\gamma^1)(-B^3) && (34)\\ &= -\frac{id}{2}(-2\gamma^3)(-B^3) && (35)\\ &= -id\alpha^3B^3 && (36) \end{aligned}$$

Therefore, we finally obtain:

$$H_{E1} = -d\beta(\vec{\sigma}\cdot\vec{E} - i\alpha\cdot\vec{B}) \tag{37}$$

In atoms and molecules with one unpaired electron, the electric term dominates over the magnetic one, and therefore, we obtain the familiar expression

$$H_{E1} = -d\beta\vec{\sigma}\cdot\vec{E} \tag{38}$$

where

$$\vec{E} = -[\vec{\nabla}, V/q] \tag{39}$$

V is the potential from the Dirac-Coulomb Hamiltonian.

i.2 Appendix B: Derivation of the effective eEDM Hamiltonian, and why $E_{eff} = 0$ for the non-relativistic case

Let us start with the commutator, $[\frac{-d_e}{e}\beta\sigma \cdot \nabla, H_o]$.

$$\begin{aligned} [\beta\sigma \cdot \nabla, H_o] &= [\beta\sigma \cdot \nabla, c\alpha \cdot p] + mc^2[\beta\sigma \cdot \nabla, \beta] + [\beta\sigma \cdot \nabla, V] \\ &= 1 + 2 + 3 \end{aligned} \tag{40}$$

Note that the summation over the number of electrons is not mentioned,it does not change the overall derivation. Also, the potential, $V = V(x, y, z)$, is general, and not necessarily central, since we are dealing with molecules.

Let us first evaluate 1:

$$[\beta\sigma \cdot \nabla, c\alpha \cdot p] = \frac{ic}{\hbar}[\beta\sigma \cdot p, \alpha \cdot p] \tag{41}$$

$$= \frac{ic}{\hbar}[\beta \sum_j \sigma_j p_j, \sum_k \alpha_k p_k] \tag{42}$$

$$= \frac{ic}{\hbar} \sum_{j,k} p_j p_k [\beta\sigma_j, \alpha_k] \tag{43}$$

This is allowed, since p_j and p_k are only the components of p, and are, hence, numbers.

$$\begin{aligned} \therefore [\beta\sigma \cdot \nabla, c\alpha \cdot p] &= \frac{ic}{\hbar} \sum_j p_j^2 [\beta\sigma_j, \alpha_j] \\ &+ \sum_j \sum_{k \neq j} p_j p_k [\beta\sigma_j, \alpha_k] \end{aligned} \tag{44}$$

Let us evaluate the first term's commutator:

$$
\begin{aligned}
[\beta\sigma_j, \alpha_j] &= \beta\sigma_j\alpha_j - \alpha_j\beta\sigma_j && (45)\\
&= -\beta\gamma_5\alpha_j^2 + \alpha_j\beta\gamma_5\alpha_j && (46)\\
&= -\beta\gamma_5 + (-\beta\alpha_j\gamma_5\alpha_j)(\because \alpha_j^2 = I,\ and\ \alpha_j, \beta = 0) && (47)\\
&= -\beta\gamma_5 + (-\beta\gamma_5\alpha_j^2)(\because \alpha_j\gamma_5 = \gamma_5\alpha_j) && (48)\\
&= -2\beta\gamma_5 && (49)
\end{aligned}
$$

Hence, the first term is: $-2\frac{ic}{\hbar}\sum_j p_j^2\beta\gamma_5$.

And the second term's commutator is:

$$
\begin{aligned}
[\beta\sigma_j, \alpha_k] &= \beta\sigma_j\alpha_k - \alpha_k\beta\sigma_j && (50)\\
&= \beta\sigma_j\alpha_k + \beta\alpha_k\sigma_j && (51)\\
&= \beta(\sigma_j\alpha_k + \alpha_k\sigma_j) && (52)\\
&= \beta(-\gamma_5\alpha_j\alpha_k - \alpha_k\gamma_5\alpha_j)(\because \sigma_j = -\gamma_5\alpha_j) && (53)\\
&= -\beta\gamma_5(\alpha_j\alpha_k + \alpha_k\alpha_j) && (54)\\
&= 0 && (55)
\end{aligned}
$$

$\therefore [\beta\sigma\cdot\nabla, c\alpha\cdot p] = -2\frac{ic}{\hbar}\sum_j \beta\gamma_5 p_j^2$.

Now, let us evaluate 2:

$$
\begin{aligned}
mc^2[\beta\sigma\cdot\nabla, \beta] &= mc^2\frac{i}{\hbar}[\beta\sigma\cdot p, \beta] && (56)\\
& && (57)
\end{aligned}
$$

$$
\begin{aligned}
[\beta\sigma\cdot p, \beta] &= \sum_k p_k[\beta\sigma_k, \beta] && (58)\\
&= \sum_k p_k[-\beta\gamma_5\alpha_k, \beta] && (59)\\
&= \sum_k p_k(-\beta\gamma_5\alpha_k\beta + \beta^2\gamma_5\alpha_k) && (60)\\
&= \sum_k p_k(-\beta\gamma_5(-\beta\alpha_k) + \gamma_5\alpha_k) && (61)
\end{aligned}
$$

$$= \sum_k p_k(\beta\gamma_5\beta\alpha_k + \gamma_5\alpha_k) \quad (62)$$

$$= \sum_k p_k(-\beta^2\gamma_5\alpha_k + \gamma_5\alpha_k) \quad (63)$$

$$= \sum_k p_k(-\gamma_5\alpha_k + \gamma_5\alpha_k) \quad (64)$$

$$= 0 \quad (65)$$

Finally, let us evaluate 3:

Note that the potential, V, has a one-body (electron-nucleus interaction) and a two body part (electron-electron interaction):

$$V = ev(r_i) + ev_{ij} \quad (66)$$

$$= ev + ev' \quad (67)$$

V is the potential energy, and v is the potential. The former has only one coordinate index, and hence we shall denote $\frac{\partial}{\partial x_i}$ (say) as $\frac{\partial}{\partial x}$.

$$[\beta\sigma\cdot\nabla, ev] = \beta[\sigma_x\frac{\partial}{\partial x}, ev] + \beta[\sigma_y\frac{\partial}{\partial y}, ev] + \beta[\sigma_z\frac{\partial}{\partial z}, ev] \quad (68)$$

$$= \beta\sigma_x[\frac{\partial}{\partial x}, ev] + \beta\sigma_y[\frac{\partial}{\partial y}, ev] + \beta\sigma_z[\frac{\partial}{\partial z}, ev] \quad (69)$$

$$= e\beta\sigma_x\frac{\partial v}{\partial x} + e\beta\sigma_y\frac{\partial v}{\partial y} + e\beta\sigma_z\frac{\partial v}{\partial z} \quad (70)$$

$$= -e\beta\sigma_x E_x - e\beta\sigma_y E_y - e\beta\sigma_z E_z \quad (71)$$

$$= -e\beta\sigma\cdot E_{intl} \quad (72)$$

In the second term, v', we have an additional index, j, which is not equal to i. The above mentioned argument for the commutator holds for the latter too. This is because the steps given above hold, independent of what the form of the potential is, as long as there is a dependence of the potential on x, y, and z.

The electric field term can be interpreted as the internal field, since v involves electron-nuclei and electron-electron interactions. Also, we have used $\frac{\partial v}{\partial x} = -E_x$, and so on, since the force is conservative (although it is not central, since we are dealing with molecules).

Hence, we get:

$$[\beta\sigma\cdot\nabla, H_o] = -2\frac{ic}{\hbar}\sum_j \beta\gamma_5 p_j^2 - e\beta\sigma\cdot E_{intl} \tag{73}$$

$$\therefore -e\beta\sigma\cdot E_{intl} = [\beta\sigma\cdot\nabla, H_o] + 2\frac{ic}{\hbar}\sum_j \beta\gamma_5 p_j^2 \tag{74}$$

Finally, we see that when we take the expectation value of the above expression, the first term vanishes. This is because the commutator involves two terms, both containing H_o, which implies that both the terms give an energy term corresponding to it (this is because E_{eff} is the expectation value of the unperturbed wave function, which is the eigenstate of the unperturbed Hamiltonian, by definition). Since the energy is a number, we can take it out as a common term, and the remaining two terms cancel.

Let us now look at the non-relativistic case, in detail, for completeness. Since in the non-relativistic case, we can view β as unity, we shall use this motivation to start with the commutator, $[\frac{-d_e}{e}\sigma\cdot\nabla, H_o]$, which is the same as the one that we started with, in the relativistic case, except that β has been set to unity. Also, H_o is the non-relativistic Hamiltonian.

$$\begin{aligned}[\sigma\cdot\nabla, H_o] &= [\sigma\cdot\nabla, \frac{-\hbar^2\nabla^2}{2m}] + [\sigma\cdot\nabla, V] \\ &= 1+2+3\end{aligned} \tag{75}$$

If we recast the ∇s in the first term as momenta, then we can directly see that the end result is zero, since when we expand the dot products of both the terms involved in the commutator, the components of momenta are just numbers, and can be taken out. The second term is calculated in a way similar to that in the previous derivation, except that the β is missing. Hence, we obtain:

$$[\sigma\cdot\nabla, H_o] = -e\sigma\cdot E_{intl} \tag{76}$$

The right hand side is the eEDM operator, and when we take its expectation value (which is E_{eff}), it is equal to the expectation value of the left hand side, which is zero, as discussed in the previous derivation. Hence, for a non-relativistic case, E_{eff} is zero.

Finally, let us comment on the case of a finite nucleus. Independent of whether we choose a point nucleus or a finite one, the commutator, $[\beta\sigma\cdot\nabla, ev]$, gives the same result,

since v is conservative (this can be seen in the following classical way: if the force can be represented as the negative gradient of the potential, and if its curl is zero, then it is conservative). Therefore, independent of whether we use a point or a finite nucleus, the non-relativistic E_{eff} is zero, and the relativistic may not be zero. However, the value of E_{eff} itself depends on the type of finite nucleus that we use, since each model for a finite nucleus modifies the electron-nucleus potential differently in the near-nuclear region, which means that the wave function we finally obtain is expected to be slightly different, and therefore E_{eff} is expected to be slightly different too.